A spatially explicit modelling approach for predicting and managing the effects of coral reef stressors

by

Russell Anderson Milne

A thesis
presented to the University of Waterloo
in fulfillment of the
thesis requirement for the degree of
Doctor of Philosophy
in
Applied Mathematics

Waterloo, Ontario, Canada, 2022

Examining Committee Membership

The following served on the Examining Committee for this thesis. The decision of the Examining Committee is by majority vote.

Supervisors:	Chris Bauch Professor, Dept. of Applied Mathematics University of Waterloo
	Madhur Anand Professor, School of Environmental Sciences University of Guelph
Internal Members:	Brian Ingalls Professor, Dept. of Applied Mathematics University of Waterloo
	Mohammad Kohandel Professor, Dept. of Applied Mathematics University of Waterloo
Internal-External Member:	Jeremy Pittman Assistant Professor, School of Planning University of Waterloo
External Examiner:	Ben Bolker Professor, Dept. of Mathematics and Statistics McMaster University

Author's Declaration

This thesis consists of material all of which I authored or co-authored: see Statement of Contributions included in the thesis. This is a true copy of the thesis, including any required final revisions, as accepted by my examiners.

I understand that my thesis may be made electronically available to the public.

Statement of Contributions

- Chapter 2: The work in this chapter was performed by Russell Milne (RM), under the supervision of Profs. Chris Bauch (CB) and Madhur Anand (MA), resulting in a co-authored paper published in the Bulletin of Mathematical Biology [171]. Contributions were as follows: RM, CB and MA conceived of the study. RM developed the model and associated MATLAB code, performed analysis, and wrote the first draft. All authors revised the manuscript.

- Chapter 3: This chapter is based on a manuscript to be submitted to Ecological Modelling. RM conceived of the study, developed the model and associated MATLAB code, performed analysis, and wrote the first draft. CB and MA supervised the work. All authors revised the manuscript.

- Chapter 4: This chapter is based on a manuscript in preparation. RM conceived of the study, developed the model and associated MATLAB code, performed analysis, and wrote the first draft. CB and MA supervised the work. All authors revised the manuscript.

Abstract

Coral reefs represent simultaneously one of the most beloved and one of the most endangered ecosystems in the world. Millions of people visit coral reefs every year for tourism purposes, and millions of people living in areas adjacent to reefs have reef fish as a key part of their diet, but both of these important services provided by reefs are under threat by anthropogenic stressors. These include overfishing, which is known to cause regime shifts to an equilibrium dominated by macroalgae instead of coral; nutrient loading, which facilitates greater nutrient uptake by macroalgae, allowing them to overgrow coral; sedimentation, in which coral and algae alike become smothered by particulate matter, leading to food web disruption; and many others such as ocean warming and acidification due to climate change. Outbreaks of crown-of-thorns starfish (CoTS), a fast-acting coral predator, are also projected to become more serious in the future, as more CoTS larvae survive at elevated nutrient concentrations. Due to the large number of reef organisms (including many coral species, macroalgae, and CoTS) that reproduce by dispersing their larvae into the ocean, the fact that sedimentation can be caused by soil erosion many miles inland, and the spatial variation in fishing pressure and nutrient input that arises from different human land use patterns, these reef stressors are explicitly spatial in nature. As the large spatial scales that coral reef dynamics take place on make comprehensive field studies expensive in money, time, and labour, determining optimal strategies for managing these stressors cannot rest on field work alone. In this thesis, we build and parametrize three spatially explicit mathematical coral reef models of intermediate complexity, and use these to produce ecological predictions and conservation recommendations for reefs with high levels of anthropogenic stress. We show that coral and herbivorous fish populations respond to fragmented habitats induced by overfishing in opposite ways, and that spillover from marine protected areas can sustain herbivorous fish populations even in heavily overfished areas. We demonstrate that local economic transitions from fishing to tourism can facilitate larger-scale recovery first of fish and subsequently of coral within approximately 30 years. We show that on reefs experiencing CoTS outbreaks, slight increases in fishing and nutrient loading rates could cause sharp transitions to states with less coral and continuous CoTS presence. We predict how future CoTS outbreaks would affect coral cover on reefs adjacent to two growing cities (Cebu City, Philippines and Jeddah, Saudi Arabia), and evaluate four strategies for CoTS management in these cities. We evaluate the resilience of reef fish in four different functional groups to sedimentation caused by deforestation, as well as the robustness of reef fisheries to decline in fish stock stemming from deforestation, and show that flexible harvesting strategies can mitigate this decline. Our work joins novel ecological theory with concrete recommendations for reef ecosystem management, and represents a substantial step forward for understanding marine spatial dynamics.

Acknowledgements

First, I would like to thank my supervisors, Profs. Chris Bauch and Madhur Anand, for supporting me throughout my journey, giving me a long leash to build my own research projects, and showing patience during the times when things weren't going according to plan. Furthermore, I would like to thank my examiners, Profs. Brian Ingalls, Mohammad Kohandel, Jeremy Pittman, and Ben Bolker, for taking the time to read this thesis.

Next, I would like to thank my family. Mom, thanks for always wanting me to be at my best, and putting so much effort into helping me do so. Dad, thanks for taking time out of your busy schedule to discuss research, math, and whatever else came to mind. Blair, thanks for being my brother and my friend, and for listening to my stories about the quirks of grad student life and telling me your own about audio engineering.

I would also like to thank my collaborators past, present, and future: thanks are due to Prof. Frédéric Guichard for giving a chance to an enthusiastic undergrad back in 2015, to Prof. Alison Derry and Jorge Negrín Dastis for showing me the wonders of copepods, and to Prof. Hao Wang for recognizing (and helping me reach) my research potential.

Similarly, I would like to thank Yiwen Tao for proving that true friends can reconnect after being separated for over a year and by eleven time zones, and Mehrshad Sadria for constantly spreading positive energy, especially during the times when I really needed it. I look forward to the first paper we write that has all three of our names on it.

Creating this thesis would also have been much harder without the logistical and technological support that I received. I would like to thank Pedram and Rhonda for taking care of my workstation while I was in Vancouver, and the developers of RustDesk for making remotely accessing my various computers relatively painless.

Having a supportive environment made a huge difference in my research output. Many thanks to everyone in the 2022 iteration of the Bauch lab (and de facto lab member Maliha) for making me enjoy coming to the office and attending lab meetings. I will also thank lab alumni Tom, Brendon, Saptarshi, Jyler, Vadim, Mark, and Vivek, for being decent human beings. Others I'd like to thank include, but are certainly not limited to: Shervin, for the trips to St. Jerome's; Yao, for being a great next-door neighbour; Greg and Juju, for the interesting conversations; Ziyuan, Wenwen, Ruikun, Yating, Shiyu, and the rest of my Chinese friends (as well as Chris West), for entertaining my curiosity about China; Stefan, for the music recommendations; and Atiyeh, for being the best student I ever TAed. Relatedly, I will thank the Butlers (Jimmy, Russell, and Karl) for hosting me in August 2021. If I ever write a paper pertaining to dairy farming, you'll be the first to know.

Lastly, I would like to thank Merlin the cat, who made truly wondrous contributions to this thesis, which this page is too small to contain the acknowledgements for.

Dedication

This thesis is dedicated to Ronald Gordon Milne (1931 – 2020), whose decision to take me on hiking and kayaking trips when I was young almost certainly influenced the direction that my future research would go in.

Table of Contents

List of Figures

List of Tables

Chapter 1

Introduction

The coral reef is one of the most iconic ecosystems existing anywhere on Earth. People collectively spend billions of dollars every year on tropical vacations during which they can see coral firsthand, and return with their waterproof cameras full of pictures of coral reefs and their animal inhabitants. However, coral reefs are also highly important from an ecological perspective, as they constitute one of the highest-biodiversity ecosystems in the world [23, 252, 25]. In addition to the various coral species themselves, reefs are home to many kinds of fish (as anyone who has been to a reef will tell you), which form a large and intricate food web. This food web is similar to those found on land in some respects, featuring herbivorous, omnivorous, and carnivorous species; fish that eat other fish are properly referred to as "piscivores". The herbivores in this food web mainly feed on photosynthetic algae that inhabit, and compete with coral for space on, the seabed. This includes fast-growing macroalgae, an umbrella term for large algae (such as seaweeds) that resemble underwater shrubs, as well as even faster-growing turf algae, which bears similarity to grass. Also present are predators of coral, such as the crown-of-thorns starfish (CoTS). CoTS are voracious coral predators with a fast life cycle, and can thus quickly reduce healthy reefs to rubble. Finally, of vital importance are the fluxes of nutrients such as nitrogen and phosphorus, which primary producers on the reef such as algae need to uptake to grow and survive.

Figure 1.1: Coral often builds incredibly complex structures. (Photo: wewe yang, Pexels)

1.1 Mathematical modelling of spatial processes in ecology

Using mathematical models to express the dynamics of interacting species is a concept with a long and rich history. We are nearing the centenary of the textbook in which Alfred Lotka first applied equations describing oscillatory chemical reactions to a predator-prey system [152], as well as that of the work of Vito Volterra on fluctuations in Adriatic Sea fish catch [255]. The Lotka-Volterra predator-prey model based on their results, probably the simplest and easiest to understand mathematical representation of an ecological system, is reproduced below:

$$\begin{aligned} \frac{\mathrm{d}N}{\mathrm{d}t} &= \alpha N - \beta NP \\ \frac{\mathrm{d}P}{\mathrm{d}t} &= \gamma\beta NP - \delta P \end{aligned} \tag{1.1}$$

Here, the population of a prey species is denoted by N, while that of a predator species is denoted by P. Within the model, prey are born at a rate α. They are eaten by predators at a rate β; the term for this is dependent on both N and P, as it represents an interaction between the two species. Predators use the energy they obtain from consuming prey to reproduce, with a constant γ representing the efficiency at which eaten prey are converted into predators, and die at a rate δ. Variations on the Lotka-Volterra model have since been

produced. Among the most notable of these is the Rosenzweig-MacArthur model [209], which features an explicit carrying capacity (K) for the prey, and represents predation as a saturation function in N (with half-saturation constant s). This latter assumption is based on the fact that predators cannot spend all of their time hunting for prey, so the rate of predation is therefore taken to scale sublinearly with prey abundance. This model is reproduced below:

$$\begin{aligned} \frac{\mathrm{d}N}{\mathrm{d}t} &= \alpha N\left(1-\frac{N}{K}\right) - \beta P \frac{N}{s+N} \\ \frac{\mathrm{d}P}{\mathrm{d}t} &= \gamma\beta P \frac{N}{s+N} - \delta P \end{aligned} \tag{1.2}$$

However, both the Lotka-Volterra and Rosenzweig-MacArthur models (without any further modification) represent dynamics within a population that is spatially uniform. In other words, neither takes into account how the population levels of these two interacting species may vary at different locations. However, real-life ecological populations are often far from well-mixed, and the wealth of biotic and abiotic interactions in an ecosystem can create rich spatial and spatiotemporal patterns [164]. These range from the large-scale migration of birds at specific points in the year [127] to the patchwork of different plant communities that establish themselves following forest fires [246], to invasive species spreading into new habitats [132]. Aquatic ecology in particular features highly connected habitats and organisms capable of dispersing tremendous distances (see Section 1.4). As a result, a variety of different mathematical frameworks have been constructed that treat their included species and abiotic factors as varying over space as well as time. One way of doing this is by modelling the local dynamics of each species involved at multiple locations using the ordinary differential equation approach detailed above, and introducing coupling between equations for the same species in different locations to represent population migration. This approach separates space into discrete habitats, which are known as "patches". A simple implementation of a two-patch model, in which a predator and a prey species can move between two separate areas, is as follows:

$$\begin{aligned} \frac{\mathrm{d}N_1}{\mathrm{d}t} &= \alpha_1 N_1\left(1-\frac{N_1}{K_1}\right) - \beta_1 P_1 \frac{N_1}{s_1+N_1} + m^N_{1,2} N_2 - m^N_{2,1} N_1 \\ \frac{\mathrm{d}P_1}{\mathrm{d}t} &= \gamma_1\beta_1 P_1 \frac{N_1}{s_1+N_1} - \delta_1 P_1 + m^P_{1,2} P_2 - m^P_{2,1} P_1 \\ \frac{\mathrm{d}N_2}{\mathrm{d}t} &= \alpha_2 N_2\left(1-\frac{N_2}{K_2}\right) - \beta_2 P_2 \frac{N_2}{s_2+N_2} + m^N_{2,1} N_1 - m^N_{1,2} N_2 \\ \frac{\mathrm{d}P_2}{\mathrm{d}t} &= \gamma_2\beta_2 P_2 \frac{N_2}{s_2+N_2} - \delta_2 P_2 + m^P_{2,1} P_1 - m^P_{1,2} P_2 \end{aligned} \tag{1.3}$$

Here, $m^N_{i,j}$ represents the migration rate from patch j into patch i for prey, and $m^P_{i,j}$ the same for predators. Due to the wide ranges of many species, this framework can easily be extended to cover more than two patches (see e.g. [172]), up to a finite but arbitrarily

large number. The resulting network of interconnected patches, including the species that inhabit them, is referred to as a "metacommunity"; see Figure 1.2 for a schematic of a 3-patch predator-prey metacommunity. Any increase in number of patches beyond that has the effect of turning space into a continuous variable, changing the system into a reaction-diffusion PDE model (see e.g. [238]).

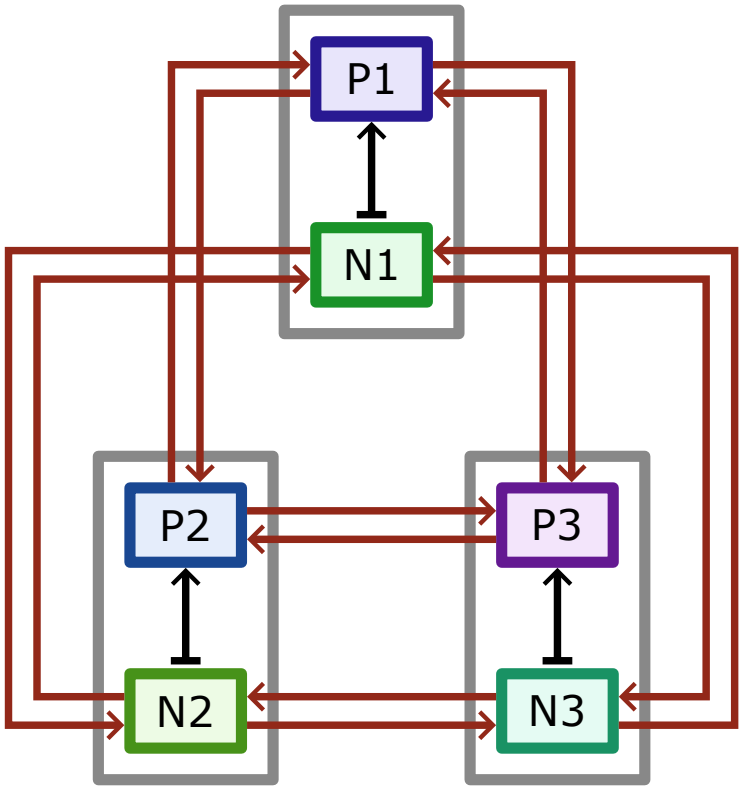

Figure 1.2: Schematic of a model of a predator species and a prey species that are each spread across three patches. Black connectors represent predation; in these connectors, pointed heads denote positive effects (increasing predator abundance due to eating prey) and rectangular heads denote the corresponding negative effects (loss of prey due to predation). Red arrows represent migration between patches.

Note also that environmental conditions may differ from patch to patch, with one of the two patches represented in the model potentially being better suited for prey growth, predator survival, hunting, et cetera. This is reflected in the fact that parameters in a spatial model may vary across patches. For instance, α_1 in the above model denotes the intrinsic prey growth rate in patch 1, while α_2 denotes that rate in patch 2, which need not be identical to α_1. This heterogeneity in environmental conditions can lead to significant

differences in local dynamics if the patches within the model are fairly isolated, although spatially distinct populations can become synchronized if between-patch dispersal is high enough [186]. Within a metacommunity, "source" habitats for a given species are those in which conditions for that species's growth are good enough that the species population can grow to its theoretical maximum and offload surplus members to other patches, while "sink" habitats are less favourable ones in which the species in question would go locally extinct if not for immigration from neighbouring patches [99]. Ultimately, the spatial layout of sources and sinks determines whether a species's habitat is closer to being one contiguous area or many mostly disjoint components (a fragmented habitat). When viewed independently of habitat loss, habitat fragmentation can potentially have both positive and negative effects on biodiversity and species abundances [30, 81, 272], indicating that it is a complex phenomenon with nontrivial consequences. Of course, habitat fragmentation can be carried out by human activities such as urban development [151, 122] and logging [239]. Because of the anthropogenic origin and complex effects of habitat fragmentation, studying it is critical for understanding how ecosystems will evolve under human influence.

1.2 Anthropogenic effects in ecological models

We currently inhabit the Anthropocene, a time when many environmental changes are inextricably linked to human activity. This means that important insights can be gained from including a human aspect in ecological models, whether explicitly or implicitly. A simple example of this is how some ecological quantities, such as the amount of demand for fish to eat, can scale with population size [219]. Consider the following Lotka-Volterra-style predator-prey model featuring two fish species N and P, which are harvested at the respective rates $h_{_N}$ and $h_{_P}$ in addition to deaths due to predation or natural causes:

$$\begin{aligned} \tfrac{\mathrm{d}N}{\mathrm{d}t} &= \alpha N - \beta NP - h_{_N} N \\ \tfrac{\mathrm{d}P}{\mathrm{d}t} &= \gamma\beta NP - \delta P - h_{_P} P \end{aligned} \tag{1.4}$$

Although considering $h_{_N}$ and $h_{_P}$ as constants does make the mathematical analysis of the model easier, greater realism can be achieved by treating them as a function of human population size. (A great deal of ecological systems are far from equilibrium [176, 47], so more complicated models will have additional parameters that also depend on human-related forcing functions.) To illustrate this, let X be the human population of an area adjacent to a reef. Suppose we assume that harvesting rates have a linear dependence on population size, or in other words that the number of fish harvested (and eaten) per person

does not change with the population. Then, we can arrive at the following formulations for the two harvesting rates, for $\hat{h}_{_N}$ and $\hat{h}_{_P}$ their baseline values and k a scaling coefficient:

$$h_{_N} = \hat{h}_{_N} \frac{kX}{X(t=0)}; \quad h_{_P} = \hat{h}_{_P} \frac{kX}{X(t=0)} \tag{1.5}$$

Here, $t = 0$ designates the start of the simulation. In this way, ecological models can be calibrated based on past population data from censuses, e.g [195], and run using future population data from predictions, e.g. [247]. (Relatedly, large-scale interactions between economic strength and ecosystem health themselves have been modelled using Lotka and Volterra's predator-prey model [177], as well as another model of competing species attributed to them [259], indicating that this framework need not be restricted to modelling individual species.)

However, human activity can also affect the health of coral reef ecosystems in much more complex ways. An example is the fact that actions taken by humans involving the sea and its life, such as fishing or marine conservation, are done because human priorities dictate that they must be. If these priorities change, then so will human interactions with the environment, and hence so will the populations of the marine species that humans interact with. Which course of action humans take ultimately rests with a concept called "utility", which is simply the amount of benefit gained by pursuing a given economic or behavioural strategy. Consider the following illustrative example, where a resource-extraction community has two resources available to it, namely ore O and forest F. Hence, two economic strategies dominate in this community, namely mining and logging. Let z be the percentage of economic activity in the community that consists of mining (rather than logging). We can then express the amount of ore available for extraction by describing its decrease using a differential equation:

$$\frac{\mathrm{d}O}{\mathrm{d}t} = -\delta_{_O} z O \tag{1.6}$$

Here, $\delta_{_O}$ is a constant representing how quickly ore is extracted. Note that if all economic activity in the community is composed of logging, then no additional ore will be mined, causing $\frac{\mathrm{d}O}{\mathrm{d}t}$ to equal zero. We can also do the same thing for the amount of forest that is available for use. Ore only regenerates on geological timescales, but forests can regrow (albeit slowly), so the formulation is slightly different. Let F represent the percentage forest cover in the community, on a scale from 0 to 1, and suppose that the managed forest is allowed to spread into previously clear-cut areas. (This may occur due to restrictions preventing logging in such areas in order to avoid overexploitation.) The spread of the forest in this manner can be viewed as an interaction between forested and

unforested land, and therefore the rate of forest expansion depends on both F and $1 - F$. If we denote $\delta_{_F}$ as the rate that forest is removed during logging operations, and r as the rate that it naturally regrows, then we get the following:

$$\frac{\mathrm{d}F}{\mathrm{d}t} = -\delta_{_F}\,(1 - z)\,F + rF\,(1 - F) \tag{1.7}$$

What about z? Clearly, if mining is more profitable than forestry, then most economic agents in the community would want to engage in mining, and vice versa. We can express these preferences as utility functions. If $e_{_O}$ denotes the utility gained from mining and $e_{_F}$ denotes the utility gained from logging, then it would be natural to take $e_{_O} = k_{_O}O$ and $e_{_F} = k_{_F}F$, for $k_{_O}$ and $k_{_F}$ scaling constants representing how profitable the two strategies are. This approach has been used in prior studies such as one that modelled transitions between grasslands and forests that arise because of human economic preferences for agriculture or silviculture [111], and another that used a model of two different fishing strategies (focused on sustainability or individual profit) to generate early warning signals for fish stock collapse [205]. (Note that a community switching economic strategies due to differences in utility is ultimately based on individual-level switches [16], when these switches are viewed in aggregate.) This paradigm of utility tradeoffs has also been used in studies of how the relative priority placed on economic and conservation goals can affect outcomes such as the spread of forest pests [20] and the preservation of both forest and grassland biomes [125].

Since the aforementioned utility functions will necessarily change over time as the availabilities of the two resources do, we could also derive a differential equation to model changes in z, where such changes represent shifts in the percentages of economic activity in the community that mining and logging make up. This will be proportional to the difference between $e_{_O}$ and $e_{_F}$. We can additionally assume that if economic agents see their neighbours using and making money from a particular strategy, they will be more likely to engage in it themselves. This effect can be modelled using techniques from evolutionary game theory [118], namely by scaling the difference between $e_{_O}$ and $e_{_F}$ by a factor of $z\,(1 - z)$ to represent the fact that switching strategies becomes harder if the community is dominated by one or the other. (On a macroeconomic scale, this also corresponds to the fact that the success of a new mining or logging operation may depend on the presence of supporting infrastructure and workers with the right skills, neither of which may be present in a community which is heavily invested in a different economic strategy.) Therefore, our differential equation for z is as follows, for κ a scaling constant governing how quickly economic agents switch strategies:

$$\frac{\mathrm{d}z}{\mathrm{d}t} = \kappa z\,(1-z)\,(k_{_O}O - k_{_F}F) \tag{1.8}$$

Here, we can see that if mining is substantially more profitable than logging, then z will approach 1 (i.e. all economic activity in the community consists of mining), and likewise if logging is more profitable, then z will approach 0.

1.3 Spatial dynamics in marine ecosystems

Spatial dynamics are important to consider when modelling terrestrial ecosystems, but they are downright vital when modelling marine ones. There are many reasons for this, but perhaps the simplest and most intuitive is the nature of ocean currents and the way that they are used by marine organisms. Phytoplankton and zooplankton, the foundations of nearly all marine food webs, drift with the currents for their entire lives (the word "plankton" itself is derived from an Ancient Greek word meaning "wanderer"). Additionally, many species that are immobile as adults spend the early stages of their development in a stage in which they have the same characteristics as plankton. This includes macroalgae [190, 140], which is a large form of algae that is rooted to the seabed and hence resembles underwater grass or shrubbery, as well as coral itself [204, 170, 57]. The amount of time that these species spend being carried about on the currents before they settle and begin the mature phase of their lives is referred to as their "pelagic larval duration", or PLD. Because of the strength of ocean currents, larvae of a species with a PLD of a couple weeks can travel dozens of miles down the coast [251]. This means that the local population dynamics of species such as coral that are commonly thought of as not moving can instead depend on processes occurring in comparatively distant locations.

Outbreaks of crown-of-thorns starfish (CoTS) are an example of a coral reef stressor that is inherently spatially explicit. CoTS larvae, like the larvae of many marine organisms, have the potential to disperse to areas great distances away from where they were originally produced [244]. This means that a typical CoTS outbreak can involve reef areas far apart from one another. For instance, genetic studies on CoTS collected at different locations on the Great Barrier Reef during the most recent outbreak there showed no appreciable genetic differences between CoTS in these areas [107], pointing to significant gene flow among CoTS populations within an area 1000 miles long. Similarly, CoTS populations in areas spread across the Pacific Ocean such as the Great Barrier Reef, Japan, Tahiti and Hawaii have been found to cluster together genetically [273], suggesting that connectivity via larval dispersal is possible between these disparate populations. As CoTS outbreaks

are a regional-scale phenomenon rather than a local-scale one, implementing methods for controlling these outbreaks is a regional-scale task. During an outbreak on the Great Barrier Reef, CoTS are typically not removed from every location where they appear, due to the great time and labour costs of doing so [137]. Instead, a smaller number of locations are focused on, chosen based on criteria such as the potential for CoTS in one area to spread further across the reef and the capability of local coral to recover if CoTS are removed. This means that deciding which parts of a very long reef to actively manage during a CoTS outbreak is effectively an optimization problem.

Figure 1.3: Coral reefs host a wide variety of fish. (Photo: Francesco Ungaro, Pexels)

The larvae of benthic organisms are not the only things on a coral reef that can travel long distances. Reef fish are also highly mobile: telemetry data has shown that reef species can disperse over a kilometer or more of coastline [169]. This has implications both for conservation of coral ecosystems and for the maintenance of reef fisheries, which provide food for many of the human inhabitants of reef-adjacent areas. Marine protected areas (MPAs), which often have strict restrictions on how much fishing, if any, is allowed within their boundaries, have been set up around the world in order to protect the populations of reef fish and other marine species [155]. Depending on the dispersal ability of reef fish and how they are affected by habitat fragmentation, it may be just as useful to maintain a network of small but interconnected MPAs as it is to maintain a large but comparatively

isolated one [228]. Additionally, improved yield in reef fisheries that are outside of but adjacent to an MPA has been observed [213]. This is an example of source and sink populations in the real world: areas that could be overfished under normal circumstances instead can have relatively stable fish populations (and therefore stable fish catch levels) due to receiving fish that disperse out of nearby MPAs, which is known as the "spillover effect" (see e.g. [43, 69]).

The dynamics of coral ecosystems can also be driven by processes outside of the ocean entirely. Much of the sediment that is deposited onto reefs originates from soil that is eroded during rainfall events and carried by rivers to the sea [21]. A certain degree of sedimentation is natural, and turbid waters do occur near the mouths of rivers whose catchments have little human disturbance [11]. However, sedimentation can be exacerbated by forest clearance: removing trees from an area means that the soil in that area is no longer held firmly in place by the trees' roots, an effect that is magnified on mountain slopes and other areas with steep gradients [108, 278]. The result of this is that important reef processes such as algal photosynthesis and herbivorous fish feeding can be affected by human activities many miles inland.

1.4 Mathematical coral reef models

Due to the necessity of devising strategies for protecting coral reefs against the numerous threats that they face, as well as the difficulty of conducting field experiments on very large spatial scales, mathematical models of coral reefs have recently been developed to provide additional insights on their dynamics. For instance, many coral reefs throughout the world have seen shifts towards algae rather than coral dominating most available space [168]. Ecologists have debated whether this was the result of the reefs in question passing a tipping point between two basins of attraction (one representing coral dominance and the other representing algal dominance) or instead being a simpler state shift without bistability, with evidence from the field on both sides [72, 182, 218]. A mathematical approach was first utilized in a 2007 seminal paper by Mumby *et al.*, which demonstrated the possibility of bistability in a model of a coral reef under biologically realistic parameter regimes [181]. The Mumby model is a low-dimensional dynamical system that tracks the proportions of a seabed area that are covered by coral (C), macroalgae (M), and turf algae (T), and is reproduced below:

$$\begin{aligned} \tfrac{\mathrm{d}M}{\mathrm{d}t} &= aMC - \tfrac{gM}{M+T} + \gamma MT \\ \tfrac{\mathrm{d}C}{\mathrm{d}t} &= rTC - dC - aMC \\ T &= 1 - M - C \end{aligned} \tag{1.9}$$

In this model, macroalgae overgrow coral at a rate a and algal turf at a rate γ, while coral overgrow algal turf at a rate r. Coral die at a rate d, and algal turf is assumed to colonize the newly available area due to its rapid population dynamics. Grazers such as herbivorous fish and sea urchins eat both macroalgae and algal turf at a rate g. When macroalgae is consumed in this way, the empty space is colonized by algal turf, expressed as the term $\frac{gM}{M+T}$ because grazers are assumed to consume both kinds of algae in the proportions that they are available. (The equivalent term for the grazing of algal turf, $\frac{gT}{M+T}$, is omitted in this model because turf is assumed to instantly regrow into areas where it has been grazed.) Due to its nonlinearity, this grazing term proved to be the key to finding bistability, leading to the conclusion that reduction in herbivorous fish populations (potentially due to overfishing) can induce a dramatic shift to a seabed covered by macroalgae. Later mathematical modelling work continued to shed light on if and when bistability in coral reef ecosystems was possible. In 2011, Fung *et al.* developed an expanded state-transition model similar to the one above, but with algal turf represented as its own compartment and explicit mechanistic terms for the reproduction and spatial expansion of coral and algae [89]. Using this model, they performed a search of the model's parameter space for values that produced multiple stable states. They found that discontinuous phase shifts between bistable equilibria could happen, particularly for reefs under significant anthropogenic stress, but also that parameter regimes featuring alternative stable states were more common near the extremes of the parameters' empirical ranges. Follow-up work by Arias-Gonzalez *et al.* using the same model demonstated the possibility of phase shifts from coral to algal dominance through nutrient input or sedimentation instead of fishing pressure increases [17], underlining the complexity present on coral reefs.

The state-transition models described above represent local dynamics: the one used by Fung *et al.* is accurate for lengths of coastline on the order of 10^1 to 10^3 metres [89]. However, fundamental reef processes such as fish migration, coral larval dispersal, and the cycling of nutrients such as nitrogen and phosphorus take place over larger scales still. In 2016, Spiecker *et al.* built a integro-differential reef model to examine how trophic cascades (i.e. fluctuations in the population level of one species due to fluctuations in its predators or prey) are affected by these long-range reef processes [228]. Within this model, the reproduction of coral and macroalgae is governed by explicitly nonlocal functions. Specifically, in any given location x on the coastline, the growth rate of coral or macroalgae in x is equal to the integral over all locations y of the number of coral larvae or macroalgae propagules produced at point y times the probability that a larva or propagule created at y will eventually settle onto the seabed at x. The findings by Spiecker *et al.* include that a network of small but interconnected MPAs (with a substantial spillover effect) causes trophic cascades inside and outside MPAs to become more similar to each other, showing how the large degree of connectivity that is possible in marine ecosystems can lead to the

convergence of dynamics in ostensibly heterogeneous local areas.

With time, the importance of mathematical models as tools for coral reef conservation and planning has grown significantly, as evidenced by the number of different problems facing coral reefs that they have been applied to. For example, a recent review of the literature on CoTS has called on mathematical modellers to perform simulations of CoTS dynamics over large spatial scales [196]. Additionally, the paradigm of models of intermediate complexity for ecosystem assessments (MICE) has gained traction recently [106, 175], as a way to create testable theory in the domain of marine ecology and coral reef management. This approach avoids the issues with overfitting that come with larger models, and hence MICE can produce results that can be applied to broad ecological scenarios. In addition to the greater focus on modelling, mathematical concepts such as the aforementioned bistability and regime shifts, as well as transient versus asymptotic ecosystem behaviour [47] and optimization approaches to conservation [228, 87] and fisheries management [136, 201] have become widespread in the literature, which opens the door for further analysis of problems faced by coral reefs using mathematical tools. In this thesis, three such problems are addressed by building models within the MICE framework and using their results both to inform theory and to provide concrete recommendations for ecosystem management.

1.5 Thesis outline

The remainder of this thesis is organized as follows. In Chapter 2, we use a coupled social-ecological metacommunity model to examine the transient effects on coral of economic transitions in reefside communities from fishing to tourism, as well as how coral and herbivorous fish populations respond to habitat fragmentation driven by overfishing. This work represents the first time that the timeframe and spatial scope of coral recovery induced by economic shifts has been modelled, and we believe that the results contained therein will also prove useful for the design of marine protected areas. This chapter has been published in the Bulletin of Mathematical Biology [171].

In Chapter 3, we use a similar spatially explicit reef model, featuring crown-of-thorns starfish (CoTS), to model CoTS outbreaks off the coasts of two large, growing cities with offshore coral reefs within the range of CoTS. We also determine levels of fishing pressure and nutrient loading that are likely to cause qualitative changes on reefs with CoTS outbreaks. Additionally, we devise four different strategies for local CoTS removal to address outbreaks, and determine the effectiveness of each of these strategies in our focus cities. This represents the first time that future CoTS outbreaks have been simulated in, and CoTS management strategies have been tailored to, areas outside the Great Barrier Reef.

This chapter will be submitted to Ecological Modelling.

In Chapter 4, we construct a model that couples seabed interactions between coral and algae, trophic interactions between fish, and sedimentation driven by deforestation. We use this model to determine how quickly deforestation can cause different fish functional groups to decline, simulating over a wide range of possible local terrain and hydrodynamic characteristics. We also evaluate the extent to which flexible harvesting strategies can stabilize these declining fish populations, as well as how robust reef fisheries yield is to deforestation-related stress. Within this chapter, we have built the first dynamical system model linking forest and reef processes, and hence performed the first explicitly time-dependent analysis of how deforestation will affect reef fish populations and the harvesting thereof. This paper is being prepared for submission.

Finally, in Chapter 5, we summarize our results and discuss the broader themes evident in our work. We also suggest further avenues of research that utilize spatial models to answer questions in marine ecology.

Chapter 2

Local overfishing patterns have regional effects on health of coral, and economic transitions can promote its recovery

This chapter is based on the paper: RA Milne, CT Bauch, M Anand. 2022. Local overfishing patterns have regional effects on health of coral, and economic transitions can promote its recovery. Bulletin of Mathematical Biology, 84: 46. DOI: 10.1007/s11538-022-01000-y

2.1 Abstract

Overfishing has the potential to severely disrupt coral reef ecosystems worldwide, while harvesting at more sustainable levels instead can boost fish yield without damaging reefs. The dispersal abilities of reef species mean that coral reefs form highly connected environments, and the viability of reef fish populations depends on spatially explicit processes such as the spillover effect and unauthorized harvesting inside marine protected areas. However, much of the literature on coral conservation and management has only examined overfishing on a local scale, without considering how different spatial patterns of fishing levels can affect reef health both locally and regionally. Here, we simulate a coupled human-environment model to determine how coral and herbivorous reef fish respond to overfishing across multiple spatial scales. We find that coral and reef fish react in opposite ways to habitat fragmentation driven by overfishing, and that a potential spillover effect from marine protected areas into overfished patches helps coral populations far less than it does reef fish. We also show that ongoing economic transitions from fishing to tourism have the potential to revive fish and coral populations over a relatively short timescale, and that large-scale reef recovery is possible even if these transitions only occur locally. Our results show the importance of considering spatial dynamics in marine conservation efforts, and demonstrate the ability of economic factors to cause regime shifts in human-environment systems.

2.2 Code availability

The code for simulating the model is available on Zenodo (DOI: 10.5281/zenodo.5534958).

2.3 Introduction

Coral reefs are home to very high levels of biodiversity [23, 252, 25], and provide vital services to humans such as harvesting of reef fish and ecotourism [59]. Overfishing has long been known to be a major stressor of reefs [207, 167, 162], due to its ability to shift areas from a coral-dominated to a macroalgae-dominated state [167, 27]. Such shifts, when considered on a regional scale, can disrupt connectivity on a reef and give rise to fragmented rather than connected habitats. This has been shown to alter the composition of species present [45, 30], although the overall effects of fragmentation are ambiguous [272]. Additionally, as the economies of reefside communities transition from being based

on fishing to tourism, areas that were previously overfished may see a regime shift in the opposite direction, back to coral dominance. However, the speed of such a shift, as well as whether one can happen regionally due to local-scale economic transitions, is yet to be seen. Here, we use a spatially explicit coral reef model using a coupled human-environment framework to investigate these multi-scale processes, and to determine their implications for the future viability of both coral reefs and the communities that depend on them.

Overfishing of reef fish has been cited as one of the most prominent threats to the livelihood of coral reefs (e.g. [207, 167, 162]). This is due to the fact that many commercially valuable species of reef fish, and especially parrotfish, are predators of macroalgae [157, 83], which can overgrow coral and outcompete it for available space. Fishing pressure on heavily-harvested coral reefs in the Pacific has been estimated at or above 50 percent of organisms from many different commercially viable species per year [184, 147]. Many of the species surveyed were being fished above levels predicted to be sustainable, including half of all parrotfish species in Hawaii [184], and harvesting rates in general were often far above the rates associated with a shift to a macroalgae-dominated state according to past modelling results [27, 28]. Further complicating matters is the fact that other coral reef stressors, such as nutrient loading, have interacting effects with overfishing that increase the propensity of an overfished system for a regime shift even further [274, 17].

While overfishing is known to have deleterious effects on coral reefs, including causing regime shifts, fishing can safely be performed at lower rates without these risks. Harvesting rates associated with small-scale subsistence fishing, which have previously been estimated at one tenth of commercial rates [63], have been found to be between one seventh and one third of the estimated upper limits for sustainability of coral populations [142]. Many communities situated adjacent to coral reefs are in the process of transitioning from economies based around commercial fishing to those more heavily based around tourism, including those in the Pacific [26, 78] and the Caribbean [26, 68]. After this transition, fishing operations would typically be on a smaller scale; the wide gap between commercial and subsistence fishing rates suggests the possibility that these economic transitions could drive regime shifts. In particular, this raises the question of how quickly a reef that has previously been under very high fishing pressure can recover following such an economic transition. In addition to this, as commercial fishing is an important industry both in terms of how much revenue it generates [59, 97, 189] and how many people depend on it for food [167, 97], it is necessary to balance the needs of the fishing and tourism industries as well as the coral reef itself. Ideally, a reefside community should have a healthy reef as well as sustainable fishing and tourism industries; therefore, finding conditions for the coexistence of these is imperative.

In addition to featuring a wide array of trophic interactions such as the linkages that

cause coral to be harmed by overfishing, coral reef ecosystems are also very complex spatially. Part of this is due to their sheer size. The Great Barrier Reef is the largest marine protected area in the world [165], and the Caribbean Sea similarly features a large network of reefs offshore of various islands. Reefs within a given region are also incredibly heterogeneous in their internal composition, with sites dominated by coral, macroalgae, and algal turf all being present [279]. Similarly, different reefs, and different areas of a reef, are highly connected due to the dispersal of coral larvae [233, 243], fish [3, 15, 24] and nutrients, and these dispersal processes themselves have different effects across different spatial scales [243]. Therefore, damaging one part of a reef also should have farther-reaching effects on areas that it is connected to. However, most modelling of overfishing and other coral reef stressors has been done strictly at local scales (see review in [29]). Because of this, an increased focus on multi-scale effects of overfishing has the potential to uncover many new insights.

Owing to coral reefs' size and complexity, concepts pertaining to nonlocal processes are often seen in field and theoretical literature related to reefs. For instance, previous models considering connectivity between coral reef habitats implicitly [75] and explicitly [228] have emphasized the importance of the spillover effect, where dispersal of coral larvae or fish from relatively undisturbed reefs into adjacent fished areas can help counteract the degradation caused by overfishing. A potential counteracting effect is large-scale and commercial harvesting in areas that are nominally protected, as seen with many species associated with coral reefs [46, 129, 126]. Fishing boats routinely travel sizable distances away from their home ports [77, 44], and outside fishers often employ overly damaging fishing techniques against marine protected area (MPA) regulations [46]. Hence, an MPA without enforced boundaries is liable to have substantial fishing pressure from adjacent areas outside it. In light of this, it is important to understand how processes such as nonlocal fishing pressure and the spillover effect can interact to affect reef health over broader spatial scales.

Echoing the spatial heterogeneity present in coral reef ecosystems, the debate over the best conservation strategy for coral is also spatial in nature. Habitat connectivity has been cited as important for the design of marine protected areas (MPAs) on coral reefs [14, 34, 233], as it also has with other types of marine ecosystems [146], and its prominence in the literature has been steadily increasing over time [19]. However, the debate over the importance of connectivity is not closed, as it rests on the distances that the species being protected can disperse. This is also related to the spillover effect. Reef species that are capable of long-range dispersal will have stronger spillover effects, so populations in MPAs that are geographically far apart will be able to reinforce one another. In contrast, the spillover effect will be weaker when considering species with less capability to disperse, so

MPA connectivity is a more important consideration for the conservation of these species. One recent paper concluded that the dispersal abilities of Caribbean reef fish are insufficient to traverse the gaps between current MPAs [24], whereas other work has found that marine species disperse over such great distances that the importance of connectivity in designing MPAs is minimal [60]. Because of these discrepancies in the literature, and given the importance of establishing sound conservation strategies for coral reefs, more research on the optimal configuration of MPAs is needed.

Analogous to the debate over connectivity of MPAs is that over the relative threats posed by habitat loss and habitat fragmentation. Again, this is underpinned by the dispersal abilities of the species that would be protected. Although habitat fragmentation is a great concern in terrestrial ecosystems, marine species generally have greater dispersal ability and are therefore affected less by it. Fragmentation has been shown to have highly variable effects on the functioning of coral reefs and other marine ecosystems [272], including on abundance and biodiversity of reef fish [30], and the effects of habitat fragmentation via degradation due to overfishing may also be countered by mechanisms such as the spillover effect. Recent calls have been made for more research on the variety of responses that marine communities have to fragmentation, especially research that integrates dynamics over both local and regional scales [272]. Hence, it is necessary to build a robust, multi-scale theory around how important connectivity and fragmentation are for the viability of the many species that inhabit coral reefs.

In this paper, we use a coupled human-environment model to determine the effects of overfishing on coral reefs across both local and regional scales, and provide policy solutions for managing overfished reefs. We identify how economic transitions can lead to regime shifts from macroalgae to coral dominance, and show that these transitions, when occurring locally, can promote both healthy reefs and a sustainable economy with fishing and tourism both being viable. We test the ability of coastal communities to stop coral decline via temporarily subsidizing the tourism industry, and find that such short-term subsidies can drive long-term coral recovery. We contrast the spatial effects of fish and coral dispersal with those of nonlocal harvesting inside MPAs, and show the importance of strict enforcement of MPA boundaries. We also determine that coral and herbivorous fish have very different responses to habitat fragmentation, with the implication that MPA design needs to take into account divergent needs of multiple species.

2.4 Methods

2.4.1 Model formulation

To simulate the dynamics of a coral reef, we adapted a model of Spiecker et al. [228] featuring herbivorous fish, coral, macroalgae, nutrients and detritus. We chose this model because it is mechanistic and based around recruitment and mortality rates (as opposed to state transition models, e.g. [181]), which is important as the regional-scale dynamics we investigate strongly involve processes like the production and dispersal of coral larvae. In [228], an integro-differential system is used to capture the dynamics in many different areas of a reef habitat, with nonlocal processes such as organismal dispersal being spatially continuous. Since our aim was to capture the effects of overfishing within specified areas rather than at individual points, we converted this system into a metacommunity version by simulating a linear network of patches along a coastline, interconnected via dispersal of the model's components. We kept the assumption made in [228] that dispersal from one patch to another would follow a Gaussian pattern, declining with increasing distance between the two patches in question. In order to perform an in-depth examination of overfishing, especially as it relates to economic transitions between fishing-based and tourism-based economies, we added a novel differential equation to the model representing the proportion of economic activity in each patch related to tourism (rather than fishing), with change over time driven by the relative economic utility gained from these strategies. We also introduced a dynamic fish harvesting rate that depends on economic strategies in each patch and incorporates harvesting by fishing boats outside their local patch. The biological components of our human-environment model are below, for i the index of a given patch:

$$\begin{aligned}
\tfrac{dH_i}{dt} &= \tfrac{r_{H_i} M_i}{k_{H_i}+M_i} H_i - m_{H_i} H_i - \xi_i H_i + g_{H_i} \\
\tfrac{dC_i}{dt} &= (1 - M_i - C_i)\, g_{C_i} - m_{C_i} C_i \\
\tfrac{dM_i}{dt} &= (1 - M_i - C_i)\, g_{M_i} - m_{M_i} M_i - \tfrac{r_{H_i} M_i}{k_{H_i}+M_i} H_i \\
\tfrac{dD_i}{dt} &= m_{H_i} H_i + m_{C_i} C_i + m_{M_i} M_i - \gamma_i D_i + g_{D_i} \\
\tfrac{dN_i}{dt} &= q_i - e_i N_i + f_i \gamma_i D_i - \left(\tfrac{r_{M_i} N_i}{k_{M_i}+N_i} \right) M_i + g_{N_i}
\end{aligned} \tag{2.1}$$

Within the model, there are five biological components. Each one represents a certain functional group or abiotic factor rather than focusing on individual species, an approach also used in e.g. [181, 18]. These are herbivorous fish H, coral C, macroalgae M, detritus D and nutrients N. Coral and macroalgae compete for space offshore, and therefore their total abundance is restricted in the model, i.e. $M + C \leq 1$. Any space not colonized by coral or macroalgae is assumed to be covered by algal turf or bare rock. The herbivorous

fish population has been normalized to be on the same scale as coral and macroalgae, and hence is expressed in terms of its density over an arbitrary area. (Scaling constants with units of area^{-1} are therefore omitted due to being equal to 1).

In the model, herbivorous fish are assumed to eat macroalgae using a Holling Type II functional response, represented as a mathematically equivalent Hill function with maximum growth rate r_H, half-saturation constant k_H, and Hill coefficient 1. The fish reproduce at the rate at which they eat macroalgae, die of natural causes at a rate m_H, and are harvested at a variable rate (detailed below). Coral and macroalgae reproduce via the dispersal of larvae and propagules [75], so their growth rate is nonlocal; these dynamics are explained below. Coral die of natural causes at a rate m_C, while macroalgae die of natural causes at a rate m_M and are eaten by fish as detailed above. Detritus is formed by organisms that die of natural causes at one-to-one rates, and decays into nutrients at a rate γ. Nutrients are formed from detritus at the same rate, scaled by a conversion constant f, and are uptaken by macroalgae as mentioned above. Nutrients also enter the system via inorganic processes (e.g. river outflows) at a rate q and leave it (e.g. by ocean currents) according to the linear term $e \times N$. These processes can be seen in a schematic of the local dynamics of the model (Fig. 2.1).

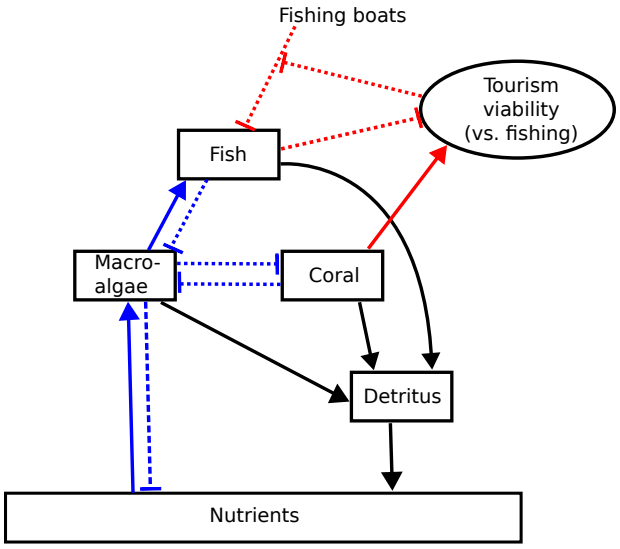

Figure 2.1: Schematic showing local interactions between model components. Red lines represent economic interactions, blue ones represent trophic and competitive ones, and black ones represent cycling of materials. Solid lines denote positive feedback, while dashed lines denote negative feedback.

The functions in the model representing dispersal between patches are below. For coral

and macroalgae, these are part of their growth rates, whereas for the other components these are mathematically equivalent to passive dispersal.

$$\begin{aligned} g_{M_i}(t) &= \sum_j \left(\frac{N_j}{k_{M_j}+N_j}\right) r_{M_j} M_j \theta_{M_j}(i) \\ g_{C_i}(t) &= \sum_j r_{C_j} C_j \theta_{C_j}(i) \\ g_I(t) &= -I_i(t) + \sum_j I_j \theta_{I_j}(i), \; I \in \{H, D, N\} \end{aligned} \tag{2.2}$$

Coral larvae are created in each patch at a rate r_C. This is constant in [228], but we took it to vary temporally, since coral reproduction events happen at specific times during the year [235] and to allow for a mechanism for macroalgae to overgrow coral during the majority of the year. Macroalgae propagules are created in each patch at a rate depending on the available nutrients, which is governed by a saturation function with maximum growth rate r_M and half-saturation constant k_M. At each time step, the new coral larvae and macroalgae propagules are distributed among patches according to their distances from whichever patch the larvae and propagules originated in. Dispersal of new larvae and propagules out of each patch is governed by a Gaussian dispersal kernel centred on that patch that has been discretized (see e.g. [150]), and the intrinsic growth rate for coral or macroalgae in one patch is the sum of the larvae or propagules created anywhere that disperse into that patch. This rate is scaled down by the factor $(1 - M - C)$ for both, to represent their shared carrying capacity.

In addition to their local dynamics, fish, detritus and nutrients are assumed to undergo passive dispersal between patches. The dispersal rates for these are governed by Gaussian dispersal kernels in the same way as coral and macroalgae reproduction are. Adult coral and macroalgae are assumed not to move. The standard deviations of these dispersal kernels biologically represent the ability of fish, coral larvae and macroalgae propagules to disperse outside of their home patches, with smaller values meaning more local retention. We chose baseline values of the standard deviations of each kernel to be 1, indicating relatively large dispersal ability. The standard deviations for detritus and nutrients are the same as those for fish, coral larvae and macroalgae propagules since dispersal by the latter groups is dependent on physical factors such as tides and ocean currents, which also drive dispersal by the former groups.

We complemented the biological components of the model by adding a state variable z encompassing local economic strategies, in a format similar to that used previously for quantifying support for conservation [242]. The differential equation governing z is below, for i the patch index:

$$\frac{dz_i}{dt} = (1 - z_i)\,\kappa_i z_i\,(c_{z_i} + k_T C_i - k_F h_{H_i} H_i) \tag{2.3}$$

When formulating z, we considered two economic strategies, namely fishing and ecotourism, and let z_i be the proportion of economic agents in patch i engaging in ecotourism. In our model, z changes according to the relative utility of both strategies. z increases when a large amount of coral is present (and hence ecotourism is more profitable), and it decreases when large quantities of fish are available to be harvested (measured by the quantity $h_{H_i} H_i$, where h_{H_i} is the commercial fishing rate in patch i). We use the parameters k_T and k_F to scale how strongly support levels for tourism and fishing, respectively, depend on the underlying biological conditions, and we define c_z as the degree to which one strategy is more profitable than the other due to external factors. Additionally, z changes due to social pressure using the replicator dynamics found in [242], under the assumption that economic agents in a patch will be more likely to use a particular strategy if their neighbours are also using (and profiting from) it. We take κ to be the base rate at which economic agents can switch their strategies.

z is coupled back into the model via the dynamic fishing rate, as only economic agents engaging in fishing are assumed to fish at the higher commercial rate. This can be seen in the local schematic (Fig. 2.1). This dynamic fishing rate is as follows, for i the patch index:

$$\xi_i(t) = \sum_j \left(h_{H_j} (1 - z_j)\,\theta_{B_j}(i) + \tilde{h}_{H_j} z_j \theta_{B_j}(i) \right) \tag{2.4}$$

In each patch, the dynamic fishing rate is set to be the weighted average of two different rates: h_H, the commercial rate, and $\tilde{h}_H$, a background subsistence rate. This is due to the assumption that any economic agents engaging in fishing (i.e. $1 - z$) would harvest according to the commercial rate, and that the dynamic fishing rate in any given patch would approach the subsistence rate if economic activity in that patch approached 100 percent tourism. A Gaussian dispersal kernel is used to quantify the amount of time that fishing boats from any given patch spend in each patch in the system (including their own), and hence the nonlocal fishing pressure in each patch; this is denoted σ_B.

2.4.2 Model parametrization

To obtain the kinetic rates for herbivorous fish growth, we surveyed the doubling times of all parrotfish species in FishBase [88], the same method as that used in previous modelling

papers (e.g. [28, 242]). We took $r_H = 0.7$ yr^{-1} and $k_H = 0.5$, since the majority of species were categorized as having doubling times less than 15 months and nearly all of the rest were in the category of having doubling times of 1.4 to 4.4 years. Our values produce a reproduction rate similar to the linear rates used in previous work [28, 242] when macroalgae cover is at its maximum of $M = 1$. Coral reproduction rate for different species has been estimated at annual doubling [2], an average of 5.7 larvae per colony per year [216], and ten eggs per polyp in a yearly spawning session [113]. We took $r_C = 5$ yr^{-1}, a value in the middle of this range. Macroalgae are known to grow very quickly, and tenfold yearly growth under optimal conditions has been reported [211]. Spiecker *et al.* deemed a value of 15 yr^{-1} for macroalgae growth rate to be biologically plausible, and their sensitivity analysis found most state variables to be minimally responsive to changes in it, so we took r_M to be the slightly lesser value of 12 yr^{-1}. We kept the value of $m_C = 0.44$ yr^{-1} from previous studies [242], and used the low natural mortality rate of 0.1 yr^{-1} for herbivorous fish and macroalgae.

When considering nutrient dynamics on coral reefs, we looked specifically at nitrogen. This was done because macroalgae and other primary producers on pristine coral reefs have shown N-limitation, but those closer to developed areas are often saturated with nitrogen due to anthropogenic input and therefore are P-limited instead [144, 86, 143]. Coral reefs have high rates of nutrient exchange with the surrounding oceanic water [153] and short residence times [188], so we took e to be a high rate of 0.6 yr^{-1}. Nutrient input into coral reefs and other marine ecosystems has been estimated as on the order of 100 to 1000 kg N km^{-2} yr^{-1} in most areas [254, 165], with higher values for areas of dense human settlement, or equivalently between 0.3 and 10 kmol N km^{-2} yr^{-1} per capita depending on the flow rates of local rivers [225]. Nitrogen concentration of water entering wetlands adjacent to the Great Barrier Reef has been measured at 200 μg N L^{-1} under flood conditions [6]. We therefore considered values of q ranging from 20 to 120 kmol N yr^{-1}, representing the total amount of nitrogen exported into a patch of approximately 1 km^2 with low to intermediate population density (i.e. areas most likely to contain pristine reefs). We took γ to be 1 yr^{-1} under the assumption that all detritus would decompose within a year [76, 54], and used a value of 20 kmol N for f as nutrient input from detritus decomposition was expected to be an order of magnitude less than input from external loading [256]. We used a half-saturation constant for nutrient uptake by macroalgae (k_M) of 80 kmol N yr^{-1}, close to the median of the values reported in previous studies [194, 159] after adjusting units to make k_M on the same scale as N. This choice also meant that nitrogen availability was close to saturation at the upper ranges of q that we tested, as expected.

We used a baseline of 0.5 yr^{-1} for the commercial fishing rate h_H; this value has been used in prior human-environment modelling work on coral reefs [242] and is consistent with

available data for reef fish harvesting [184, 147]. We took the subsistence fishing rate $\tilde{h}_H$ to be 0.05 yr^{-1}, one tenth of the baseline commercial rate [63]. Unless we were simulating economic transitions or the effects of tourism subsidies (see below), we took c_z to be zero, indicating no external economic pressure in favour of fishing or tourism. We fit the other social parameters (κ, k_T, k_F) by simulating the system for different orders of magnitude of these parameters, and choosing values for which z converged to equilibrium at 0 or 1 after a plausible length of time following a shock. We ultimately took $\kappa = k_T = k_F = 1$.

2.4.3 Numerical methods

To perform the simulations mentioned below, we integrated our model using MATLAB's ODE45 function. This was done as our system is nonstiff, as the maximal rate of change within the system is less than that in the model of Spiecker et al. [228], which was integrated using ODE45.

In order to investigate local dynamics and check when regime shifts are expected to take place, we simulated a one-patch version of the model while varying harvesting rate (h_H) and nutrient loading rate (q). This allowed us to determine how the ability of overfishing to push coral reefs into a macroalgae-dominant regime is mediated by nutrient loading. For each run of the model, i.e. for each deterministic pair of values (h_H, q), we determined the post-transient average values of coral and macroalgae cover, as well as herbivorous fish abundance. We defined different regimes as discrete regions of parameter space (harvesting rate vs. nutrient loading rate) with qualitatively similar dynamics. We did not encounter bistability for any parameter values within the ranges specified above, similarly to how bistability was found to be rare in another coral model with comparable complexity [89]. We tested this by simulating the model from initial conditions between 0 to 1 (aside from the two boundary cases) for coral, macroalgae and economic strategy, and ranging from just above 0 to double the highest observed values in our initial simulations (i.e. those in Figure 2.2) for the other variables. Therefore, each regime corresponds to one specific set of long-term model behaviour.

To evaluate whether overfishing-driven habitat loss or fragmentation is more detrimental to coral and herbivorous fish, we simulated a network of 25 patches in which a fixed number of patches were heavily overfished ($h_H = 0.8$) and the rest were fished at subsistence levels ($h_H = 0.05$). We varied both the number of overfished patches (to test the effects of habitat loss) and their configuration (to test the effects of habitat fragmentation). Configurations that we used included one where all overfished patches formed a contiguous area in the middle of the simulated landscape, with large contiguous areas of non-overfished patches on either side, and several where overfished and non-overfished patches alternated

Parameter	Value	Units	Description
r_H	0.7	yr^{-1}	Herbivorous fish maximum intrinsic growth rate
k_H	0.5	unitless	Half-saturation constant for herbivorous fish growth
m_H	0.1	yr^{-1}	Mortality rate for herbivorous fish from natural causes (i.e. non-harvesting)
h_H	$0.05 - 0.5 - 0.8$	yr^{-1}	Commercial fish harvesting rate
$\tilde{h}_H$	0.05	yr^{-1}	Subsistence fish harvesting rate
r_C	5	yr^{-1}	Coral intrinsic growth rate
m_C	0.44	yr^{-1}	Coral mortality rate
r_M	12	yr^{-1}	Macroalgae intrinsic growth rate
k_M	80	kmol N	Half-saturation constant for macroalgae growth
m_M	0.1	yr^{-1}	Macroalgae mortality rate
γ	1	yr^{-1}	Detritus decomposition rate
q	$20 - 60 - 120$	kmol N yr^{-1}	Nitrogen loading rate
e	0.6	yr^{-1}	Nitrogen flushing rate
f	20	kmol N	Scaling constant for conversion of detritus into nutrients
κ	1	yr^{-1}	Rate at which economic agents can switch strategies
c_z	$0 - 0 - 5$	unitless	Economic utility for tourism (as compared to fishing) from external sources
k_T	1	unitless	Scaling constant for how strongly tourism utility varies due to coral cover
k_F	1	yr	Scaling constant for how strongly fishing utility varies due to fish catch

Table 2.1: Parameters, their units, and their associated values in Chapter 2

in a repeating pattern. Each of these patterns involved taking specifying a certain number of patches to be overfished and taking the rest to be non-overfished, and spacing groups of overfished patches evenly throughout the system (where each group consisted of a fixed number of patches). For each run of the model, we took the average post-transient values of coral cover and herbivorous fish abundance across the landscape as a whole, in overfished patches and in non-overfished patches. This allowed us to easily separate the local and regional effects in each scenario. We also took different values of σ_B to control for the effects of nonlocal harvesting, using values of 0.25 (for a system in which fishing is almost entirely done locally) and 1 (for a system in which substantial amounts of harvesting takes place outside of fishing boats' local patches).

To determine the relative effects of the spillover effect and fishing across MPA boundaries, we determined the long-term average values (at equilibrium or over one periodic orbit) of herbivorous fish and coral in a 25-patch system while varying their dispersal abilities (σ_H and σ_C) and the amount of time fishing boats spend locally (represented by the mean value of the discretized Gaussian distribution generated by σ_B). In the simulated system, approximately half of the patches (13 of 25) were overfished ($h_H = 0.5$) and the rest were fished at subsistence rates. The overfished patches were either located in a contiguous stretch in the middle of the simulated area (the "contiguous case") or alternating one-to-one with non-overfished patches (the "fragmented case").

To determine the long-term effects of economic transitions between a fishing-based economy and a tourism-based one, as well as check conditions for the coexistence of fishing and tourism, we ran simulations that treated c_z as a time-dependent function, rather than its static baseline value of zero. We ran different simulations to represent long-term economic trends and temporary subsidization of the tourism industry. For long-term trends, we made c_z increase linearly from 0 to a maximum value of 5 over a span of five years. For short-term subsidization, c_z was initialized at a positive constant value (taken to be integer values from 1 to 5), held there until a time $\tilde{t}$ (taken to be integer values from 1 to 15), and then reset to 0. As above, we used a 25-patch system. In the long-term trend scenario, we altered c_z in a varying number of connected patches (1 to 25) in the middle of the simulated area to test the effects of both local and regional economic shifts.

In both long-term and short-term scenarios, we initialized the system using initial conditions representative of the macroalgae-only regime, and determined the amount of time taken before the overfished patches shifted back to a coral-dominated state (defined as over 50 percent coral cover) and healthy fish population levels (fish density of 1). These values were chosen to represent typical average coral and fish levels in the coral-dominated regime (see Results section), and to be high enough that the systemwide average attaining these levels would indicate a regional-scale recovery. We also checked the long-term average

coral cover in these systems, to test whether recovery was temporary or permanent. The initial conditions that we used in overfished patches were 90-99 percent macroalgae cover with the rest of the seabed covered by coral, fish density equal to the amount of coral cover, fishing being 99 percent of the economic activity, and detritus and nutrients being at their average steady-state levels reached under these conditions. We also took h_H as the constant value of 0.5 in each patch to preclude the possibility of natural recovery.

2.5 Results

2.5.1 Local dynamics and regime shifts

We found three distinct regimes that the system's local dynamics can take (Fig. 2.2). The first of these featured cyclical dynamics, with coral dominant most of the time and macroalgae always present. In this regime, tourism eventually composed all economic activity (Fig. 2.3), as z rose and fell depending on the relative abundances of coral and fish but was always higher at the end of a cycle than at its beginning. Due to the lack of fishing pressure, the herbivorous fish and macroalgae populations followed oscillatory boom-bust patterns similar to those found in the Rosenzweig-MacArthur model. The second regime featured stable, nonzero levels of coral, macroalgae and herbivorous fish. Here, macroalgae was dominant over coral, with coral cover of the seabed typically above 10 percent but below 30 percent. Economic activity converged to a state where only fishing was viable, although very long transients were possible depending on the social parameters (Fig. 2.3). However, fish populations were higher in this regime than they were in the cyclical coral-dominant regime. The third regime was characterized by local extinction of both coral and herbivorous fish, with macroalgae taking up all available space on the seabed. Economic activity tended towards the all-fishing equilibrium while there were still fish available to catch. However, after a certain point in time, changes in economic behaviour became minimal as coral and fish populations were both roughly zero and no economic utility could be gained from either of them.

The boundaries between the different regimes are sharp, and transitions between the regimes can be driven by both overfishing and excessive nutrient loading (Fig. 2.2). Both the macroalgae-dominant and macroalgae-only regimes occur when economic activity converges to the fishing-only equilibrium, while the coral-dominant regime is coterminous with the area of parameter space in which economic activity converges to the tourism-only equilibrium. This indicates that in the macroalgae-dominant regime, some coral survived despite the fact that coral-related ecotourism was not economically viable.

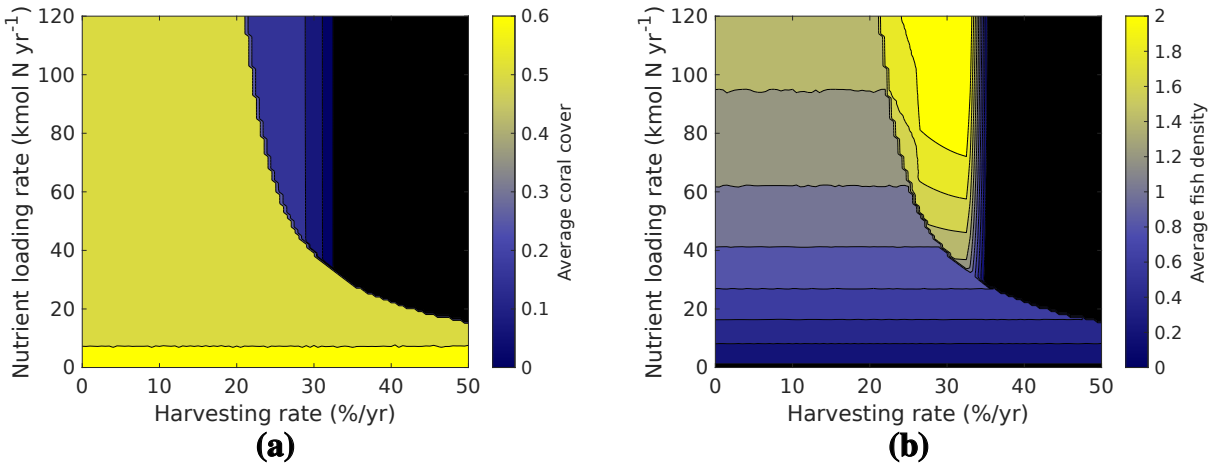

Figure 2.2: Levels of coral cover (Fig. 2.2a) and herbivorous fish density (Fig. 2.2b) in one patch as a function of harvesting rate and nutrient loading rate, showing three distinct regimes. Values taken are the equilibrium value or the average over one limit cycle.

2.5.2 Spatial effects of local overfishing

We found that herbivorous fish and coral responded in opposite ways to the two patterns of local overfishing that we tested (Fig. 2.4). Herbivorous fish abundance was lower on average when overfished patches were contiguous (i.e. they were harmed more by habitat loss than fragmentation). In fact, the case where overfished patches alternated with non-overfished ones saw no decrease in average herbivorous fish abundance compared to the baseline. In contrast, coral had greater declines in the alternating-patch scenario, corresponding to habitat fragmentation as a result of overfishing. There, coral cover was uniformly low across the system, whereas in the contiguous-patch scenario large amounts of coral survived in the patches away from the stressed area.

Increasing the proportion of patches that were overfished resulted in the expected linear decline in systemwide coral cover, as patches shifted one by one from being in the coral-dominant regime to the macroalgae-only regime. However, this masked nonlinear effects on coral in the overfished and non-overfished patches (Fig. 2.5). In the scenario where overfished patches were contiguous, coral cover fell off sharply in them but remained almost constant in the non-overfished ones. When overfished and non-overfished patches formed an alternating pattern, the decline in coral cover was steeper and was linear in both kinds of patches, and coral was completely extirpated at a ratio of two overfished patches for every one non-overfished one.

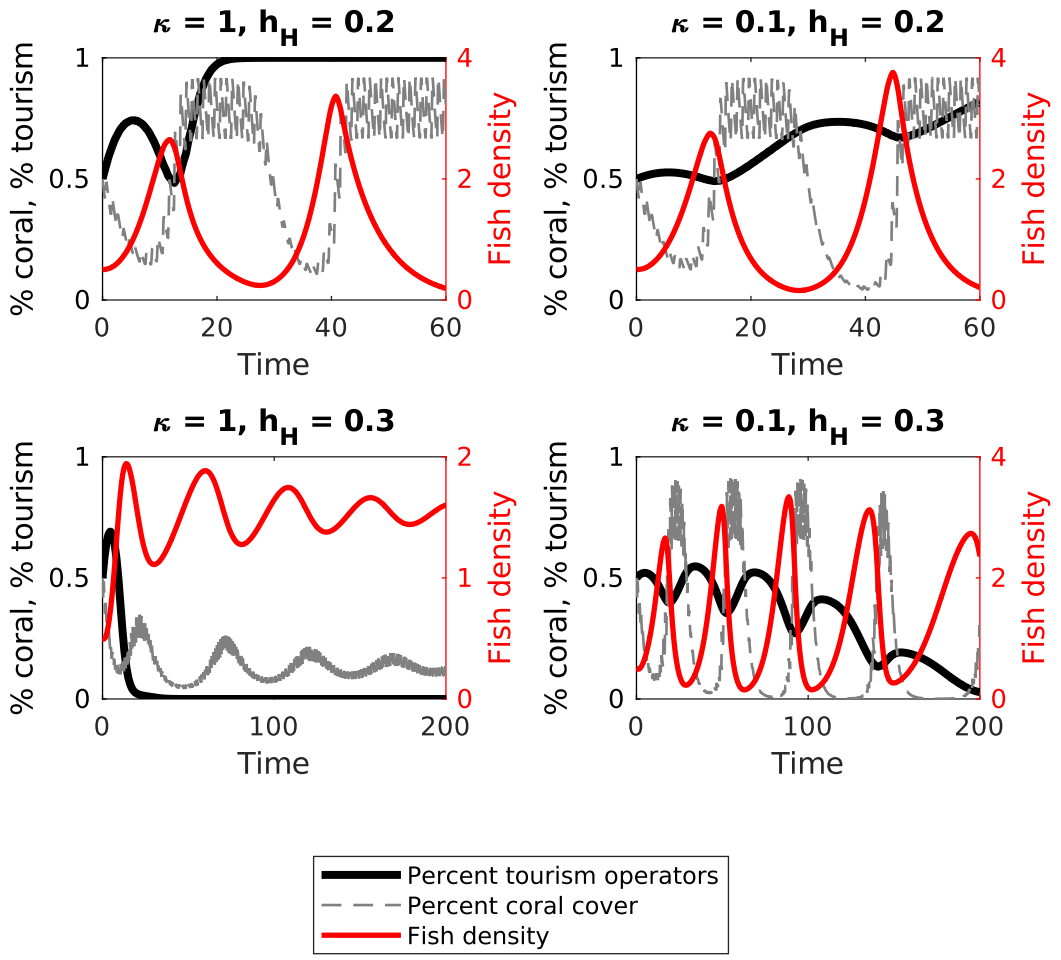

Figure 2.3: Time series showing coral cover, fish density and percentage of economic agents engaging in tourism for different values of κ and h_H, within a single patch. The top two graphs show dynamics in the cyclic coral-dominant regime, while the bottom two show transient dynamics in the high-fish regime.

As with habitat fragmentation, we found that the combination of nonlocal harvesting and the spillover effect had very different impacts on coral and herbivorous fish (Fig. 2.6). For the case with contiguous strings of overfished and non-overfished patches, increasing fish dispersal ability (and hence the strength of any potential spillover effect) caused an increase of average fish density across the system by over 20 percent (Fig. 2.6b). This held regardless of how much time fishers spent locally. In the case where overfished and non-overfished patches alternated, and therefore any overfished patch could receive some spatial

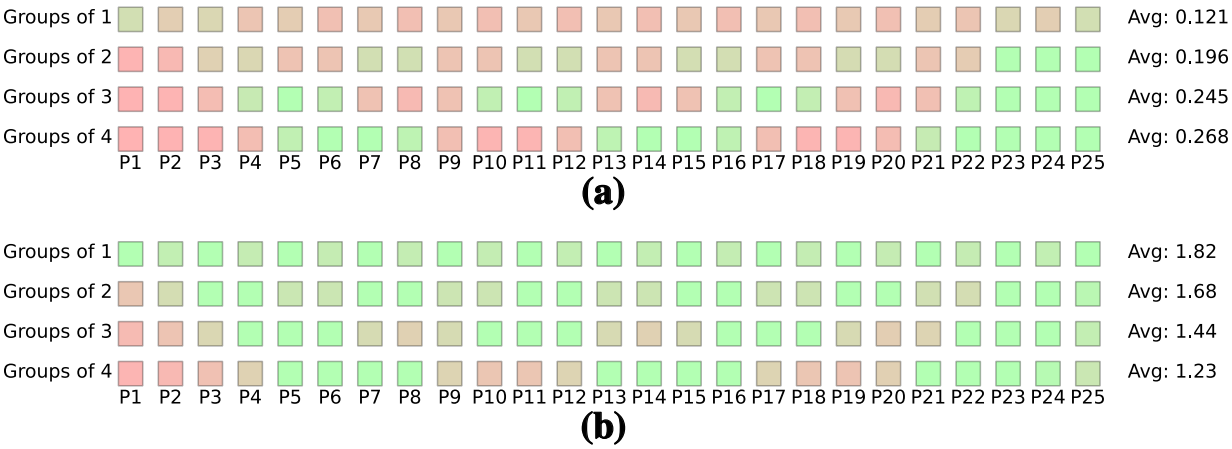

Figure 2.4: Coral cover (Fig. 2.4a) and fish density (Fig. 2.4b) in each of 25 patches, on a scale from red (low) to green (high), showing variation between contiguous and fragmented reefs. Here, 12 of 25 patches are overfished (arranged in groups of 1, 2, 3 and 4), and $\sigma_B = 0.25$. Averages of coral cover and fish density for the entire system are also provided for each configuration.

subsidies from an adjacent MPA, average fish density was higher than in the contiguous case (Fig. 2.4, Fig. 2.6b) with little dependence on fish dispersal ability in most cases. Coral larval dispersal ability had almost no effect on the abundance of fish or coral, with the exception of when both coral and fishing boats were almost entirely confined to their local patches. In contrast, we found that unauthorized fishing across MPA boundaries could lower coral cover by significant amounts, especially in the fragmented case (Fig. 2.6a) where we found losses of over thirty percent.

2.5.3 Economic transitions

When we simulated systemwide transitions from a fishing-based to a tourism-based economy, we found that herbivorous fish returned to healthy levels after about 15 to 20 years, with the system returning to a coral-dominated state after an additional 10 years (Fig. 2.7). This was dependent on the degree to which coral was previously extirpated, as expected. Local economic transitions resulted in systemwide fish recovery when they occurred in as little as 12 percent of patches (Fig. 2.7b), and systemwide coral recovery happened when at least 56 percent of patches transitioned (Fig. 2.7a). (This meant that under some conditions, herbivorous fish were predicted to recover but coral was not.) The recovery times for fish and coral following these local transitions were typically longer by a few years

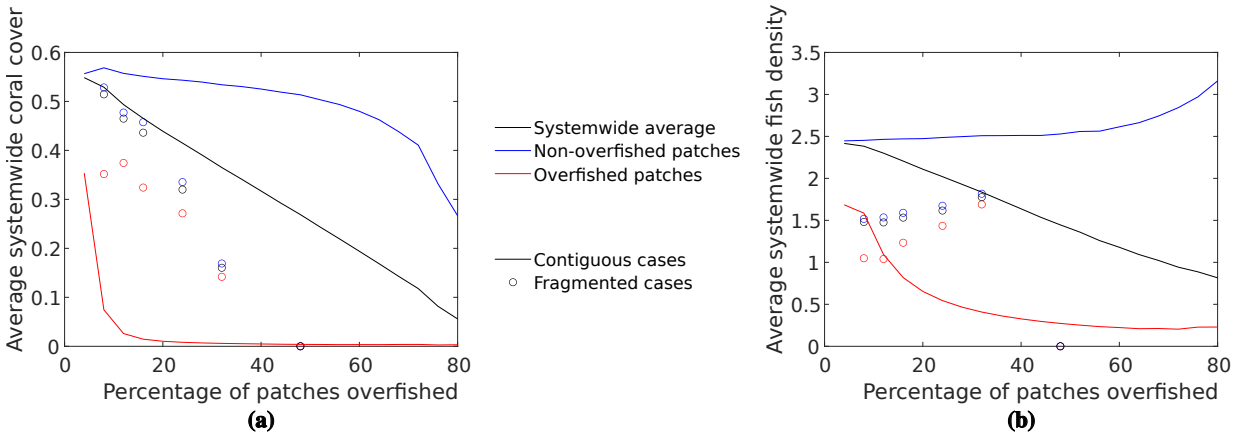

Figure 2.5: Average coral cover (Fig. 2.5a) and fish density (Fig. 2.5b) across a 25-patch system as a function of percentage of patches overfished, showing cases where overfished patches are contiguous and dispersed throughout the system. Values are shown for the system as a whole as well as for both overfished and non-overfished patches. Here, $\sigma_B = 1$.

than they were when the entire system transitioned, although the recovery times increased nonlinearly as the number of patches decreased towards the minimum number for which a recovery would take place, indicating the possibility of a bifurcation.

In our simulations involving short-term subsidization of the tourism sector in a heavily overfished system, we found that depending on how much tourism was subsidized and for how long, four different outcomes were possible (Fig. 2.8). In increasing order of subsidy length or amount, these were the status quo (macroalgae dominance), a temporary recovery of the herbivorous fish population, a temporary recovery of both fish and coral, and a permanent shift to a tourism-based economy with healthy fish and coral populations. When fish and/or coral recovered, temporarily or permanently, this happened after the tourism subsidies had finished, indicating that tourism subsidies set off a positive feedback loop in terms of fish and coral populations.

2.6 Discussion

We found that habitat fragmentation (via overfishing and subsequent shift to conditions more favourable to macroalgae) strongly affected both coral and herbivorous fish. However, the effects of habitat fragmentation on these two functional groups were opposite to one another. When holding constant the percentage of patches that were overfished, coral

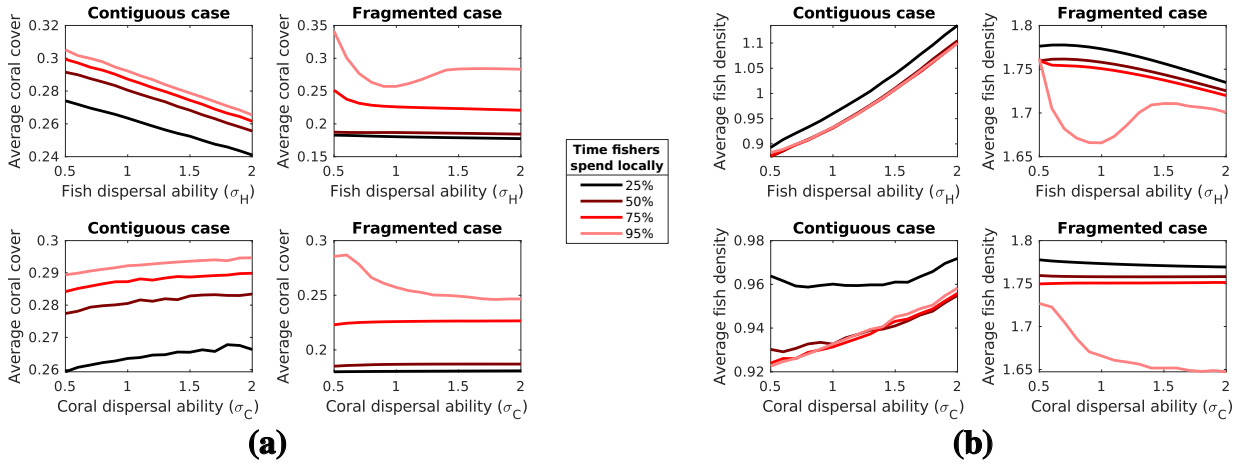

Figure 2.6: Average coral cover (Fig. 2.6a) and fish density (Fig. 2.6b) in a 25-patch system for different values of σ_H, σ_C and σ_B. Here, 13 of the 25 patches were overfished. Note the differences in scale on the vertical axes.

cover was higher when long strings of non-overfished patches were adjacent to each other. In contrast, herbivorous fish populations were highest when overfished patches alternated with non-overfished ones, This is consistent with the results of Bonin et al. [30], who found that habitat fragmentation had only a temporary negative effect on reef fish, and when disentangled from habitat loss its long-term effects were neutral or even positive.

In a similar vein, we found that dispersal ability of herbivorous fish had much different effects on their abundance in contiguous and fragmented habitats. We found that the abundance of herbivorous fish was strongly dependent on their dispersal ability in scenarios where there were long stretches of overfished patches that could potentially receive spillover, although this saturates when MPAs and overfished patches alternate with each other and form a fragmented pattern. In these areas, herbivorous fish always exhibited a strong spillover effect, elevating the fish population size and hence the potential fish catch regardless of their dispersal ability (as there was always a place outside of any MPA for them to disperse into).

Our results suggest that a strategy of placing MPAs in the middle of overfished areas [43] would be effective in maximizing both fishing yield and standing fish populations, potentially by even more than the 20 percent increase predicted by Cabral et al. Our results also recommend the enforcement of MPA boundaries by requiring fishing operations to harvest mostly locally (above 75 percent in their home patches), as doing so is predicted to greatly boost coral populations while maintaining increased fish yield from the spillover effect. Although it has recently been shown that more mobile species show increased

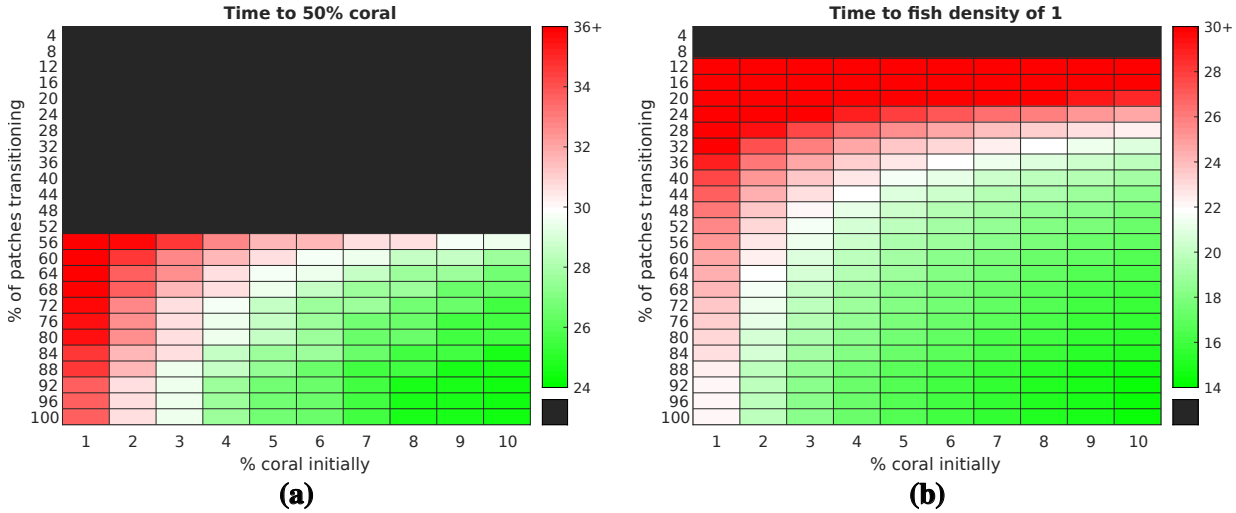

Figure 2.7: Time taken for average coral cover in a 25-patch system to return from a degraded state to 50 percent (Fig. 2.7a) and average fish density to return to 1 (Fig. 2.7b), following long-term economic transitions from fishing to tourism. Black boxes indicate that coral or fish was not observed to recover to the stated thresholds within 200 years.

spillover tendencies and that some spillover is present regardless of whether habitats are fragmented or not [69], we believe that our study is the first to look at the interaction between these two factors.

The differing responses of coral and herbivorous fish to habitat fragmentation and dispersal ability can be explained by their different life history traits. When coral larvae disperse into an adjacent patch, if that patch is completely occupied by macroalgae, the coral larvae will be much less able to establish themselves. This can be seen in Fig. 2.6, where we found that coral larval dispersal ability has minimal effect on system coral cover. Our results here are in accordance with field results showing that the presence of macroalgae can inhibit both coral larval settlement and coral recruit survival after settlement [141, 260]. Hence, overfishing can cause coral to decline not just by removing predation pressure on faster-growing algae, but also by preventing colonization by coral larvae. (This latter mechanism is implicitly implemented in the model, since the faster intrinsic growth rates of macroalgae mean that existing macroalgae within a given patch that is dominated by it tends to outcompete coral larvae dispersed in from other patches, meaning that perturbation away from a macroalgae-dominant state via coral larval influx is generally not feasible.) This feedback loop can drive a shift to the macroalgae-dominant regime, and its presence explains why we found sharp regime boundaries (Fig. 2.2).

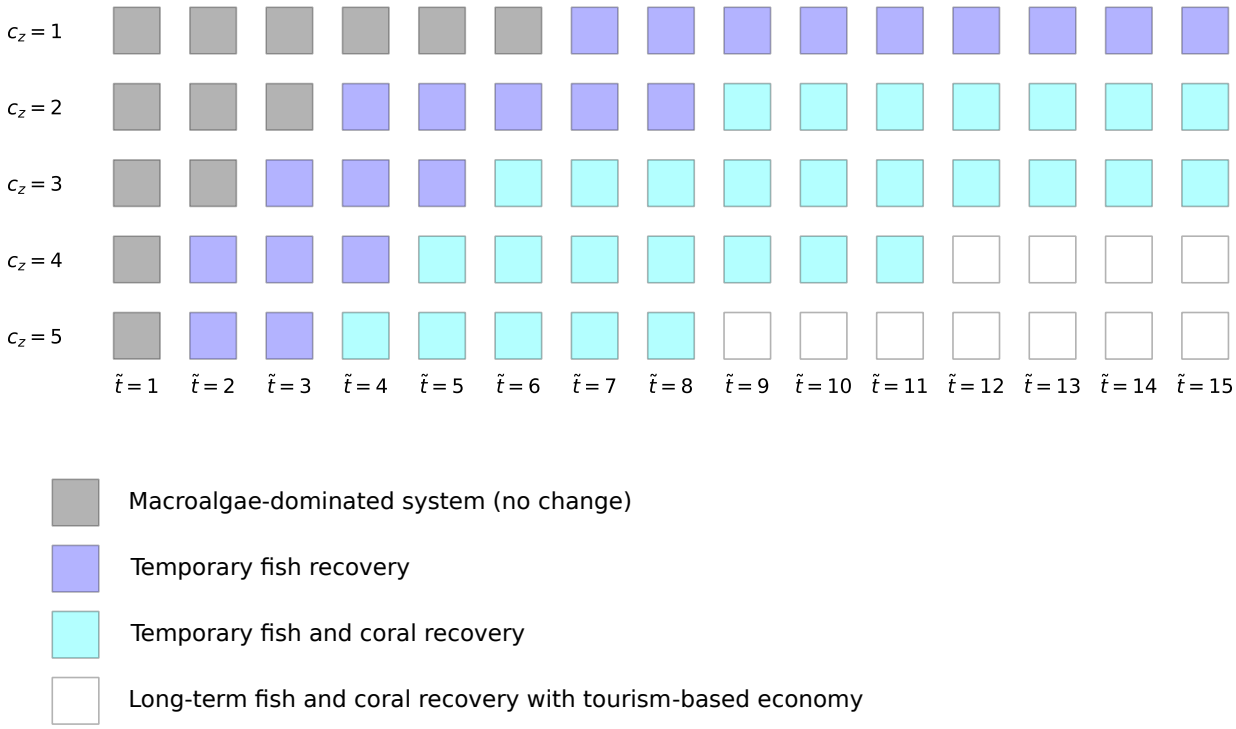

Figure 2.8: State reached by an overfished, macroalgae-dominated system after temporary subsidies to ecotourism. The four states shown differ in their transient and steady-state behaviour.

In the case when overfishing took place in a contiguous area, coral reacted very differently to an increase in the proportion of overfished patches depending on the local fishing rate. The average coral cover in overfished patches saw a steep dropoff after only a small number of patches became overfished, due to the breakdown of spatial subsidies. However, coral cover in the non-overfished patches (representing MPAs or areas fished at small-scale subsistence rates) remained at reasonably high levels, even when most patches were overfished and nonlocal harvesting was prevalent. This indicates the possibility of a conservation trap, in which a conservation-dependent species (in this case coral) is maintained via costly human intervention even though shifting the system to a more sustainable state would require less money and effort [49].

Given the predicted high discrepancy between coral health in overfished and non-overfished patches (or outside and inside MPAs) in the contiguous case, a manager could reasonably believe that only by implementing strict conservation measures can the coral be protected. However, we found two alternatives that may be considered if maintaining

an MPA is not financially feasible. Firstly, the regime we found with high fish populations and stable coral cover (Fig. 2.2) features z converging to the fishing-only equilibrium, indicating that the coral population is not conservation-dependent. This is achievable for harvesting rates between 20 and 30 percent per year, similar to what has been seen in a previous model [242]. Secondly, we found that promoting ecotourism can shift a system back to a coral-dominated state over an appreciable timeframe, even if such promotion is temporary (Fig. 2.8) or spatially limited in scope (Fig. 2.7). These additional options allow coral reef managers more choice in the strategies they have for reef protection.

We found that following a large-scale economic transition that reduced fishing pressure on previously degraded reefs, fish could be expected to return to healthy levels after 14 to 20 years, with coral following about 10 years afterward. This is comparable to measured recovery times of reef ecosystems following other disturbances. For example, a recent long-term study on resilience of Caribbean coral and parrotfish populations found that percentage coral cover had risen from 36 to 47 percent, in line with pre-disturbance levels, seven years after a 2010 coral bleaching event [231]. Extending this rate of recovery of slightly less than two percent cover per year to the scenarios that we tested, which had much lower initial conditions for coral, yields recovery times very similar to what we found (Fig. 2.7). The same study found that parrotfish recovery after the disturbance, when assisted by a law enacted the same year that banned their harvesting, happened at a greater magnitude than coral recovery, echoing our findings that herbivorous fish recovery during an economic transition serves as a leading indicator for coral recovery.

Another long-term study found no significant increase in coral cover from low starting points (about 10 and 20 percent cover) in the six years following a period of disturbances [119], in accordance with our result that recovery from such levels should not be expected within that timeframe. Shifts to macroalgae-dominated regimes taking 14 years, about half the length we found for a shift in the other direction, have been observed in the field [17]; the difference can be explained by factors such as macroalgae's ability to inhibit coral larval settlement (Fig. 2.6) and its higher intrinsic growth rate. Additionally, prior modelling results suggest that coral is able to recover after major hurricanes that happen once every 20 years, provided other environmental conditions are favourable [181, 180], which is also comparable to our results. This correspondence between our socially-driven transitions and the biologically-driven ones seen in previous field and modelling work helps validate the social component of our model, and indicates that coupled social-environmental interactions will be a useful addition to coral research going forward.

In addition to the spatial dynamics of coral and herbivorous fish, our results also show that different economic strategies (fishing and tourism) can coexist at a regional level. Specifically, we found that economic transitions from fishing to tourism along some parts

of a reef can result in herbivorous fish populations rebounding across the system, enough so that fishing remains viable where the economic transitions did not take place. Our findings are supported by recent modelling results showing that fishing and tourism can coexist in the same area [82], as well as field observations that different economic strategies in marine communities have complex, overlapping distributions [212]. Similarly, our results suggest that reef health and fish catch can be effectively balanced by using strategies that we identified, such as selecting local areas in which tourism would be temporarily subsidized or annual harvesting rates would be limited to intermediate levels. As economic models of fishing that both take into account marine protected areas and are spatially explicit have only been put forward recently [268, 82], we believe that spatial modelling of economic strategies on coral reefs is an area ripe for future research.

When determining the strength of the spillover effect and the differing responses of fish and coral to habitat fragmentation, we took $c_z = 0$, which assumes that the relative profitability of fishing and tourism depends solely on environmental conditions. Although this eliminated a potential confounding factor in these analyses, it also represents a simplification compared to real-life systems, and our results on reef recovery via economic transitions indicate that variation in c_z can have a significant environmental impact. This opens the door for future research on how changing economic conditions could lead to more or less fragmented reefs (and hence alter species composition). Based on our results (see for instance Figs. 2.2 and 2.8), we predict that positive values for c_z would boost coral growth, while negative values could increase fish populations or lead to macroalgae dominance, depending on the underlying biological conditions. (Hence, having a variety of local-scale values for c_z could provide another way to generate a fragmented system.) Since the ecosystem shifts we found when c_z was temporarily increased occurred a few years after the changes were made, we also predict that periodically varying c_z could result in complex patterns of coral and macroalgae dominance, and potentially a decoupling between coral cover and the preferences of economic actors.

In our simulations regarding fishing-to-tourism transitions, we started all patches at the same low values for coral cover and fish density, and assumed that h_H had the systemwide value of 0.5. As indicated by our results, the spatial configuration of overfished areas and MPAs makes a big difference in the abundance of each reef species, and hence considering how heterogeneous initial conditions affect the transition to a healthy reef would be useful. We especially believe that determining the extent to which habitat connectivity can aid a coral reef's recovery following an economic shift is an interesting avenue for future research. Additionally, due to the large ranges of many aquatic species, we believe that simulating economic changes in coral reef models larger than 25 patches could produce great insights as to which areas will be most hospitable for reef species going forward.

Chapter 3

Preparing for and managing crown-of-thorns starfish outbreaks under heavily stressed conditions

This chapter is based on the paper: RA Milne, CT Bauch, M Anand. 2022. Preparing for and managing crown-of-thorns starfish outbreaks under heavily stressed conditions. To be submitted to Ecological Modelling.

3.1 Abstract

Crown-of-thorns starfish (CoTS) outbreaks rank among the greatest threats to coral throughout the Indo-Pacific. In the future, reefs already stressed by CoTS will be further burdened by overfishing and nutrient loading. How much these two factors will exacerbate CoTS outbreak severity is still uncertain. Furthermore, the CoTS management literature has focused on the Great Barrier Reef, whereas outbreak damage is rising across the Indo-Pacific. Here, we use a metacommunity model to simulate CoTS outbreaks in areas with high anthropogenic stress. We model outbreaks on reefs adjacent to two cities within the range of CoTS that have less prior literature coverage: Cebu City, Philippines, and Jeddah, Saudi Arabia. We observe that urban growth can drive complex patterns of multi-stressor interaction. We find that CoTS removal on intermediate spatial scales significantly improves regional-scale coral health, and provide guidelines under which each of four CoTS management strategies is optimal for conservation. We find that coral decline due to overfishing can be sharper on reefs with CoTS, and that nutrification can induce a shift from discrete outbreak waves to continuous CoTS presence. Our work shows the importance of long-term planning for reef management, and highlights how reef stressors can interact in potentially unforeseen ways.

3.2 Code availability

The code for simulating the model is available on Zenodo (DOI: 10.5281/zenodo.6516167).

3.3 Introduction

Crown-of-thorns starfish (*Acanthaster planci*; CoTS) are a voracious predator of coral, having been cited as the primary cause of short-term decline in coral cover across the Indo-Pacific region [40, 66]. Rapid increases of CoTS populations, deemed "outbreaks", can devastate a coral reef in a very short period of time [196]. In recent years, outbreaks of CoTS have become more frequent across its entire range [120]. Field studies have linked this with increased nutrient input into coastal waters [39, 18], which is concerning as nutrient loading rates are projected to rise well above current values over the next few decades [226, 276]. In addition to CoTS outbreaks and nutrient loading, overfishing represents another rising source of stress for coral populations [208], but whether the effects on coral of overfishing interact with those of CoTS outbreaks in an additive, synergistic

or antagonistic manner is still an open question [74]. Most CoTS modelling efforts have been done on the Great Barrier Reef, meaning that the development of management best practices in other areas under threat by CoTS is still ongoing. Here, we use a model of intermediate complexity, specifically a dynamical system metacommunity model of a coral reef, to evaluate the potential future threats posed by CoTS and how they can be addressed. We specifically focus on how future increases in fishing rates and nutrient loading can alter the effects of a CoTS outbreak, with case studies drawn from reef areas throughout the range of CoTS.

The presence of multiple interacting stressors on coral reefs has long been known [121], and many of these stressors have high predicted future impact on coral as well. Nutrient loading [101, 226, 100], overfishing [265, 208], CoTS outbreaks [131], sedimentation [101], bleaching due to increased ocean temperatures [48, 193], and ocean acidification [193, 131] have all been cited as future points of concern. Hence, much research has been done recently on the interacting effects of multiple coral reef stressors (e.g. [28, 93, 274, 257]). These interactions have often been nonlinear, with both positive and negative feedback [85], indicating that different stressors can have unforeseen effects on each other and are potentially more dangerous together than when considered individually. However, despite the possibility for complex interactions to emerge, few studies have examined how other stressors can exacerbate or inhibit the frequency and severity of CoTS outbreaks [74]. Previous work using qualitative models to examine the effects of fishing and nutrient loading on CoTS populations predicted varying patterns of interaction with a high degree of uncertainty [18], suggesting that complex relationships between these stressors are possible.

CoTS larvae can disperse over long distances [244], and hence CoTS outbreaks happen over wide spatial scales [107]. Hence, spatially explicit modelling of coral reefs under threat by CoTS has attracted research attention in recent years [251, 160]. However, long-term ecological data that could be used to fit large-scale models is scarce [119], and hence the metacommunity and regional-scale CoTS models in existence have mostly been fit for conditions on the Great Barrier Reef, owing to the larger availability of data there. CoTS have been found across the entire Indian and Pacific Oceans, from the Red Sea [273] to Southeast Asia [271] and Polynesia [271, 245], and the number of recorded outbreaks (including those in regions outside the Great Barrier Reef such as these) has significantly increased since 1990 [120]. Because of this, it is important to develop strategies for their management that are robust to conditions in many different regions. Models of intermediate complexity (e.g. [175]) are especially important in this regard, as more complex models may produce predictions with greater uncertainty [106, 18]. A corollary of this is that significant gaps in the literature can be filled by using a model of intermediate complexity, especially in the context of generating ecological predictions and management recommendations for a wide

variety of different regions.

Nutrient loading is a major source of concern for coral reefs, both now [274, 17] and in the future [101, 226, 100]. In the coming decades, urban areas are predicted to expand both in land area [148, 53] and population [247]. Because of this, anthropogenic nutrient input to adjacent coastal areas is expected to go up by significant amounts, in some cases doubling or tripling by 2050 (e.g. [226, 8]). This increase in nutrients can make reefs more vulnerable to CoTS, as it may cause blooms of phytoplankton. Phytoplankton are the primary food for CoTS larvae [196], with relationships having been observed between CoTS larval survival and phytoplankton concentration [79] and therefore nutrient input [39], leading to the conclusion that increased nutrient availability is itself a potential cause of outbreaks [18].

Another reef stressor projected to become more of a concern in the future is overfishing [265, 208]. Similarly to nutrient loading, relationships between human population and offshore fishing pressure has been established [232], including in coral-dense regions such as the Philippines [219]. The ability of increases in fishing rate to cause phase shifts on coral reefs is well-documented in both modelling [28, 89, 38] and field literature [72]. As CoTS is a primary predator of coral, a CoTS outbreak could cause a coral-algal phase shift induced by overfishing to happen earlier or with greater speed. Additionally, field research has found a correlation between fishing rate and CoTS density on reefs [73], as well as a link between the presence of large, commercially valuable fish on a reef and its recovery following a disturbance partially caused by CoTS [119]. This suggests that even when a phase shift does not happen, strong interaction effects between overfishing and CoTS could still cause significant damage to reefs.

Since CoTS is responsible for much of the degradation in reefs throughout the Indo-Pacific region [185], many strategies for its management have been proposed. Historically, the most widely used of these was manual removal and subsequent disposal on land, which is costly and labour-intensive [198]. Hence, other options for CoTS management have been recently explored. CoTSBot, an autonomous underwater vehicle designed for CoTS eradication, has been developed for use on the Great Barrier Reef [1], and cheap and widely available chemicals such as citric acid powder and vinegar have been shown to be effective for controlling CoTS [269, 33, 41]. The government of Australia introduced the Crown-of-thorns Starfish Control Program in 2012 on the Great Barrier Reef, two years after the start of the current outbreak there. Removal of CoTS from all locations on the Great Barrier Reef is impractical due to the scale of the potential effort involved, so management instead strategically focuses on high-priority locations [137]. Given the limited resources available, optimization of CoTS management strategies (especially prior to severe outbreaks) can help protect areas under threat by CoTS to the maximum extent possible.

In this paper, we use a dynamical system model to determine the characteristics of CoTS outbreaks in different parts of their range, how these will change with increased anthropogenic stress, and how they can be best managed. We find that the intensity of CoTS outbreaks depends nonlinearly on both fishing and nutrient loading rates, whose relative importance on a reef with CoTS presence can hence change as urban development increases. We use growth projections for two major cities with adjacent coral reefs (Cebu City, Philippines, and Jeddah, Saudi Arabia) to predict the potential severity of future CoTS outbreaks there. We simulate application of different CoTS management strategies to reefs off the coast of Cebu and Jeddah to evaluate their effectiveness in advance of future outbreaks. We find that each of four different methods of prioritizing local patches for active CoTS removal may be the most effective, depending on the conservation objective sought, and that CoTS removal on intermediate spatial scales (e.g. 20 km of coastline) can promote coral health across larger regions. We also determine that establishing a marine protected area at a strategically-located site near Cebu City can insulate coral there against serious CoTS outbreaks.

3.4 Methods

3.4.1 Model

In order to model the population dynamics of coral, crown-of-thorns starfish (CoTS), and other functional groups present on a reef that interact with them, we adapted a spatially explicit, mechanistic model first used by Spiecker *et al.* [228]. This model was chosen as CoTS outbreaks occur over large spatial scales, necessitating the use of a spatial model, and because it contained explicit terms for fishing and nutrient loading rates, which we intended to vary to match future predictions. That model was composed of integro-differential equations, but we intended to represent a patchy landscape with a resolution of 1 km (see Numerical Methods subsection and Appendix A), so we converted it into a metacommunity model of ordinary differential equations. The components of the original model are herbivorous fish H, coral C, macroalgae M, detritus D and nutrients N. We retained that model's terms, and added a component for CoTS, which we denote S. Our modified equations for the model components in [228] are below, where the subscript i denotes local dynamics in patch i:

$$
\begin{aligned}
\frac{\mathrm{d}H_i}{\mathrm{d}t} &= \frac{r_{H_i} M_i}{k_{H_i}+M_i} H_i - m_{H_i} H_i - \xi_i H_i + g_{H_i} \\
\frac{\mathrm{d}C_i}{\mathrm{d}t} &= (1 - M_i - C_i)\, g_{C_i} - m_{C_i} C_i - l_{S_i} S_i C_i \\
\frac{\mathrm{d}M_i}{\mathrm{d}t} &= (1 - M_i - C_i)\, g_{M_i} - m_{M_i} M_i - \frac{r_{H_i} M_i}{k_{H_i}+M_i} H_i \\
\frac{\mathrm{d}D_i}{\mathrm{d}t} &= m_{H_i} H_i + m_{C_i} C_i + m_{M_i} M_i + m_{S_i} S_i - \gamma_i D_i + g_{D_i} \\
\frac{\mathrm{d}N_i}{\mathrm{d}t} &= q_i - e_i N_i + f_i \gamma_i D_i - \left(\frac{r_{M_i} N_i}{k_{M_i}+N_i}\right) M_i + g_{N_i}
\end{aligned}
\tag{3.1}
$$

A detailed schematic of the model is presented in Figure 3.1. In the model, herbivorous fish consume macroalgae according to a saturation function with maximum rate r_H and half-saturation constant k_H. (This is equivalent to a Holling Type II functional response.) Herbivorous fish die of natural causes at a rate m_H, and are fished out at a rate ξ. Coral and macroalgae reproduce by dispersing their larvae and propagules, respectively, so the model functions representing their population growth are part of their dispersal functions g_C and g_M (see Equation 3.2). Coral and macroalgae also compete for space on the seabed, so it is assumed that they have a shared carrying capacity, which is normalized to 1. Coral and macroalgae die of natural causes at rates m_C and m_M, macroalgae is eaten by fish in the manner described above, and coral is destroyed by CoTS at a rate l_S. All dead organisms (including CoTS) become detritus, which in turn decays at a rate γ. Nutrients are measured in kilomoles of nitrogen, on the scale expected to be found in an offshore patch of 1 km^2 surface area [254, 225]. We chose nitrogen because it is the most common limiting nutrient in pristine reef systems [143], and because nitrogen addition has been especially cited in existing literature as being damaging for coral [276]. Nutrients are generated by decomposing detritus, subject to a scaling constant f; they also are assumed to be fed into the system at a rate q and washed out of it at a rate e. Nutrients are also uptaken by macroalgae, with the dynamics of this being explained below. The model parameters are further described in Tables A.1 and A.2.

Since this model encompasses both local-scale and regional-scale dynamics (using a patchy landscape), we modelled the dispersal of the model components with functions describing the transfer of material from each patch to each other patch, denoted g_X for each corresponding state variable X. The dispersal functions for all model components other than CoTS are shown below:

$$
\begin{aligned}
g_{M_i}(t) &= \sum_j \left(\frac{N_j}{k_{M_j}+N_j}\right) r_{M_j} M_j \theta_{M_j}(i) \\
g_{C_i}(t) &= \sum_j r_{C_j} C_j \theta_{C_j}(i) \\
g_I(t) &= -I_i(t) + \sum_j I_j \theta_{I_j}(i), \; I \in \{H, D, N\}
\end{aligned}
\tag{3.2}
$$

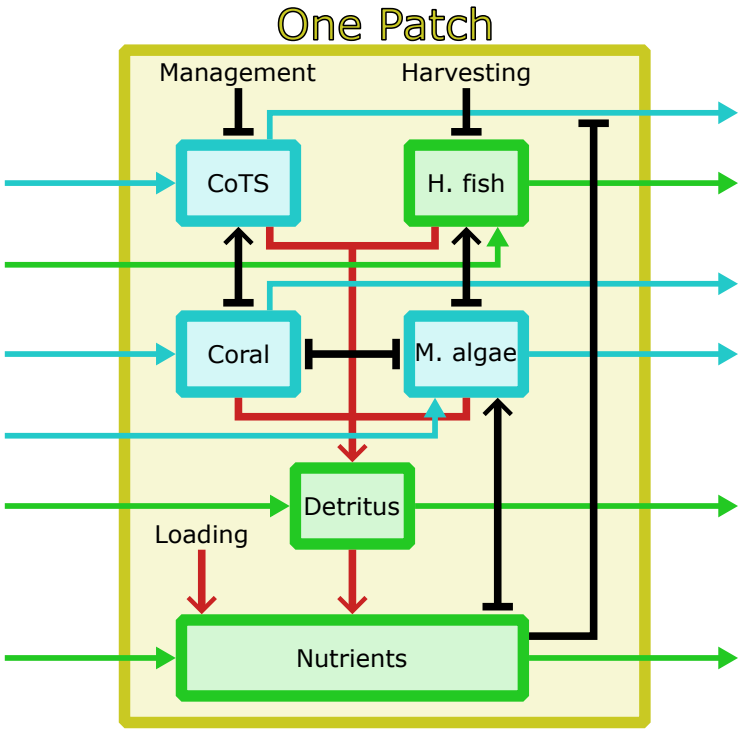

Figure 3.1: Diagram representing interactions in the model. All connections within the box marked "One Patch" are local. Black connectors denote trophic and competitive interactions; for these, pointed heads denote positive effects and rectangular heads denote negative effects. Red connectors represent materials cycling. Teal arrows represent gains and losses of organisms due to larval dispersal, whereas green arrows represent all other forms of dispersal.

Since coral and macroalgae reproduce via dispersal, but adults of those functional groups do not move, g_C and g_M include those functional groups' intrinsic growth rates. CoTS were also handled in this manner (see Equation 3.5). For each patch i, the growth rates for coral and macroalgae in i are expressed as the sum over all patches j of the number of larvae or propagules produced in patch j that eventually settle in patch i. The intrinsic growth rates of coral and macroalgae are r_C and r_M, respectively. Macroalgae growth is additionally assumed to depend on the availability of nutrients, modelled with a saturation function with half-saturation constant k_M. We also took r_C to be a periodic function, to represent the annual reproduction cycle of coral [235]. (This took the form of a repeated Gaussian function, with its peak at mid-year. The value of r_C at the beginning of each year was very small, about 10^{-10}, so we assumed that the tails of the distribution

could be safely ignored.) Herbivorous fish, detritus, and nutrients were instead assumed to follow passive dispersal; their dispersal functions are written above in a similar way to g_C and g_M to highlight the differences in the latter.

The harvesting rate in each patch ξ_i was also assumed to be nonlocal, as fishing boats were assumed to be non-stationary. This was done in order to test the effectiveness of marine protected areas (MPAs) as tools for protecting coral against CoTS, since illegal harvesting inside MPAs by fishing boats based outside them has been identified as a problem [46, 129]. For a baseline harvesting rate h_{H_i} and a discretized probability distribution θ_{B_i} that were both defined for each patch i, this was as follows:

$$\xi_i(t) = \sum_j h_{H_j} \theta_{B_j}(i) \tag{3.3}$$

Each probability distribution related to dispersal (θ_{X_i}, for $X \in \{H, C, M, D, N, B\}$ and for each patch i) was taken to be a discretized Gaussian. θ_{B_i} for each patch i contained the amounts of time that fishing boats originating in i would spend in each patch in the system, with mean i and standard deviation 1 to represent a wide range. θ_{C_i} and θ_{M_i} for each patch i were used to model larval dispersal for broadcast-spawning functional groups (C and M). The means of θ_{C_i} and θ_{M_i} for each patch i were taken to be $i + k_{\text{PLD},X} k_{\text{curr}} k_{\text{sc}}$, where $k_{\text{PLD},X}$ is the average pelagic larval duration of functional group X in days, k_{curr} is an index of current strength scaled so that 1 represents conditions on the Great Barrier Reef, and k_{sc} is a scaling constant that was fit to qualitatively replicate dynamics on the Great Barrier Reef (with units of day^{-1}). The parameters governing the shapes of the θ distributions for macroalgae and coral were determined and validated based on observed variation in pelagic larval duration for each functional group, as well as conditions on the Great Barrier Reef; k_{curr} was varied based on conditions in the specific area being simulated. Further information on the distributions used in the model is contained in Table A.3.

To model the population dynamics of CoTS, we implemented a novel differential equation describing their vital processes. This DE is as follows:

$$\varepsilon \frac{\mathrm{d}S_i}{\mathrm{d}t} = g_{S_i} - m_{S_i} S_i \tag{3.4}$$

CoTS reproduce by dispersing larvae into the ocean [203, 251], and hence most movement by CoTS over the spatial scale that we consider is done by larvae [196]. Therefore, we assumed that CoTS movement would be done by larvae, and combined their reproduction and dispersal into a single term, as was done with coral and macroalgae. This nonlocal growth term is as follows:

$$g_{S_i}(t) = \sum_j \left(\frac{N_j}{k_{S_j} + N_j} \right) r_{S_j} l_{S_j} S_j C_j \theta_{S_j}(i) \tag{3.5}$$

CoTS and coral were assumed to follow predator-prey dynamics with respect to each other. As coral is represented as a percentage cover of the seabed and CoTS is represented as a population size, we assumed that coral is destroyed by CoTS at a rate l_S, and that CoTS reproduces at a rate $r_S l_S$. We took the CoTS-coral predation terms to be linear in each. Since CoTS is known to experience boom-bust population cycles, and hence can sustain very high reproduction rates while coral prey is available, we decided against taking its predation rate to be a saturation function; we also did not expect any loss in CoTS predation efficiency at low coral density, due to adult coral being sessile and therefore easy for CoTS to locate. CoTS larvae originating in a given patch i are sent to each patch in the system according to a probability distribution function θ_{S_i} with a mean of $i + k_{\mathrm{PLD},S} k_{\mathrm{curr}} k_{\mathrm{sc}}$ and a standard deviation of σ_S, which is similar to coral and macroalgae reproduction. We assumed that CoTS larval survival depends on the availability of phytoplankton, and hence on nutrient concentration [39]. Previous modelling work has described the relationship between phytoplankton concentration and CoTS larval survival using a logarithmic function [160]. We used a saturation function of N in our equation for CoTS larval production and distribution g_S, with half-saturation constant k_S, which is similarly concave down as well as being zero when no nutrients are present (thus making it unnecessary to translate the function to achieve this property). We assumed that CoTS dies of natural causes at a rate m_S. Additionally, as CoTS outbreaks are known to happen very rapidly [249], we assumed that CoTS-related dynamics happen over a faster timescale than the dynamics of the other model components. Hence, we took ε to represent the difference in timescales, as has been done in previous ecological models featuring fast-slow dynamics [58]. Full model parametrization details are available in Appendix A.

3.4.2 Numerical methods

In order to determine how different conditions on a reef can affect the characteristics and outcomes of a CoTS outbreak, we ran simulations of the model in which parameters representing reef conditions were varied and looked for trends in CoTS density and coral cover. To specifically examine how the presence of CoTS affects the relationship between fishing rate and coral cover, we ran the model for varying values of h_H, with and without the presence of CoTS. This was done for different values of q and k_{curr}, representing typical conditions in three specific reef areas. In the case with CoTS, we set the initial condition $S_i(t = 0)$ to be 0.5 for $i = 1$ (the furthest upstream patch) and 0 for all other values of i,

to capture the initial spread of CoTS at the start of an outbreak and all further dynamics. For each simulation, we took the average coral cover in all patches over a window from the start of the initial outbreak to 50 years after. This was compared to a baseline value, namely the average coral cover in each simulated reef area with $h_H = 0$ and CoTS absent.

Similarly, to determine how different levels of nutrient loading can affect specific features of a CoTS outbreak, we looked at different metrics representing the characteristics of an outbreak for different values of q and k_{curr}. The specific metrics that we used were average CoTS density in the system after time $t = 15$ years (representing whether CoTS remained in the system, or became locally extinct or was washed out on the currents), maximum length of time that average CoTS density was above 1 systemwide (indicating whether outbreaks were discrete events or CoTS had a continuous presence), and number of discrete peaks in CoTS density over the 50-year simulated timespan (representing the period of an outbreak cycle, or the length of time between outbreaks). In these simulations, we took q ranging from 0 to 80, covering nutrient loading values associated with rural and low- to mid-density urban areas, and k_{curr} ranging from 0 to 2 (i.e. from no current at all to a current with double the strength of those on the Great Barrier Reef).

In order to determine the extent to which future increases in fishing and nutrient loading driven by urbanization will exacerbate CoTS outbreaks, we ran numerical simulations with varying rates of nutrient input level (q) and fishing rate (h_H). We ran the model with 100 patches, with the values of q in each patch chosen to represent specific urban areas in 2020 and 2050 (see Appendix A). The two cities chosen were Cebu City, Philippines and Jeddah, Saudi Arabia; both of these have offshore coral reefs [112, 149, 219] and are within the range of CoTS [31, 104]. For each city, we tracked coral cover and CoTS density over 30 years (2020 to 2050) where q and h_H continually increased according to predictions. We also performed these simulations for static q and h_H, starting both in 2020 (to provide a baseline for comparison) and in 2050 (using predicted values for q and h_H, to test short-term coral response to an outbreak starting in that year). For Cebu City, we also simulated cases in which an MPA was established on parts of Mactan and Cordova Islands and urban development there was limited, to examine the efficacy of this conservation strategy. We controlled for the effects of nutrient availability on CoTS larval survival [79, 267] by taking $k_S = 30$ (the baseline value) and 3. Additional details on the model fitting and parametrization for these scenarios are available in Appendix A.

To evaluate the effectiveness of different CoTS management strategies, both in general and for our two focus cities, we ran a variation of our model in which local-scale active management of CoTS was simulated. This was done by periodically evaluating different management criteria for each patch, selecting a fixed number of patches ρ to prioritize for management based on these criteria, and scaling up CoTS mortality rate by some

constant ω in the selected patches until the next update of the management criteria. We considered three different management criteria, based on removing CoTS from patches with the highest CoTS density, the greatest ability for coral to recover, and the greatest potential for CoTS to spread to other patches, as well as an additional criterion equal to the average of these three. The methods for selecting patches according to this criteria are detailed in Appendix A, where they are referred to as Φ_{CoTS}, Φ_{Rec}, Φ_{Spr}, and Φ_{Avg}.

For each management criterion, patches with negligible CoTS densities ($S < 0.01$) were not considered in order to avoid spending resources on removing CoTS from areas where their presence was minimal. During runs of the model, the management criterion that was being applied was evaluated either at the start of each month (i.e. at $t = \frac{n}{12}$ for $n \in \mathbb{N}$) or at the start of each week (i.e. at $t = \frac{n}{52}$ for $n \in \mathbb{N}$). Upon evaluation of the management criterion for each patch i, the ρ patches with the highest criterion values were selected to be actively managed (i.e. their death term for CoTS was changed from $-m_S S$ to $-\omega m_S S$) until the end of the current month or week when the criterion would be recalculated.

In order to check the performance of each different management strategy at removing CoTS, we ran our model using each criterion with parameter values representing rural areas of the Great Barrier Reef, where the real-life versions of these criteria were developed for. (Here, we took $\rho = 20$ and $\omega = 2$.) We then calculated the average CoTS density in the system as an index of overall performance, and looked at CoTS densities in each specific patch to determine how each management strategy affected local CoTS dynamics. (The average in question was taken of CoTS densities in all patches, creating a single time series.)

To evaluate the effectiveness of active CoTS management at preserving coral in Cebu City and Jeddah, we ran the the model with management, taking parameter values representing each city. This included nutrient loading q and fish harvesting rate h_H increasing over time, as detailed above. Since resources for conservation are limited, and not all local areas can be actively managed, we considered values of ρ (the number of patches that CoTS is actively removed from) ranging from 0 to 50 (out of 100 patches total). We took ω, the change in CoTS mortality rate due to active removal, to be integer values from 1 to 6, where $\omega = 1$ represents the baseline case where no additional CoTS mortality due to management is observed. For each run of the model, we evaluated local and regional levels of coral cover and CoTS density over the 30 years (2020 to 2050) that the model was run for. (To produce a single systemwide value for coral cover, we took a spatiotemporal average, namely the average coral cover at all points in time in all 100 patches within the model.) In Cebu, we also simulated a combination of active CoTS removal and establishment of the MPA at Mactan (see above) to check whether these two conservation strategies provided additional benefit when used together.

3.5 Results

3.5.1 Future prediction case studies indicate more frequent CoTS outbreaks with longer coral recovery times

In our case studies for both Cebu City and Jeddah, we found that projected increases in nutrient loading (q) and fishing rate (h_H) will have substantial effects on the frequency and severity of crown-of-thorns starfish outbreaks (Figure 3.2). We found that coral would recover from simulated outbreaks under conditions representative of 2020 in both cities after 15 to 20 years, but under conditions based on forecasts for 2050, coral took longer than 30 years to recover in both cities (Figures B.2a and B.2c). In Cebu, our additional simulations of 2050 conditions featuring a marine protected area along the coast of Mactan and Cordova Islands with limits on urban development there showed much greater reef health than the baseline 2050 case (Figure B.2a), despite fishing pressure and nutrient loading rates taking the elevated 2050 values everywhere else along the coastline. Our findings on coral recovery time were robust to potential uncertainty in the dependence of CoTS larval survival on nutrient concentration (k_S), although the level that coral populations reached at the most severe point in a CoTS outbreak was affected by k_S, particularly in Jeddah (Figures B.2b and B.2d).

We also found that continual increases in nutrient loading and fishing rate caused the frequency of CoTS outbreaks to increase (Figure 3.2), and in particular caused the predicted second outbreak wave to occur sooner after the first by approximately 5 years. In both cities, increasing nutrient loading and fishing pressure led to coral populations becoming more variable compared to the case with q and h_H constant (Figures 3.2a, 3.2c, B.2a and B.2c). CoTS also had a much greater maximum density in Cebu under the scenario with increasing stress (Figure 3.2b), and Jeddah shifted from outbreaks being mostly discrete events to CoTS having a continuous presence throughout the system even in between waves (Figure 3.2d).

3.5.2 Overfishing and nutrient loading both drive strong nonlinear effects in potential CoTS damage to coral

We found that adding CoTS to a reef altered how fishing rate increases on that reef affect coral health, creating a threshold effect capable of producing "ecological surprises" at intermediate levels of fishing pressure (Figure 3.3). When CoTS are not present, we found increases in fishing rate to correspond to steady, usually linear declines in average coral

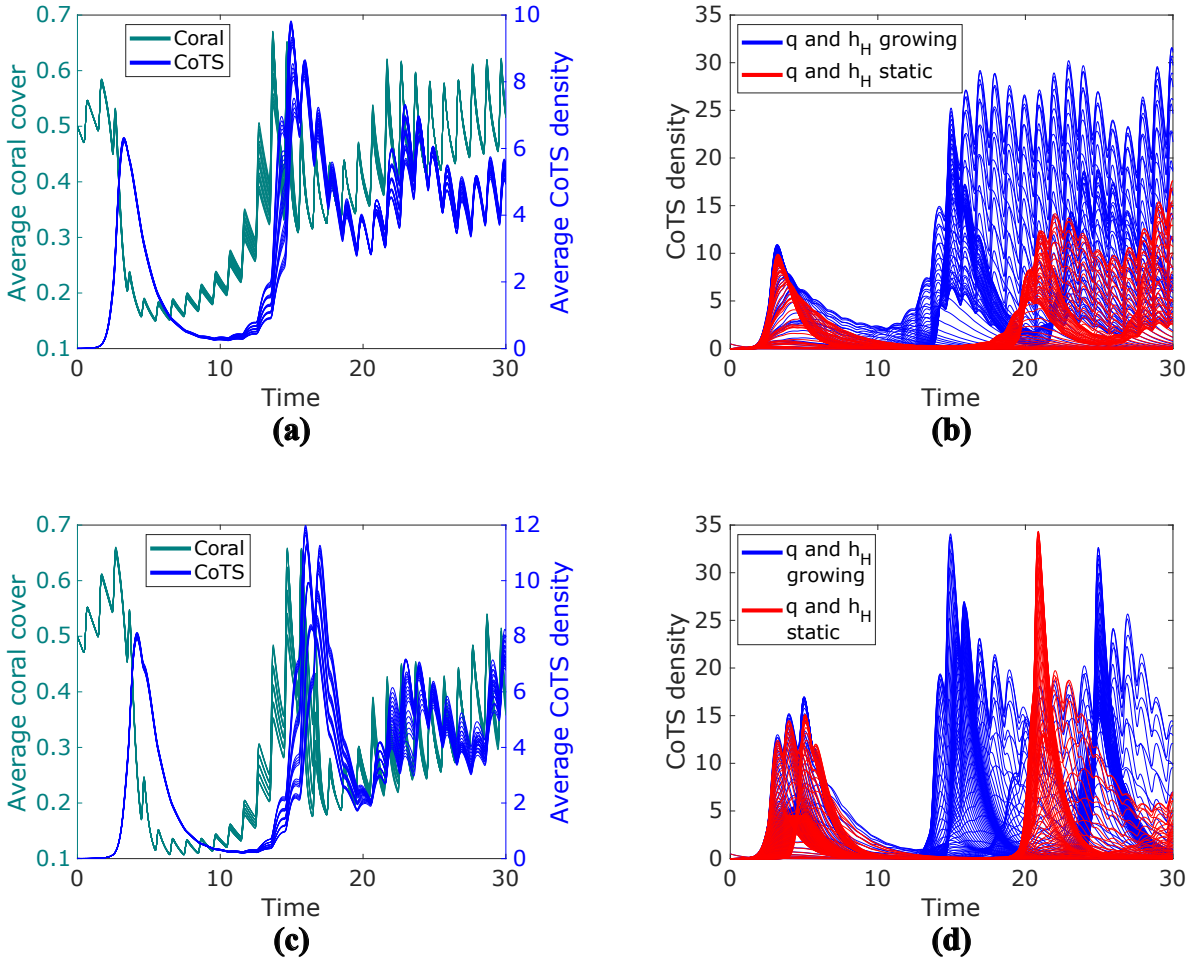

Figure 3.2: Case studies for Cebu, Philippines and Jeddah, Saudi Arabia. Figures 3.2a and 3.2b show simulated dynamics for Cebu, while figures 3.2c and 3.2d represent Jeddah. Figures 3.2a and 3.2c show coral cover and CoTS density in each city for continually increasing values of q and h_H (up to $\pm 10\%$ from baseline predictions) starting in 2020. Figures 3.2b and 3.2d show the density of CoTS in individual patches offshore from each city starting in 2020. There, CoTS densities are plotted for both static and continually increasing values of q and h_H. Time is measured in years in this and all other graphs in this section; outbreaks are identifiable as the slow waves rather than the fast (yearly) ones.

cover. Increasing nutrient loading rate caused this decline to be steeper, as seen in the differing responses of coral in each of the three tested scenarios in Figure 3.3. Introducing CoTS resulted in this relationship instead becoming mostly flat: for each tested scenario

(the Great Barrier Reef, the Red Sea, and the internal waters of the Philippines), average coral cover was approximately the same when there was no fishing as when 20 to 25 percent of fish were harvested annually. However, in systems with CoTS, a threshold effect occurred for fishing rates at or slightly above 30 percent annually, where average coral cover dropped significantly. The addition of CoTS decreased average coral cover in all three tested scenarios, as expected. This effect was stronger for higher rates of nutrient loading (which also strengthened the threshold effect), as well as when currents were slower and more CoTS were locally retained.

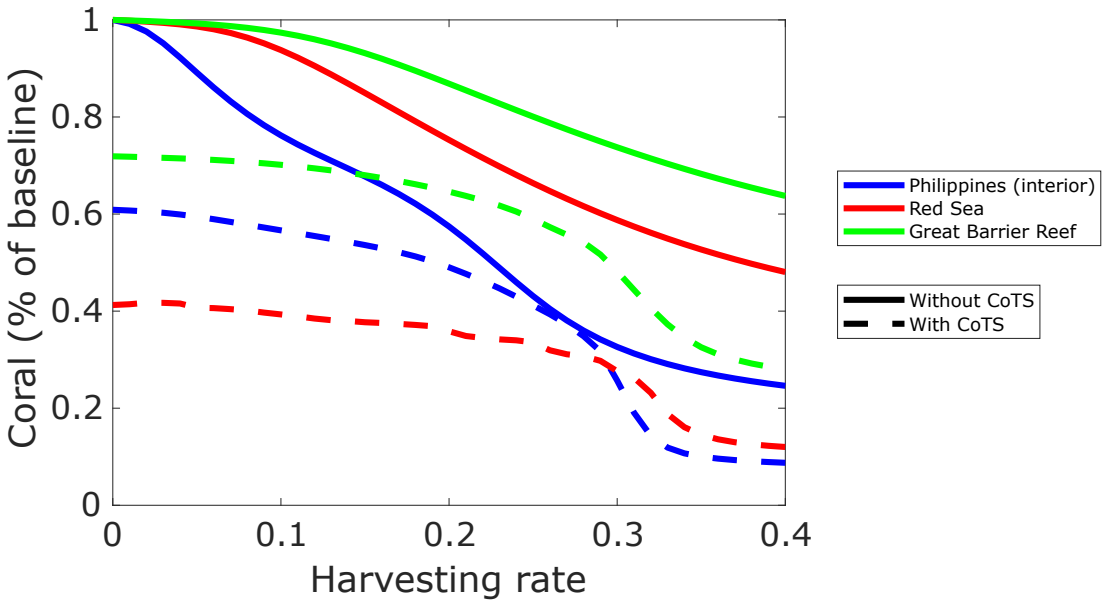

Figure 3.3: Plot showing average coral cover over a 50-year window for different levels of harvesting rate h_H, with and without crown-of-thorns starfish presence. Graphs are shown for simulations of reefs adjacent to rural areas in three different regions (interior waters of the Philippines, the Red Sea, and the Great Barrier Reef), which differ from each other in terms of ocean current strength and amount of nutrient loading.

We also found that nutrient loading increases affected many different qualitative aspects of a CoTS outbreak: they had significant impacts on outbreak length, frequency and severity (Figure 3.4). In particular, we found that increasing nutrient input could cause an abrupt shift from discrete CoTS outbreaks of a few years each to continuous presence of CoTS on a reef (Figure 3.4b). Greater nutrient input also resulted in higher CoTS populations overall, particularly in areas with slow currents (Figure 3.4a), although this relationship tended to plateau at intermediate values of q. Furthermore, the threshold

of nutrient input that was necessary for CoTS survival was very low (Figure 3.4c), even though the survival of CoTS larvae was assumed to have significant dependence on nutrient availability ($k_S = 30$). We additionally found a boundary between regimes where CoTS larvae would be retained locally and where they would mostly be swept out of the system on the currents, which occurred when local currents were about 1.5 times the strength of those on the Great Barrier Reef (Figure 3.4). In terms of general trends, we found that at low rates of both fishing and nutrient loading, the primary determinant of CoTS outbreak severity was nutrient loading rate, while when both rates were high, fishing rate became the more important one (Figures 3.3 and 3.4).

3.5.3 Four different CoTS management strategies can effectively protect coral, even on highly stressed reefs

For simulations of the Great Barrier Reef, we found that each of the four CoTS management criteria (i.e. Φ_{Avg}, Φ_{CoTS}, Φ_{Rec} and Φ_{Spr}) was effective as a way to prioritize patches for CoTS removal. The four criteria did about equally well in this regard, and CoTS densities in the simulations where 20 out of 100 patches were actively managed were significantly lower than in simulations without management, particularly after the first outbreak wave (Figures 3.5 and B.1a). However, local CoTS densities were different over the course of an outbreak depending on which strategy was used. Prioritization based on promoting coral recovery or minimizing CoTS spread resulted in outbreaks in which most patches had minimal or no CoTS presence, aside from a small number that were "triaged" and had relatively abundant CoTS populations (Figures 3.5c and 3.5d). In contrast, prioritization based on CoTS density caused more patches to have some CoTS presence, but the maximum local CoTS density at any given time to be lower (Figure 3.5b).

In our simulations that applied the CoTS management strategies used on the Great Barrier Reef to Cebu City and Jeddah, we found that active removal of CoTS over intermediate spatial scales (5 to 50 km^2 of offshore reef areas) can substantially increase coral cover (Figures 3.6a and 3.6c). The incremental benefit for coral tended to saturate as the number of managed patches increased, an effect that was stronger in Jeddah; the relationship in Cebu City between coral cover and number of patches managed was more linear. We also found little additional benefit when the list of patches to be actively managed was updated weekly rather than monthly, indicating that removing CoTS over a greater area is a more efficient use of resources than surveying managed reefs more frequently.

When evaluating which of the four CoTS management strategies did the best at maintaining coral cover, we found a clear pattern in Cebu City. There, prioritizing patches

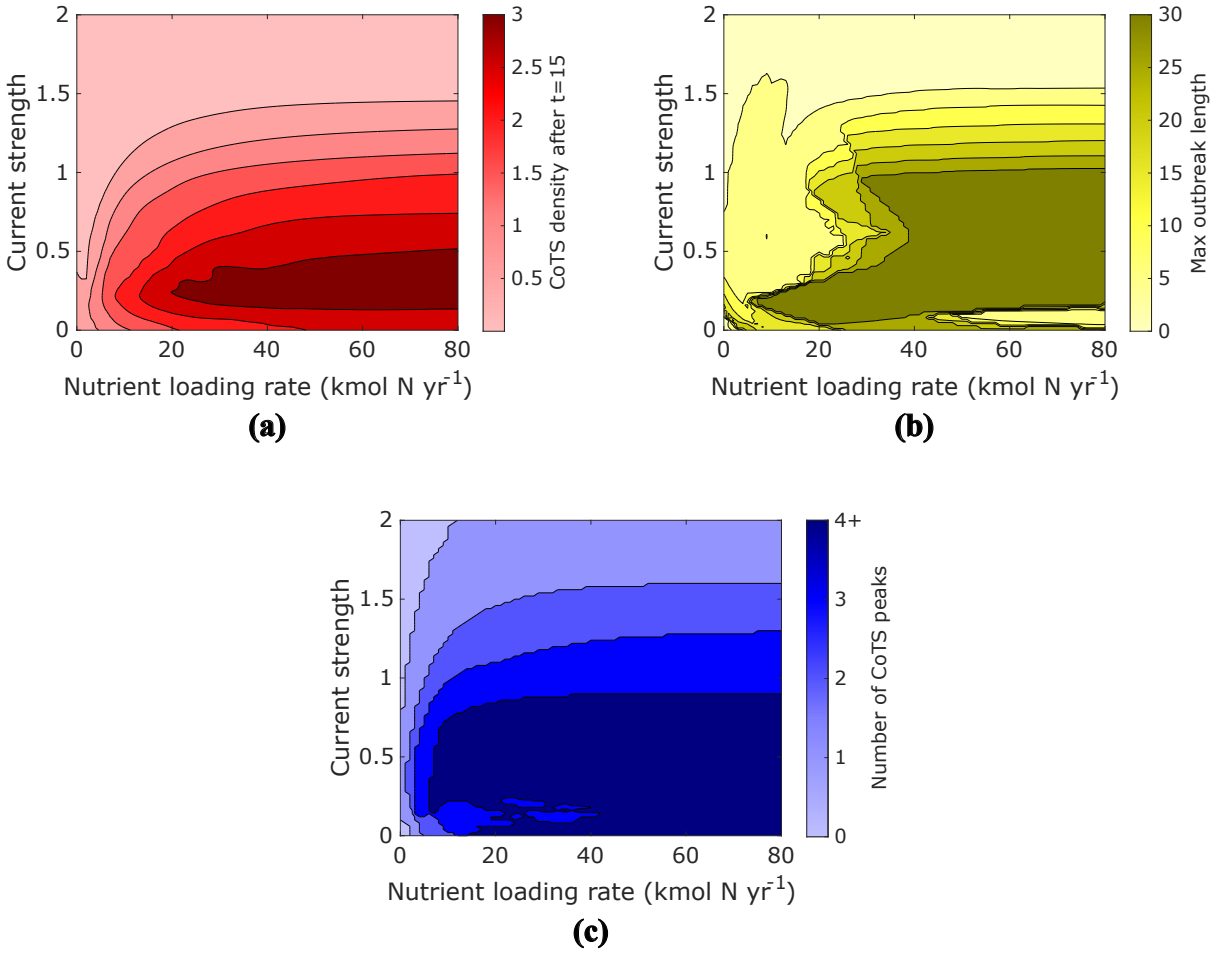

Figure 3.4: Graphs showing model behaviour for different values of q and k_{curr}. Figure 3.4a shows the average density of CoTS throughout the system after time $t = 15$ years, the approximate end of the first simulated outbreak. Figure 3.4b shows the maximum length of an outbreak in years, defined as when the systemwide average CoTS density is above 1. (High values suggest continuous presence of CoTS in most areas of the system.) Figure 3.4c shows the number of discrete peaks in CoTS density over 50 years after the start of the initial outbreak, i.e. the number of outbreaks within that timespan.

based on preventing CoTS spread resulted in the most coral when the number of managed patches was low, but prioritization based on promoting coral recovery became the best strategy when an intermediate number of patches could be actively managed, and increasing the number of managed patches further caused the averaged strategy to become

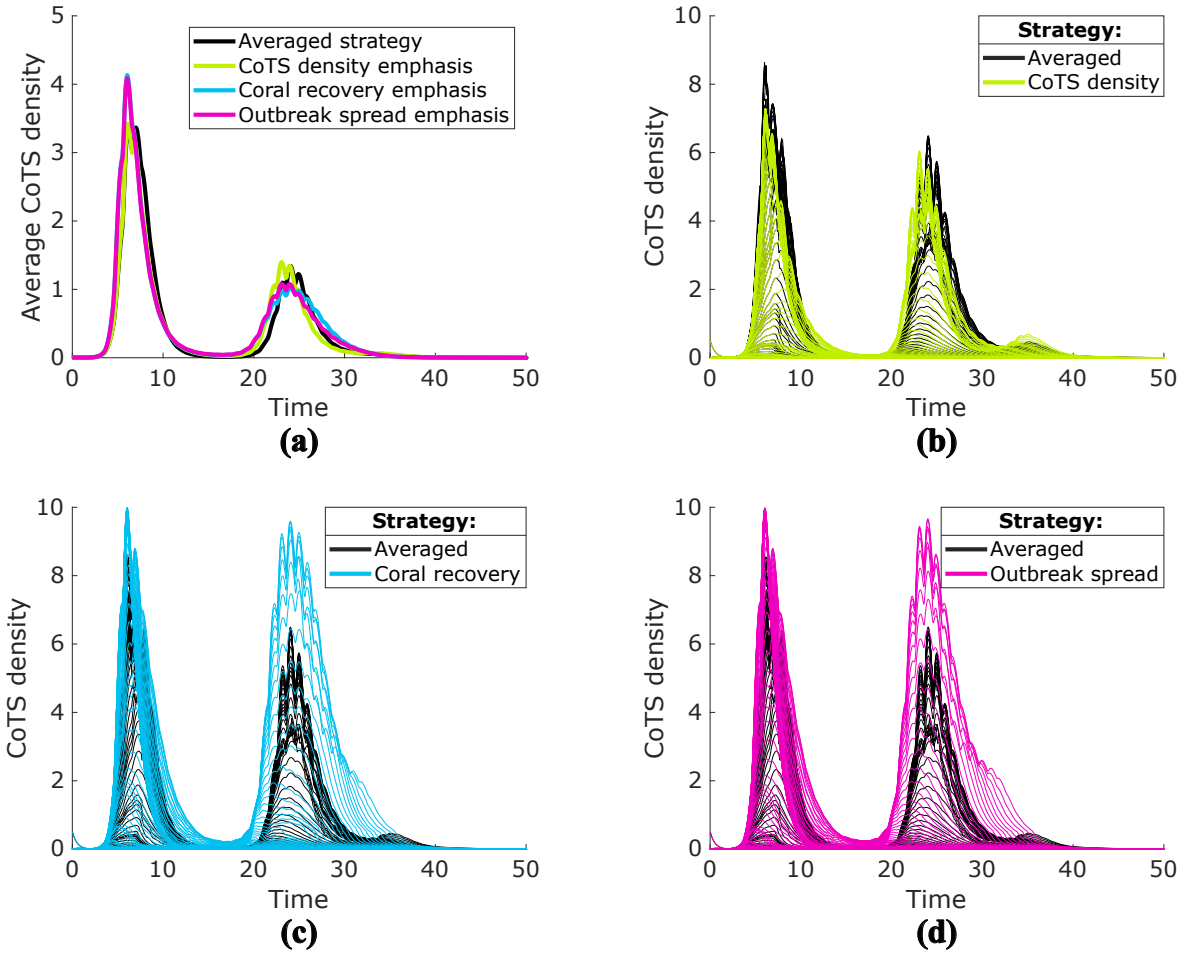

Figure 3.5: Effectiveness of different management strategies at controlling CoTS populations on the Great Barrier Reef. Figure 3.5a shows average CoTS density across 100 patches when each of the four different management strategies is applied (i.e. management using Φ_{Avg}, Φ_{CoTS}, Φ_{Rec}, and Φ_{Spr}). Figures 3.5b, 3.5c and 3.5d show CoTS densities in individual patches for the averaged strategy and each of the three others, demonstrating their different local-scale effects.

optimal (Figure 3.6b). However, this pattern did not emerge in Jeddah, where the strategy producing the most coral cover was usually to focus on the patches with the greatest capability to spread a CoTS outbreak, and occasionally to focus on patches with a high probability for coral to recover (Figure 3.6d). Focusing on patches with the highest CoTS densities did not maximize coral cover in any of our simulations.

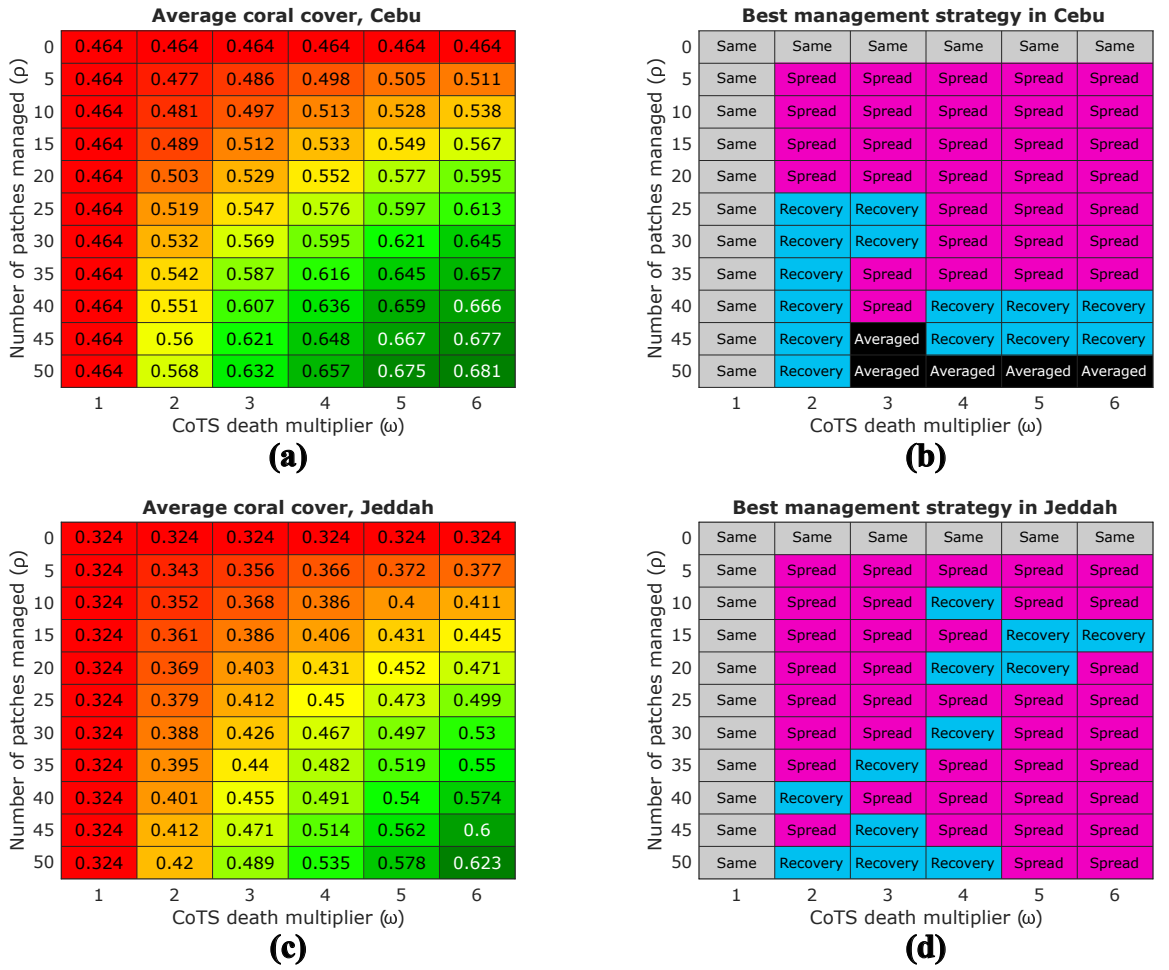

Figure 3.6: Average coral cover when applying the averaged CoTS management strategy in Cebu and Jeddah, as well as which of the four management strategies (averaged, CoTS focus, recovery focus, and spread focus) results in the most coral cover. Results are shown for different numbers of patches in which CoTS are actively removed (ρ), as well as different values for how effective active management is at boosting CoTS mortality (ω). Cases where $\rho = 0$ and $\omega = 0$ are included for comparison.

In Cebu City, we found that active removal of CoTS in 20 percent of patches, as chosen by the averaged management criterion, resulted in decreases in systemwide CoTS density that were often substantially more than 20 percent (Figure 3.7a). We also found that introducing a marine protected area in Mactan and restricting growth there had a substantial effect on reducing CoTS presence, as it did with increasing coral cover, and that

active CoTS removal had a significant additive effect when applied to a system with this MPA. Combining these two conservation strategies (instituting an MPA with development limits as well as actively removing CoTS) led to maximum local CoTS densities in Cebu City that were comparable to those in the case with no population growth and hence no growth in q and h_H (Figure 3.7b).

In Jeddah, we found that active CoTS removal in patches corresponding to 10 to 30 percent of the simulated coastline significantly decreased local CoTS densities between outbreak peaks (Figures 3.7c and 3.7d), and hence mitigated the potential problem of continuous CoTS presence. Another effect of management was to delay the peak of the initial outbreak following CoTS establishing itself in the system. However, we also found that increasing the number of actively managed patches in Jeddah sped up CoTS outbreaks, causing them to have a higher frequency (Figure 3.7c).

3.6 Discussion

Our model is, to the best of our knowledge, the first attempt to simulate crown-of-thorns starfish outbreaks in specific areas outside the Great Barrier Reef. We build on previous local-scale [175, 18] and regional-scale [251, 160] CoTS models by obtaining results for regions that feature less in the literature, but where CoTS outbreaks are nonetheless on the rise. This improves prospects for predicting the characteristics of outbreaks across the entire range of CoTS, as well as evaluating strategies for managing them.

3.6.1 Policy and management recommendations

Our model predicted that CoTS removal programs on an intermediate spatial scale, between 5 and 50 km^2 of offshore waters, could lead to improvements in coral health over larger areas (Figure 3.6). These figures are within the range of areas covered by previous CoTS control efforts [198]. While the spatial scale that we suggest for management is near the high end of this range, we note that recent improvements in CoTS removal (e.g. [33, 1]) likely indicate that CoTS removal has become more efficient in terms of time and money than it has been previously. Additionally, it has been observed that CoTS management projects over smaller spatial scales have met with little success in controlling CoTS populations over wider regions [198], echoing our recommendations for an intermediate-scale approach.

When testing the effectiveness of the four different CoTS management criteria introduced above, we found a clear pattern in Cebu as to which strategy was best at preserving

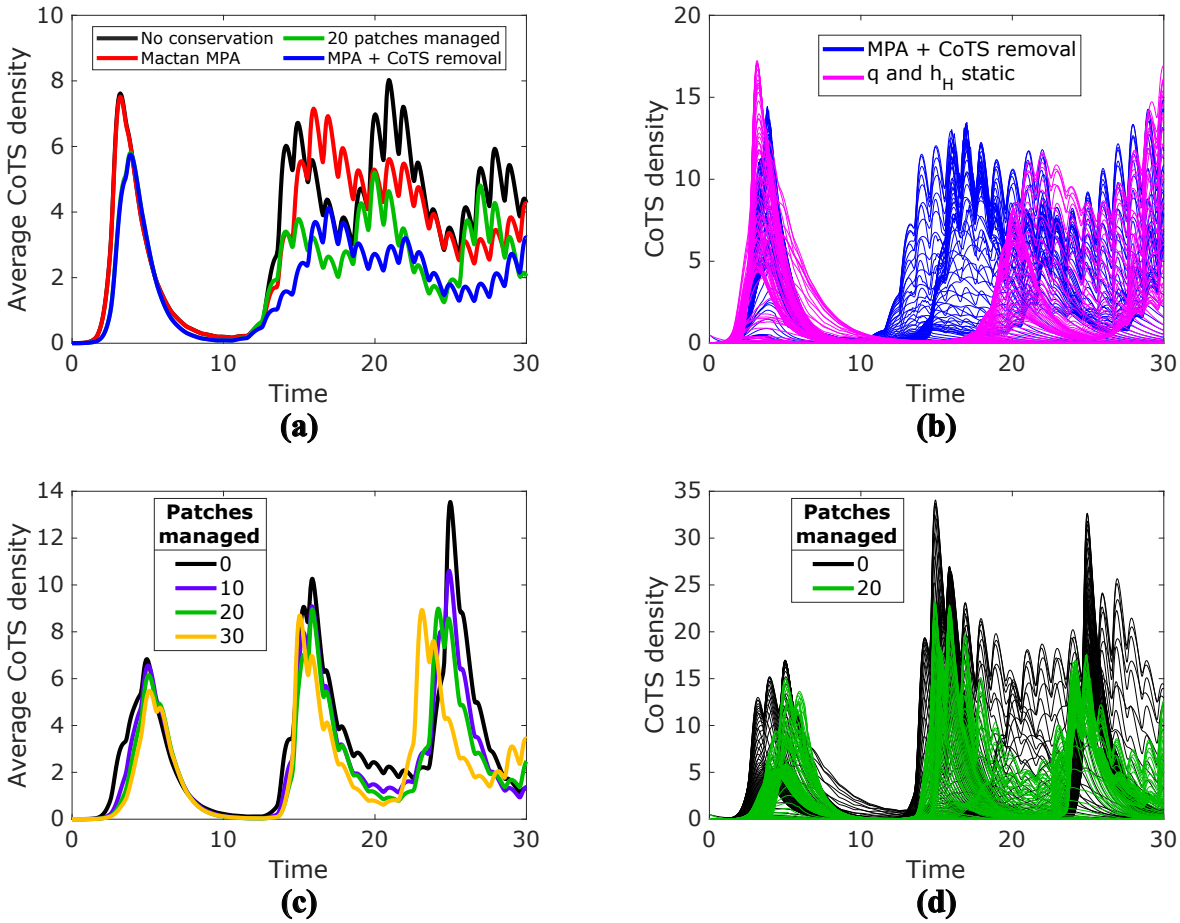

Figure 3.7: Effects of active management in Cebu and Jeddah on CoTS density. Figure 3.7a shows average CoTS densities in Cebu when 20 patches are actively managed and/or an MPA and growth restrictions are established in Mactan, compared to a baseline without conservation efforts. Figure 3.7b shows local CoTS densities in Cebu with both active CoTS management and an MPA, compared to a case where q and h_H remain at 2020 levels. Figure 3.7c shows the temporal effects of increasing the number of managed patches in Jeddah (using the averaged strategy). Figure 3.7d shows local dynamics in Jeddah for the cases with 0 and 20 actively managed patches. $\omega = 2$ in all subfigures.

coral. There, focusing on patches with high propensity to spread CoTS resulted in the most coral when resources were very limited, but when more patches were able to be managed, focusing on patches where the coral had the best prospects for recovery was better (Figure 3.6b). This has an intuitive explanation. If CoTS can only be actively removed from a

small number of patches, then preventing its spread into patches that cannot be managed protects the coral in those patches; this is similar to targeted spread prevention strategies in epidemiology (e.g. [264, 5]). However, if resources are available to remove CoTS in more patches, then CoTS from a patch being actively managed has a higher likelihood to disperse its larvae into another managed patch. In that case, preventing the spread of CoTS becomes less pressing, and expending resources protecting areas with conditions favourable to coral regrowth becomes a better strategy. This same pattern did not occur in Jeddah (Figure 3.6d), which was also due to patch connectivity. In the Red Sea, currents are much slower than in the Philippines, so dispersal ability of CoTS larvae is generally lower; this means that it is more important to focus on the few patches that do have significant ability to send CoTS larvae to other areas of a reef.

Although the strategy of removing CoTS in patches with the highest CoTS densities (i.e. prioritizing patches using Φ_{CoTS}) did not maximize coral cover in any of our simulations (Figures 3.6b and 3.6d), it did produce dynamics that were significantly qualitatively different than the strategies focusing on promoting coral recovery (i.e. using Φ_{Rec}) and preventing CoTS spread (i.e. using Φ_{Spr}). Specifically, removing CoTS from the patches in which their density was the highest prevented any patches from reaching very high levels of CoTS presence (as some did under the recovery and spread strategies), while keeping the systemwide average CoTS density close to those produced by the other management strategies (Figure 3.5). This indicates that the management strategy focusing on CoTS density is useful for avoiding the risk of any area of a reef having dangerously high CoTS levels. We also found that the averaged strategy (i.e. prioritizing patches using Φ_{Avg}) did well in promoting coral cover (Figures 3.6a and 3.6c), showing that it is also a viable option. We therefore conclude that all four of the tested strategies can be useful under certain circumstances. In particular, we recommend prioritizing patches for CoTS removal based on promoting coral recovery if substantial resources are available for conservation, based on preventing CoTS spread if resources are limited or if connectivity between parts of a reef is low, based on limiting local CoTS density if preventing severe outbreaks is the most important objective, and using an average of those three if a more holistic strategy is desired.

In addition to active removal of CoTS from vulnerable areas of a reef, we also recommend another strategy for protecting coral from the harmful effects of CoTS. In our simulations, we found that restricting urban development along the east coasts of Mactan and Cordova, near Cebu City, and establishing an MPA there resulted in greater recovery potential for coral and lower CoTS densities (Figures 3.7a, 3.7b, and B.2a). This is supported by previous findings on how MPAs on the Great Barrier Reef can reduce the susceptibility of coral to CoTS outbreaks by strengthening trophic cascades favourable to

coral [234, 251]. Furthermore, establishing an MPA and restricting urbanization at this particular location would allow for a stretch of coastline in a relatively natural state, forming a gap in between heavily built-up areas on either side. This could preserve connectivity between marine habitats outside the Cebu City area, and therefore enhance the stability of reefs outside our study area (see e.g. [233]). This includes the coral reefs of the nearby Olango island group. As some areas in these islands, such as the waters around the islands of Caohagan, Nalusuan, and Gilutongan, are already protected [12], establishing a large MPA along the coasts of Mactan and Cordova could increase the ability of species in these smaller, already existing MPAs to reinforce each other by way of the spillover effect (see e.g. [43, 69]).

We note that our results on the effectiveness of this proposed MPA were obtained when the spatial distribution of fishing boats θ_{B_i} for each patch i had a large standard deviation of 1, indicating high amounts of nonlocal fishing (and therefore lax MPA boundary enforcement). This means that if the boundaries of this MPA were rigidly enforced, its benefits for coral would likely be even stronger. We also note that in a recent survey of Philippine reefs, reefs in the two MPAs in the survey that were closest to Cebu City were not overfished, whereas a clear majority of reefs in the survey (inside and outside MPAs) were overfished. This was reflected in our initial conditions; if we took a higher initial value of h_H in our simulations of coral around Cebu City, pressure from population growth would have likely led to values of h_H that would cause a collapse in fish and coral populations before 2050 (Figure 3.3). This further increases the importance of protecting large offshore areas near Cebu City, as the margin for error regarding future reef ecosystem collapse is likely to be small.

3.6.2 Multi-stressor interaction and ecological shifts

Our results suggest specific ways in which both fishing and nutrient loading can alter the characteristics of CoTS outbreaks (Figures 3.3 and 3.4). Previous work has outlined the trophic cascades that can occur upon fishing of predators of CoTS [18]; we build on this by showing that harvesting of fish species with no direct trophic connection to CoTS can have profound effects on CoTS and coral populations. We found that a relatively steep dropoff in coral cover occurred in systems with CoTS at fishing rates of approximately 30 percent, compared to more gradual declines in systems without CoTS (Figure 3.3). Similar fishing rates resulted in state transitions in other models that were formulated differently and did not feature CoTS [28, 242], suggesting a level of herbivorous fish abundance below which coral reef ecosystem functioning is significantly diminished. We also found that increases in nutrient loading can shift a reef from a state where outbreaks are periodic to one in

which CoTS are continuously present in at least some local areas. Local observations in the Philippines have noted that CoTS outbreaks have recently become an ongoing problem there [65], in line with these predictions.

Another significant pattern that emerged in our results was the fact that when harvesting and nutrient loading rates were both low, nutrient loading was the primary driver of CoTS outbreak severity, but when both rates were high, harvesting rate was more important (see Figures 3.3 and 3.4). As a region urbanizes, fish harvesting and nutrient input both go up (e.g. [226, 219]). Our results therefore predict that the relative impacts of overfishing and nutrient loading on the severity of a CoTS outbreak can shift during the urbanization process. We therefore recommend that dynamic strategies should be used to manage CoTS, as future processes such as urban growth may change which factors are most important to mitigate for the prevention of large-scale CoTS outbreaks.

We found that continually increasing both the fishing rate h_H and the nutrient loading rate q in systems with CoTS present leads to significant shifts in reef dynamics (Figure 3.2), due to the changing interaction between these two processes over time. As nutrient loading is projected to increase more quickly than fishing rate in Cebu and Jeddah, the initial effect of rises in nutrient loading is to produce surplus macroalgae that will be eaten by herbivorous fish rather than overgrow coral. This is consistent with field data showing that herbivorous reef fish have a diet preference for macroalgae rich in nitrogen and phosphorus [96, 221]. Hence, our model predicted that the short-term dynamics in our study areas (a small increase in h_H and a larger one in q) would lead to higher herbivorous fish populations, less overgrowth of coral by macroalgae, and hence faster coral recovery after crown-of-thorns starfish outbreaks. Previous field studies have found that the presence of large, commercially valuable fish is correlated with increased coral resilience to CoTS outbreaks [73, 119], and our model demonstrates a case where this relationship can arise.

However, the model also predicted that this coral recovery would be short-lived. This was because the increases in q also meant greater CoTS larval survival, leading to more rapid outbreak onsets and greater long-term presence of CoTS. Additionally, further increases in fishing rate caused the herbivorous fish population to decline via fishing faster than it could grow due to increases in food availability (see Figure 3.3). This meant that macroalgae became the main beneficiary of additional nutrients at high fishing rates, and hence caused coral populations to increase in variability, as coral was overgrown more quickly during periods of the year when it was not spawning. This result demonstrates the possibility of complex, temporally-varying interactions between multiple reef stressors. It is also in line with our general finding that as urbanization increases, fishing rate becomes more important as a determinant of coral health and CoTS outbreak severity. Significant interaction effects between overfishing and nutrient loading have been observed before in

the field [93, 274], and a recent study has shown that overfishing and nutrient loading can switch between having synergistic and antagonistic interaction effects depending on the level of sedimentation (a third stressor) in the system [85]. Our work demonstrates that CoTS may act on other stressors in a similar way, and hence that areas where both nutrient loading and fishing rates are expected to increase may experience significant ecological shifts due to changing patterns of multi-stressor interaction.

3.6.3 Study limitations and future work

When simulating future dynamics in our focus cities, we fit some aspects of the model based on observed regional data, owing to the lack of availability of finer-grained measurements. As our model has the capability of specifying local parameters at a resolution of 1 km, we believe that if remote sensing data on features such as coral cover and current strength is available, parametrizing the model using such data would further enhance prediction accuracy. Likewise, remote sensing data on phytoplankton blooms could be used to fit local nutrient availability; see [237] for a good example of how nutrient-phytoplankton interactions can be mathematically modelled. However, many of the trends captured by our study, such as the shift to continuous CoTS presence on reefs with increased nutrient input, the sharp dropoff in coral cover on reefs with CoTS at intermediate fishing rates, and the effectiveness of controlling the spread of CoTS larvae, occurred regardless of regionally-varying inputs. Thus, we believe that our conservation and management predictions can be generalized to reefs throughout the Indo-Pacific region, albeit with variation due to present local conditions.

While studying multi-stressor interaction as it pertains to CoTS, we chose to focus on overfishing and nutrient loading due to their large potential impact on CoTS outbreaks. However, there exist other anthropogenic coral reef stressors that we did not examine in this paper. Some of these, such as coral bleaching, ocean acidification, and increased hurricane frequency, are linked to greenhouse gas emissions and climate change [193, 36]. Future work will determine how these additional stressors will affect CoTS outbreaks and coral's resilience to them, both for each stressor individually (to isolate its effects on CoTS) and for the aforementioned stressors together (in order to evaluate the multifaceted changes brought on by ocean temperature increases).

Chapter 4

Reef fish functional groups show variable declines due to deforestation-driven sedimentation, while flexible harvesting mitigates this damage

This chapter is based on the paper: RA Milne, CT Bauch, M Anand. 2022. Deforestation-driven sedimentation causes variable abundance declines across reef fish functional groups, which are mitigated by flexible harvesting. In preparation.

4.1 Abstract

Sedimentation is a major coral reef stressor, with immediate effects that include degradation of algal turf into a less productive form that suppresses herbivory. This puts pressure on reef fish populations, as well as the fisheries that harvest them. Deforestation causes much sedimentation on reefs, and is an ongoing concern in Pacific island states. Although ecosystem processes such as deforestation and fish population dynamics are usually far from equilibrium, analyses of reef fish vulnerability to deforestation that explicitly consider time-dependent effects are rare. Additionally, optimization methods for fisheries on heavily sedimented reefs are generally unexplored. Here, we construct a model coupling four reef fish functional groups with seabed dynamics and deforestation, fit using data for the Solomon Islands. We show that with predicted human population increases, highland deforestation could cause herbivorous and omnivorous fish abundances to halve within 15 to 30 years, and many fish taxa to collapse within 50 years, but that piscivorous fish and top predators are resilient to lowland deforestation. We demonstrate that flexible approaches to fishing could lead to high and temporally stable populations of herbivorous fish and top predators, offsetting stress caused by sedimentation and deforestation. We additionally show that if future human population growth causes both deforestation and increased fishing demand, future reef fish stock sizes will be unlikely to satisfy fishing demand, with local extirpation possible in the medium-term. Our results provide sustainability guidelines for reef fisheries, and demonstrate nonlinear interactions between overfishing and deforestation that may result in unforeseen ecological surprises.

4.2 Code availability

The code for simulating the model is available on Zenodo (DOI: 10.5281/zenodo.7036364).

4.3 Introduction

Sedimentation is projected to be a serious cause of coral reef degradation in the future [79, 206, 95], with a large number of reef-associated species being affected, including many reef fish taxa [262]. Much of the sediment exported onto reefs is produced either directly or indirectly by deforestation [156], and deforestation itself has been mentioned as a threat to reef fish [103]. Hence, overexploitation of local forest resources could lead to substantial declines in fish populations on adjacent reefs. However, different fish functional groups are

likely to experience different amounts of pressure. In particular, the timing of when different functional groups can be expected to decline following deforestation is still relatively unexplored. Because of the dependence of many coastal communities on reef fisheries for food [224], the effects of deforestation could additionally include a collapse in fish catch and subsequent food shortages. Therefore, optimization of fishing strategies on reefs with heavy sedimentation is a pressing concern. Here, we construct a land-sea model of intermediate complexity linking four fish functional groups, seabed dynamics, and forest cover, specifically parametrized to represent the Solomon Islands. We use this model to predict which functional groups will be most and least threatened by deforestation and its accompanying sedimentation, when these fish populations will be expected to decline to critical levels, and how fishing strategies on reefs under stress due to deforestation can be improved to ensure sustainable catches. Our results can aid in establishing which fish taxa should be paid the closest attention to in areas where deforestation is anticipated, as well as setting guidelines for safe fishing and logging levels that would minimally jeopardize reef fish.

Sediment washed onto reefs comes in large part from soil erosion [21], and cleared land tends to have significantly higher rates of erosion compared to forests [187, 261]. Hence, deforestation has been identified as a major cause of reef sedimentation [156]. When algal turf on the seabed becomes laden with sediment, it undergoes a qualitative shift to a form that is less productive and less palatable to herbivorous fish, known as "long sediment-laden algal turf" (LSAT) or a "turf algal sediment mat" [95, 240]. This results in suppression of herbivory on the algal turf, which is due to different mechanisms that vary across types of herbivorous fish based on their dental morphologies. (For instance, those with scraping teeth avoid LSAT because they would have to ingest sediment with low nutritional value when they scrape algae off the seabed.) This can lower herbivorous fish numbers [240], as herbivorous reef fish are particularly susceptible to bottom-up control [214]. This means that through land-sea linkages, deforestation has the potential to severely impact reef fish populations. Because of the potential magnitude of these long-range effects of deforestation, "ridge-to-reef" models have recently begun to be developed, in order to predict how forest clearance and other terrestrial drivers will affect future health of coral reefs (see e.g. [67, 263]).

Many existing ridge-to-reef models are static, offering a snapshot in time of what conditions on reefs may be like under different deforestation and management scenarios. However, linking deforestation to the health of coral and fish communities involves considering many interwoven processes, which may happen on different timescales [32, 217] and will often not be at equilibrium. For instance, deforestation does not necessarily happen at a constant rate [91], as the demand for cleared land or forest products that underpins it may vary. Another example of this is the differing life history strategies of fish species. Marine

fish taxa can be categorized based on factors such as lifespan and reproductive rates [139], with the implication that the population growth rates of reef fish can substantially vary due to these traits. These life history differences bear with them different levels of susceptibility to different stressors: slow-growing, long-lived species are particularly susceptible to rapid depletion due to overharvesting (see e.g. [158]), while declines in species with more rapid life history traits were seen in an Atlantic fish community following increases in ocean temperature [166]. As a result, in addition to anticipating future reef conditions, management plans must understand how quickly and in which order the events that lead to them take place. The importance of using insights from static models to inform dynamic biophysical ones has been highlighted [67], as ecosystem management benefits most from using a combination of these tools.

Deforestation has been identified as a significant environmental concern in the West Pacific and Southeast Asia in the past decades [91, 250]. The trend of deforestation within this region has manifested itself in the Solomon Islands: logging there has been estimated at seven times the sustainable yield [92]. Hence, concerns have been raised about forest loss on several of that country's constituent islands, such as Guadalcanal [10], Kolombangara [133, 261], and Rennell [123]. Of particular concern is logging on steep slopes and in highland areas, such as those found in the interior of Kolombangara [261], which has been described as a pervasive problem in the Solomon Islands [90, 102]. This is because erosion (and therefore sediment generation) can happen at a greater magnitude on such terrain [210, 223], particularly in areas where logging or other human disturbances take place [108, 278]. However, past deforestation on the Solomon Islands has been spatially uneven, and many areas still have close to complete forest cover [92, 124]. Therefore, it is important to establish expectations for how large-scale deforestation in these areas could affect local reef fish populations before it happens.

It is well-known that reef fish assemblages can be significantly negatively impacted by human activity [37]. Clear-cutting of mangroves can alter fish assemblages [222], in particular by harming the fish species that use mangroves as nurseries. In a similar example in riparian habitats, deforestation along the banks of streams reduces niche diversity among stream fish by homogenizing the landscape [275]; this has been accompanied by shifts to more sediment-tolerant species [130, 128]. Additionally, sedimentation from offshore construction has been shown to change community composition on a coral reef over a long timescale [230]. Recent studies have begun to examine how sedimentation due to inland deforestation affects the populations of different reef fish taxa [67, 263], although this work has mostly covered different groupings of herbivorous fish rather than the fish elsewhere in a coral reef food web. Therefore, ridge-to-reef models could be further used to predict population changes of many different reef fish functional groups, to provide a

holistic evaluation of fish assemblage changes.

Coral reef fisheries represent one of the main food sources in tropical island states [224]. However, many of these countries, among them the Solomon Islands, are projected to experience substantial human population growth in the next few decades [248]. This can be expected to put pressure on local fish populations. The intuitive result that more population means greater demand for fish has been observed as both increasing fishing effort over time in growing areas [219] and a correlation between population density and fishing effort [232]. These fishing rate increases will likely come in tandem with additional deforestation: empirical relationships between the population of an area and its forest cover have been obtained from observations in many different parts of the world (see e.g. [236, 253, 138]). Previous studies on multiple coral reef stressors have found that overfishing and sedimentation can have significant interaction effects [85, 74]. This suggests that through its effects on sedimentation, deforestation could have sizable long-term impacts on fisheries yield. In other words, overharvesting of one resource (forest) can potentially also lead to shortages in another one (reef fish). Hence, the maintenance of fisheries after shifts to heavily sedimented conditions has been mentioned as a priority for research [240].

4.4 Methods

4.4.1 Model building

Seabed state transitions

To model how deforestation and the sediment buildup associated with it could affect reef fish populations and the viability of harvesting them, we adapted a model of Fung *et al.* [89]. We chose this particular coral reef model because it includes a compartment for turf algae, which we make use of in our investigation of fishing potential on algal turf-dominated reefs, and because the authors included estimations of how sedimentation could affect the model parameters as part of their original derivations. This model features state transitions between coral C, turf algae T, macroalgae M, and open space Q on a seabed; as the total seabed area is constant, space is defined as $Q = 1 - C - T - M$. The original equations in [89], which we retained, are below:

$$\begin{aligned}
\frac{\mathrm{d}C}{\mathrm{d}t} &= \left(l_{C}^{s} + l_{C}^{b} C\right)\left(Q + \varepsilon_{C} T\right) + r_{C}\left(1 - \beta_{M} M\right)\left(Q + \alpha_{C} T\right) C - d_{C} C - \gamma_{MC} r_{M} M C \\
\frac{\mathrm{d}T}{\mathrm{d}t} &= \zeta_{T}\left(1 - \theta\right) Q - g_{T} \theta T - \varepsilon_{C}\left(l_{C}^{s} + l_{C}^{b} C\right) T - \alpha_{C} r_{C}\left(1 - \beta_{M} M\right) T C - \gamma_{MT} r_{M} M T \\
\frac{\mathrm{d}M}{\mathrm{d}t} &= r_{M} M\left(Q + \gamma_{MC} C + \gamma_{MT} T\right) - g_{M} \theta M
\end{aligned} \tag{4.1}$$

Here, turf algae can overgrow open space, coral can overgrow space and turf, and macroalgae can overgrow all other components. Coral larvae are produced by local brooding corals at a rate l_{C}^{b}, and by exogenous spawning corals (outside the spatial scope of the model) at a rate l_{C}^{s}. These larvae can settle on open space or algal turf, with ε_{C} being the relative rate at which coral larvae settle on turf relative to open space. Coral can also take up more space by undergoing lateral expansion, which happens at a baseline rate r_{C}. As with larval recruitment, coral can laterally expand into open space or turf, with α_{C} being the relative rate at which coral expands into algal turf compared to open space (analogous to ε_{C}). Additionally, coral lateral expansion is suppressed by the presence of macroalgae according to a factor β_{M}. Coral dies at a rate d_{C}, at which point the space it takes up reverts to being empty. Algal turf expands over space at a rate ζ_{T}, which is scaled down according to a unitless quantity θ between 0 and 1 representing grazing pressure; existing algal turf is also cleared by grazing at a rate $g_{T}\theta$, where g_{T} is the maximum rate at which turf is grazed (for scaling). Macroalgae has an intrinsic rate of growth r_{M}, and is grazed at a rate $g_{M}\theta$ analogous to the rate for algal turf (i.e. g_{M} is the maximum yearly rate that macroalgae is removed due to grazing). Macroalgae can expand over coral and turf. It does so according to the relative rates γ_{MC} and γ_{MT}, respectively, which are normalized according to its rate of expansion into open space (as with ε_{C} and α_{C}). Because we expanded this model to explicitly include the processes of herbivory and sedimentation, we took θ, r_{C}, l_{C}^{b}, l_{C}^{s}, and d_{C} to vary rather than being constant (see below). All other model features were kept identical to those in [89].

Fish trophic interactions

To this model, we added four different fish functional groups: herbivores (e.g. *Scarus dimidiatus*), omnivores (e.g. *Acanthurus triostegus*), piscivores (e.g. *Epinephelus merra*), and top predators (e.g. *Sphyraena forsteri*). All functional groups were assumed to follow logistic growth, with intrinsic growth rates of r_{H}, r_{O}, r_{P}, and r_{Z}, respectively, and carrying capacities of 1. Each functional group's growth rate was further scaled according to food availability, representing predator-prey interactions. Fish were assumed to be harvested at rates h_{H}, h_{O}, h_{P}, and h_{Z}, and all fish functional groups aside from top predators were

assumed to die due to predation at rates m_H, m_O, and m_P. (Death of top predators due to natural causes is contained in the logistic growth function.) As with the growth rates, the death rates for each functional group were scaled according to the abundance of predators of that functional group.

Since turf algae and macroalgae were assumed to be grazed at rates g_T and $g_M \leq g_T$, respectively, it can be further assumed that the relative proportions of turf algae and macroalgae consumed by grazers (such as herbivorous fish) can be represented with the ratio $\frac{g_M}{g_T} \leq 1$. Hence, we took $T + \frac{g_M}{g_T} M \leq 1$ as the scaling term for herbivorous fish growth. As rates of herbivory are negatively impacted by accumulation of algal turf sediment [94, 241], we introduced another quantity $\mu(t)$ representing this decrease, which depends on sediment quantities on the seabed (see below). We assumed that herbivorous fish would be eaten by piscivorous fish and top predators, with δ_P denoting the percentage of the diet of piscivores made up by herbivores and δ_Z^H denoting this percentage for top predators. This meant that our scaling constant for herbivorous fish predation was taken to be $\frac{\delta_P F_P + \delta_Z^H F_Z}{\delta_P + \delta_Z^H} \leq 1$. Therefore, after also accounting for the harvesting term $-h_H F_H$, we represented the differential equation for herbivorous fish as follows:

$$\frac{\mathrm{d}F_H}{\mathrm{d}t} = \frac{r_H}{1+\mu} F_H \left(1 - F_H\right) \left(T + \frac{g_M}{g_T} M\right) - h_H F_H - m_H F_H \frac{\delta_P F_P + \delta_Z^H F_Z}{\delta_P + \delta_Z^H} \tag{4.2}$$

The diet of omnivorous fish typically consists partly of primary producers (e.g. algae) and partly of other food sources such as zooplankton and small invertebrates [88]. We defined δ_O as the percentage of an omnivorous fish's diet consisting of algae, and assumed that omnivorous fish would consume turf algae and macroalgae at the same relative rates as herbivorous fish. This was scaled down by μ in the same way as in the dynamics for herbivorous fish. This implies that $(1 - \delta_O)$ percent of an onmivorous fish's diet consists of other food sources, the availability of which we modelled using a function $\phi(t)$ (see below). As with herbivorous fish, we assumed that omnivorous fish were eaten by piscivorous fish (composing $(1 - \delta_P)$ percent of their diet) and top predators (composing δ_Z^O percent of their diet), and harvested at a constant rate. Therefore, the dynamics of omnivorous fish are represented as follows:

$$\frac{\mathrm{d}F_O}{\mathrm{d}t} = r_O F_O \left(1 - F_O\right) \left(\frac{\delta_O}{1+\mu} \left(T + \frac{g_M}{g_T} M\right) + \left(1 - \delta_O\right) \phi\right) - h_O F_O - m_O F_O \frac{(1 - \delta_P) F_P + \delta_Z^O F_Z}{1 - \delta_P + \delta_Z^O} \tag{4.3}$$

As detailed above, piscivorous fish were assumed to eat both herbivorous and omnivorous fish, in proportions $\delta_{_P}$ and $(1-\delta_{_P})$, respectively. They are, in turn, eaten by top predators and harvested. Note that the proportion of top predator diet that piscivorous fish make up is $1-\delta_{_Z}^{H}-\delta_{_Z}^{O}$. As the total predation pressure on piscivorous fish is therefore $F_{_Z}\left(1-\delta_{_Z}^{H}-\delta_{_Z}^{O}\right)$, but scaling this to values between 0 and 1 involves dividing by $1-\delta_{_Z}^{H}-\delta_{_Z}^{O}$, this constant is normalized out of the differential equation governing piscivorous fish dynamics. The differential equation in question is as follows:

$$\frac{\mathrm{d}F_{_P}}{\mathrm{d}t} = r_{_P}F_{_P}\left(1-F_{_P}\right)\left(\delta_{_P}F_{_H}+\left(1-\delta_{_P}\right)F_{_O}\right)-h_{_P}F_{_P}-m_{_P}F_{_P}F_{_Z} \tag{4.4}$$

Top predators consume fish from all other functional groups, according to the proportions mentioned above. As they lack predators by definition, the sources of their mortality are assumed to be harvesting and natural causes. This yields the following differential equation for top predators:

$$\frac{\mathrm{d}F_{_Z}}{\mathrm{d}t} = r_{_Z}F_{_Z}\left(1-F_{_Z}\right)\left(\delta_{_Z}^{H}F_{_H}+\delta_{_Z}^{O}F_{_O}+\left(1-\delta_{_Z}^{H}-\delta_{_Z}^{O}\right)F_{_P}\right)-h_{_Z}F_{_Z} \tag{4.5}$$

Fung *et al.* did not explicitly include grazer populations in their model, and hence represented grazing pressure as a constant θ. We instead use a baseline rate $\tilde{\theta}$ scaled by the population levels of herbivorous and omnivorous fish relative to their theoretical maxima, with the contribution of omnivorous fish to grazing being the proportion of their diet consisting of algae. The grazing rate also decreases as sediment levels increase, so we additionally divide by $1+\mu$ (as in the grazing terms of $F_{_H}$ and $F_{_O}$) to represent this. Specifically, we take θ to be the following:

$$\theta(t) = \frac{\tilde{\theta}\left(F_{_H}+\delta_{_O}F_{_O}\right)}{\left(1+\mu\right)\left(1+\delta_{_O}\right)} \tag{4.6}$$

Deforestation and sediment dynamics

To specifically investigate the effects of deforestation and sedimentation on reef fish populations, we added three more model components representing forest cover in land areas adjacent to the reef being modelled, concentration of suspended sediment within the water column on the reef, and concentration of sediment that has accumulated on the seabed. We represented these using the variables X (measured as a percentage), $S_{_W}$ (measured in mg cm^{-3}), and $S_{_B}$ ("B" for "benthic"; measured as a dimensionless constant), respectively. A schematic of the full model can be seen in Figure 4.1.

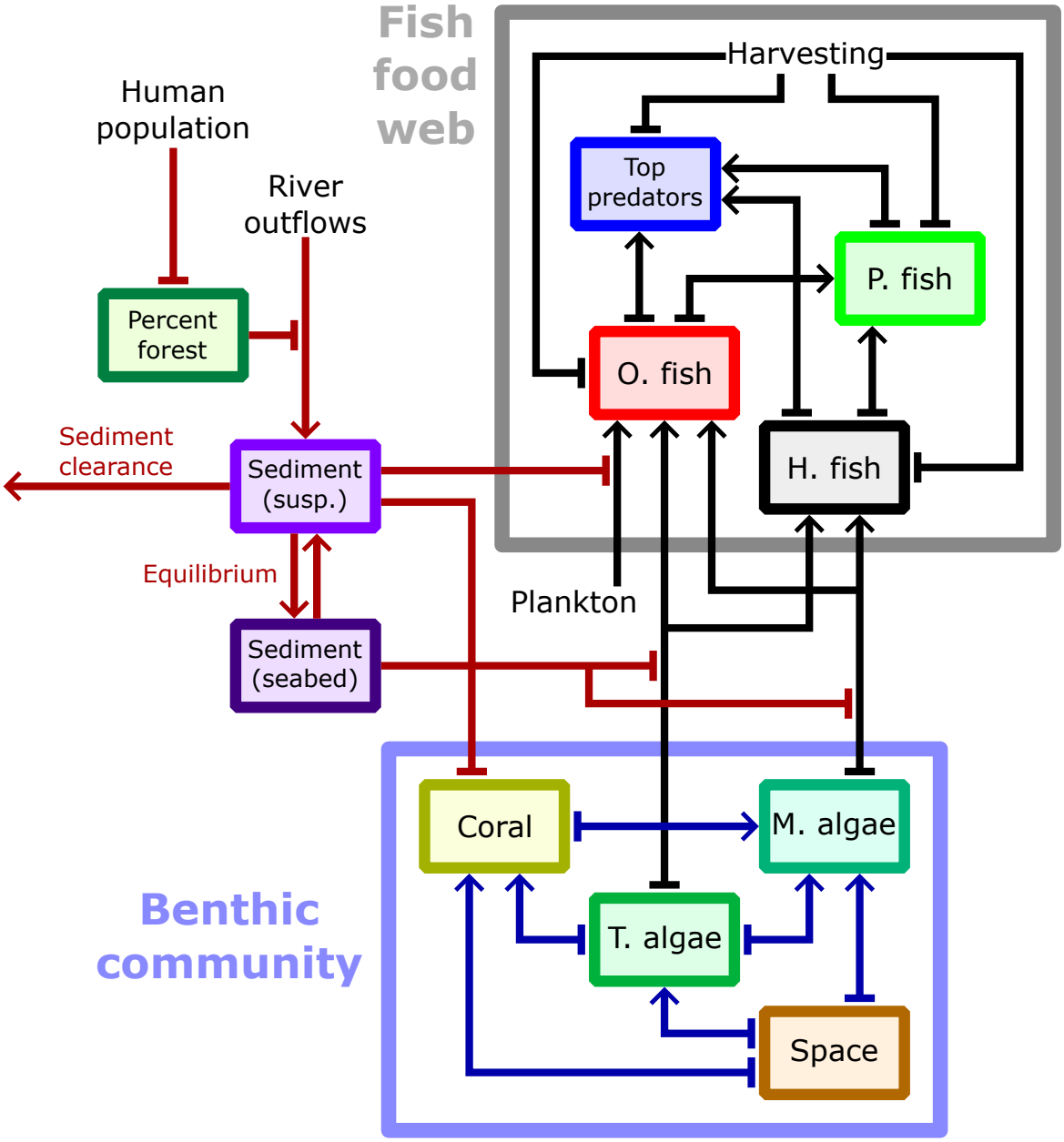

Figure 4.1: Diagram containing interactions in the model. Trophic interactions involving reef fish are shown in black, patterns of overgrowth on the benthos are shown in blue, and processes related to deforestation and sediment transport are shown in red. Pointed heads denote positive effects, while rectangular heads denote negative effects.

Changes in forest cover were modelled in a variety of different ways, to represent unmanaged deforestation and managed logging. For our baseline scenario, we assumed a steady loss of forest cover scaling with population increases. Here, we drew on the work of Tanaka and Nishii [236] which modelled the percentage change in forest cover per unit change in area population; we defined $r_{_X}$ as the linear rate of deforestation referred to as r in [236]. We used United Nations population growth estimates for the Solomon Islands [248] to obtain values for population N and population change $\frac{\mathrm{d}N}{\mathrm{d}t}$. We also assumed a background rate of forest regrowth, governed by the rate $a_{_X}$. We took the forest regrowth term to be logistic, as the rate of forest expansion into cleared land should decrease as the amount of available cleared land does; we assumed a carrying capacity of 1, or 100% forest cover. Therefore, the differential equation for forest cover, $\frac{\mathrm{d}X}{\mathrm{d}t}$, was taken to be the following:

$$\frac{\mathrm{d}X}{\mathrm{d}t} = \frac{\mathrm{d}X}{\mathrm{d}N}\frac{\mathrm{d}N}{\mathrm{d}t} + a_{_X}X(1-X) = -r_{_X}NX\frac{\mathrm{d}N}{\mathrm{d}t} + a_{_X}X(1-X) \tag{4.7}$$

Sediment export onto reefs was assumed to change due to deforestation, and specifically increase due to increased erosion when forest cover was low. The amount of sediment being deposited onto reefs due to soil erosion typically increases linearly as forest cover is reduced [187, 261]. We took $q_{_b}$ to be the baseline river sediment concentration at 100 percent forest cover, and $q_{_c}$ to represent the additional amount of sediment in rivers when all land has been cleared; both of these have units of mg cm^{-3}. We also took λ (measured in yr^{-1}) as the rate at which sediment in these rivers is exported into the water column. Once sediment is suspended in the water column above a reef, it can be washed out further into the ocean or settle on the seabed. We took e to be the rate at which sediment is washed out of a reef ecosystem, and assumed that the amount of sediment on the seabed would be in equilibrium with the amount suspended in the water column. The differential equation for $S_{_W}$ is therefore as follows:

$$\frac{\mathrm{d}S_{_W}}{\mathrm{d}t} = \left(q_{_b} + (1-X)\,q_{_c}\right)\lambda - eS_{_W} \tag{4.8}$$

Here, the term $eS_{_W}$ covers both initial export of sediment by rivers to areas beyond a reef (which first must physically pass through the reef area) and later off-shelf export of sediment in the water above a reef. This was done since both of these processes are significant [258, 84] and data that could be used to separate the two was not readily available. Because suspended sediment and sediment on the seabed are measured in different units (mass per unit volume and per unit area, respectively), and converting between these may be difficult, we opted to express sediment on the seabed as a ratio between the level at any given

time and levels corresponding to pristine conditions. A corollary of our assumption that accumulated seabed sediment is in equilibrium with suspended sediment concentration is that the growth in these two variables is proportional to each other, and expressing S_B as a ratio (i.e. indexing a value of $S_B = 1$ to pristine conditions) rather than as a differential equation eliminates the need for a growth rate constant. We therefore took S_B to be the following:

$$S_B(t) = \frac{S_W(t)}{S_W(t=0)} \tag{4.9}$$

Fung *et al.* identified sedimentation as affecting four processes in their model, namely lateral coral growth (described using r_C), larval recruitment of both local brooding and exogenous spawning corals (l_C^b and l_C^s, respectively), and coral death (d_C). The existing literature describes changes in these processes as functions of sedimentation rates, rather than the total amount of sediment either in the water column or on the seabed (see e.g. [89] Appendix B). We therefore assumed that these processes could be described as baseline rates $\tilde{r}_C$, $\tilde{l}_C^b$, $\tilde{l}_C^s$, and $\tilde{d}_C$ scaled up or down according to the sedimentation rate. Much of the redistribution of sediment on reefs is performed by parrotfish [117, 145], which bite into sediment while feeding and therefore reduce sediment buildup on reefs, lowering the effective sedimentation rate, although other herbivorous fish with different feeding methods also may have effects on sediment accumulation [145]. In a recent experiment in which areas of seabed were caged off to simulate a herbivorous fish density of zero, Akita *et al.* found that the caged areas had on average double the accumulated sediment levels compared to uncaged control sites [7]. All of the control sites in [7] were fished, and herbivorous fish landings in the area were reported as being half of what was caught in the 1990s, suggesting that herbivorous fish density there would be at most half of its theoretical maximum. Since the sedimentation rates (mass per unit area per unit time) observed by [7] were similar to pristine values observed elsewhere (see below), we therefore assumed that the sedimentation rate would begin linearly increasing when the herbivorous fish population declined below a value of 0.5, and would double when no herbivorous fish were present. Hence, we defined the sedimentation rate as follows:

$$r_{\text{Sed}} = \max[1 + (1 - 2H), 1]\, k_{\text{Dep}} S_W \tag{4.10}$$

This formulation uses a constant k_{Dep} to represent the baseline rate of sediment deposition, as well as incorporating dependence on the population of herbivorous fish. (We took k_{Dep} to have units of $100 \times \text{cm yr}^{-1}$. This is done so that the rate of sedimentation is expressed over an area rather than a volume, and hence can be calibrated to observed

field values that are measured in mg cm^{-2} time^{-1}. The scaling down of k_{Dep} by a factor of 100 was done because the field data on sedimentation rates that we fit our model to had time units of days, while time in our model is expressed in years, and we intended to keep our sedimentation rate on the same order of magnitude as the raw numbers seen in the field.) Because the three coral growth processes were negatively affected by sedimentation, we modelled them as follows:

$$r_{C}(t) = \frac{\tilde{r}_{C}\kappa_{r}}{\kappa_{r}+r_{\text{Sed}}}; \quad l^{b}_{C}(t) = \frac{\tilde{l}^{b}_{C}\kappa_{b}}{\kappa_{b}+r_{\text{Sed}}}; \quad l^{s}_{C}(t) = \frac{\tilde{l}^{s}_{C}\kappa_{s}}{\kappa_{s}+r_{\text{Sed}}} \tag{4.11}$$

Here, κ_{r}, κ_{b}, and κ_{s} are constants that determine at which sedimentation rate the corresponding coral growth rate is halved. Coral death instead increases when sedimentation rate is high. This means that the sedimentation-dependent coral death rate can be taken as the following, with κ_{d} a scaling constant:

$$d_{C}(t) = \tilde{d}_{C}\left(1 + \frac{r_{\text{Sed}}}{\kappa_{d}}\right) \tag{4.12}$$

In addition to sedimentation's effects on coral, the buildup of algal turf sediment (i.e. sediment on the seabed contained under and within areas dominated by algal turf) is known to inhibit herbivory of algae [94, 241]. As mentioned above, we modelled this by using a factor μ to divide the rates of grazing and herbivory in the model. We assume here that sediment is evenly distributed on the seabed, so the amount of sediment accumulated there is a good proxy for algal turf sediment, and hence the extent to which local algal turf is closer to being SPAT (short, productive algal turf, the kind preferred by herbivorous fish) or LSAT. This can be done because the correlation between seabed sediment load and algal turf length is roughly linear [241]. Tebbett *et al.* found that approximately doubling seabed sediment concentration from pristine values led to herbivorous fish bites on algae approximately halving, and a quadrupling of sediment concentration led to a 78% reduction in herbivorous fish bites compared to the pristine baseline (i.e. approximately another halving from the value with doubled sediment levels) [241]. Similarly, it has been found that removal of large amounts of sediment from reef flats (where seabed sediment buildup is greater) had similar effects on encouraging herbivory as removing much smaller amounts of sediment from reef areas with less sediment buildup [94], indicating the sensitivity of herbivorous fish to algal turf sediment levels. Because of this, we assumed that μ would increase logarithmically with the amount of sediment on the seabed, with a logarithm base of 2 due to the repeated halvings mentioned above. This means that our formulation for μ is as follows:

$$\mu = \max[\log_2(S_B), 0] \tag{4.13}$$

Much of the diet of omnivorous fish consists of zooplankton [88]. The phytoplankton that zooplankton eat can have their population growth limited by low light availability, such as in turbid waters, making planktonic food webs vulnerable to suspended sediment increases [109]. As zooplankton population dynamics (and hence zooplankton-phytoplankton trophic interactions) happen over a faster timescale than the rest of the model processes [70], we assumed a direct dependence of $\phi(t)$ on suspended sediment concentration. This involved scaling ϕ with light availability according to the Lambert-Beer law [110], which is the following function relating underwater light intensity I to intensity of the light source I_0, depth d, and light attenuation constant k_{att}:

$$I = I_0 e^{-k_{att} d} \tag{4.14}$$

We took the light attenuation constant k_{att} to vary based on suspended sediment concentration. A linear relationship has been found between these two quantities in estuarine waters [56], which has a slope of 60 when suspended sediments are measured in mg cm^{-3}. Furthermore, we assumed that $\phi = 1$ in pristine conditions (to bound the growth rate of omnivorous fish above by 1), and that water depth was constant. These constraints meant that we took the following form for ϕ:

$$\phi = \exp\left(-\tilde{\phi} S_W\right); \quad \tilde{\phi} = 60 \tag{4.15}$$

Algae on the seabed also undergoes photosynthesis, and coral obtains much of its energy from dinoflagellate symbionts, which in turn get their energy from photosynthesis. However, the reduction in coral growth and reproduction rates due to sedimentation (including from photosynthesis reduction) is already included in the model via processes detailed by Fung *et al.* (see above). Additionally, Fung *et al.* considered reduction in algal photosynthesis due to sedimentation, but did not include it in their model due to lack of data. We also opted not to include this. Turf algae spread very rapidly, and have been found to dominate the benthos under conditions featuring high turbidity [191] or sedimentation rates [22, 257] due to their ability to trap sediment. Therefore, we assumed that although light attenuation due to turbidity may affect the growth of turf algae, it would not appreciably affect their spread if a reasonable amount of light still reached the seabed. Conversely, the steady-state macroalgae levels reached with our baseline parameter values were low enough that any difference due to decreasing photosynthesis would be minimal.

4.4.2 Model parametrization

All parameters relating to transitions on the seabed between coral, macroalgae, turf algae and space that were used by Fung *et al.* were kept at the values specified in [89]. This includes the baseline values $\tilde{\theta}$, $\tilde{r}_{C}$, $\tilde{l}^{b}_{C}$, $\tilde{l}^{s}_{C}$, and $\tilde{d}_{C}$ for rates affected by features that we added to the model.

Growth and harvesting rates for each fish functional group, as well as diet composition ratios for omnivorous and piscivorous fish, were taken from FishBase [88]. This involved first dividing all reef-associated fish species observed in our study region (the Solomon Islands) for which data on both doubling time and use by fisheries was available into functional groups depending on their trophic level. Fish with a listed trophic level of 2.0 were assumed to be herbivorous, those with tropic level greater than 2.0 but less than 3.0 were assumed to be omnivorous (with a diet consisting partially of algae and partially of alternative sources such as invertebrates), those with trophic level at least 3.0 but less than 4.0 were assumed piscivorous due to being a full trophic level above herbivorous fish, and those with trophic level at least 4.0 were designated top-level predators. (The fish in the latter two categories could include some predators of benthic crustaceans as well as predators of fish. Hence, during our calculations below, we assumed that growth and harvesting rates would be similar between those groups.)

The omnivorous fish species for which growth and harvesting data was available had an average trophic level of 2.62, while that of the piscivorous species (other than top predators) was 3.49. Therefore, we took $\delta_{O} = 0.38$ and $\delta_{P} = 0.21$ under the assumptions that the diet of omnivorous fish would be 38% algae and 62% organisms that eat algae, and that the diet of piscivorous fish would consist of organisms with an average trophic level of 2.49, such as 21% herbivorous fish (trophic level 2) and 79% omnivorous fish (trophic level 2.62). We took the values of the top predator diet parameters to be $\delta^{H}_{Z} = 0.1$ and $\delta^{O}_{Z} = 0.3$. This was based on the assumption that top predators would eat more fish in higher trophic levels, as well as the fact that summing the trophic levels of herbivorous, omnivorous and piscivorous fish with these weights results in a trophic level of 3.08, close to the trophic level of the prey of top predators in the Solomon Islands (3.18).

The intrinsic growth rate for each functional group was set to be the average of those for each species within the functional group, while the growth rate for each species was derived from its reported doubling time using the formula $r = \frac{\ln 2}{t_D}$. As the doubling time of each species was defined using an estimated range, numerical values for each species were obtained by taking the median of this range; if the doubling time for a species was defined as being very long, without an upper bound, this numerical value was taken to be 15 years. These intrinsic growth rates were assumed to hold for pristine reefs, which

typically have about 50 percent coral cover [227] that is not edible by herbivorous fish. Therefore, we multiplied each growth rate by 2, so that herbivorous fish growth would scale based on the amount of algae present compared to its observed maximum values on pristine reefs, and the timescale of the other fish functional groups' dynamics (compared to those of herbivorous fish) would not be affected. From this, we obtained $r_{_H} = 1.51$, $r_{_O} = 1.36$, $r_{_P} = 1.45$, and $r_{_Z} = 0.69$.

The harvesting rate for each functional group was defined in the same way, based an average of harvesting rates for each species in the group. A species was assumed to have a harvesting rate of 0.5 if its use by fisheries was listed as "highly commercial", as many highly-fished species have harvesting rates at or above 50 percent annually [184]. Species whose fisheries usage was listed as "commercial" were assumed to have harvesting rates of 0.3, a value that previous modelling studies have determined to be close to the maximum rate at which fish populations can maintain themselves [28, 242], and "minor commercial" species were assumed to have harvesting rates half of that (0.15). The harvesting rate for species that were listed as being the targets of subsistence fishing (rather than commercial fishing) was taken to be 0.05, an order of magnitude lower than the highest commercial rates [63], and species of no commercial interest had a harvesting rate of 0. This process gave us $h_{_H} = 0.2$, $h_{_O} = 0.11$, $h_{_P} = 0.15$, and $h_{_Z} = 0.22$.

Sediment export onto reefs due to erosion is low in heavily forested areas, and increases with the proportion of cleared land [187, 261]. A recent survey on Isabel Island in the Solomon Islands found that over a catchment covered almost entirely by forest, sediment concentrations at the mouth of a local river (the Jejevo) had a geometric mean of 20 mg L^{-1}, or 0.02 mg cm^{-3} [124]. Since the waters at the mouth of the Jejevo have been found to be on average 15 times more turbid than those by adjacent rivers [11], we took $q_{_b}$ to have a high value of 0.02 mg cm^{-3} and a low value of 0.0013 mg cm^{-3}. In the wet tropics of northern Queensland, Australia, Neil *et al.* found a linear relationship between percentage of land cleared and suspended sediment concentration in local rivers during the wet seasons of specific years [187], thus controlling for temporal variation due to any ongoing changes in land use. Plugging 100 percent land clearance into the formulas in [187] yielded values of 72 and 14 mg L^{-1} for very wet and fairly wet conditions, respectively. Wenger *et al.* performed a similar analysis on Kolombangara Island in the Solomon Islands, based on future predictions of yearly erosion with varying percentages of cleared land [261]. That study found average suspended sediment concentration in streams to be 124 mg L^{-1} at 40 percent cleared land with no management, as well as a linear rate of increase for sediments, implying a concentration of 310 mg L^{-1} when land is fully cleared. The concentration at 100 percent forest cover found by Wenger *et al.* was similar to that found by Neil *et al.*; the difference in slope of the two relationships can be attributed to the fact that Wenger *et al.*

considered deforestation on steeper terrain. We therefore took q_c to be 0.31 mg cm^{-3} when simulating deforestation on steep terrain, and 0.043 mg cm^{-3} (the average of the two values found by Neil *et al.*) for gentler terrain. This represents the increase in sedimentation due to erosion that an entirely cleared environment has compared to an entirely forested one.

Rates of sediment export from coastal into off-shelf areas have a great deal of spatial variation (see [258] for an example of this in New Guinea, with both very high and very low amounts of off-shelf export observed). Therefore, we took e to vary over a wide range, namely from 0.1 to 0.9, with the median value 0.5 used as a baseline. We assumed λ to be 1 yr^{-1} in order to simulate conditions on reefs near river mouths. Reefs further away can receive substantially less sediment from river discharges [21]; this process was folded into e in order to simplify the model analysis (see above), as e and λ perform similar functions (limiting sediment on reefs due to local hydrodynamics).

To find a value of k_{Dep} suitable for the Solomon Islands, we related suspended sediment concentrations to rates of sedimentation in a dataset covering Isabel Island [11], using the formula $r_{\text{Sed}} \approx k_{\text{Dep}} S_W$ in the absence of data on parrotfish abundance. We used the average reported turbidity in nephelometric turbidity units (NTUs) at the Jihro inshore reef site in that dataset, which was similar to those on other inshore reefs globally [11] such as on the Great Barrier Reef [145], to estimate suspended sediment concentration. A value in mg L^{-1} was obtained from this using a linear method used in [215], taking the average slope of 18 linear functions linking NTUs to sediment density, and this was further scaled to units of mg cm^{-3}. We then divided the observed sedimentation rates on inshore reefs in this dataset by the obtained average sediment concentration. This gave us an average value of 4400 for k_{Dep}, after disregarding an outlier, which had a sedimentation rate over 20 times higher than the other sites and was therefore deemed non-representative.

While parametrizing their model, Fung *et al.* estimated from field data that a sedimentation rate of 100 mg cm^{-2} d^{-1}, or 365×10^2 mg cm^{-2} yr^{-1}, causes coral lateral growth rate to decline by half (see [89] Appendix B). Hence, we took $\kappa_r = 365$. Similar estimates by Fung *et al.* included that a sedimentation rate of 12 cm^{-2} d^{-1} causes larval recruitment of both brooding and spawning corals to decrease by 60%, and one of 13 cm^{-2} d^{-1} causes coral death rate to double. After converting units, this leads to a value of $\frac{44}{1.5}$ for κ_b and κ_s, and a value of 47.5 for κ_d.

We determined values for r_X by isolating it within the differential equation proposed by Tanaka *et al.* [236], i.e. $\frac{\mathrm{d}F}{\mathrm{d}N} = -r_X FN$. To do this, we used data on deforestation in the Indonesian part of the island of Borneo (i.e. Kalimantan) from 1973 to 2000 and from 2000 to 2010 [91], and population growth data in Kalimantan over the same years [229]. For each of these time periods, we took F to be the percentage forest cover in Kalimantan at the end of the period and N to be the population of Kalimantan at the end of the period

relative to its population at the beginning of the period, and estimated $\frac{dF}{dN}$ by dividing the change in forest cover by the relative change in population during the period. (2000 and 2010 were census years in Indonesia, and we estimated the 1973 population by assuming a linear rate of growth between the 1971 and 1980 censuses.) We used relative rates rather than absolute population numbers (as was done by Tanaka *et al.*) in order to control for population density and hence maximize applicability to different locations. From these calculations, we obtained a value of 0.18 for r_X from 1973 to 2000, and a value of 0.23 from 2000 to 2010. We therefore took 0.23 as a baseline for r_X, although we allowed it to vary in order to simulate a variety of deforestation speeds.

A long-term study (from 1990 to 2020) on changes in forest cover in the tropics found that out of the undisturbed forest in insular Southeast Asia in 1990, 16.4 percent had been deforested, and 3.7 percent had been deforested and subsequently regrew [250]. This gives an estimate that the speed of reforestation was 0.18 times the speed of deforestation in this time period. Hence, we assumed our background rate of forest regrowth a_X to be 0.18 times the baseline value for r_X of 0.23, or in other words $a_X \approx 0.04$.

4.4.3 Numerical methods

In order to determine how fish assemblages in the Solomon Islands changed with deforestation, we simulated the population dynamics of each fish functional group (F_H, F_O, F_P and F_Z) while increasing the population of the Solomon Islands based on United Nations predictions starting in 2022 [248], for varying values of the forest loss constant r_X. We did this for three values of the sediment flushing rate ($e = 0.1$, 0.5, and 0.9) to control for variation due to local conditions. For each run of the model, initial conditions for each state variable were set to the steady state reached by that variable in the case where $X(t = 0) = 1$ and $r_X = 0$ (i.e. without deforestation), to simulate effects in a part of the Solomon Islands that currently has close to full forest cover (see e.g. [92, 124]). We took fish populations in each functional group at $t = 20$ years and $t = 50$ years, (representing medium-term and long-term effects of deforestation, respectively). We subsequently normalized each population value by the corresponding population at $t = 20$ or $t = 50$ without deforestation, in order to isolate the decline in fish populations that could be directly attributable to deforestation.

To determine how the changes brought about by deforestation depend on local conditions, we ran simulations of highland deforestation with q_b (the baseline sediment concentration in local rivers) and e (the rate at which sediment is flushed out of the system) varying within their entire ranges. Here, we took $r_X = 0.23$. Initial conditions for fish were taken to be their theoretical population maxima (i.e. 1 for each functional group); all other

Param	Value	Units	Description
$r_{_H}$	1.51	yr^{-1}	Intrinsic growth rate for herbivorous fish
$r_{_O}$	1.36	yr^{-1}	Intrinsic growth rate for omnivorous fish
$r_{_P}$	1.45	yr^{-1}	Intrinsic growth rate for piscivorous fish
$r_{_Z}$	0.69	yr^{-1}	Intrinsic growth rate for top predator fish
$h_{_H}$	0.2	yr^{-1}	Harvesting rate for herbivorous fish
$h_{_O}$	0.11	yr^{-1}	Harvesting rate for omnivorous fish
$h_{_P}$	0.15	yr^{-1}	Harvesting rate for piscivorous fish
$h_{_Z}$	0.22	yr^{-1}	Harvesting rate for top predator fish
$m_{_H}$	0.1	yr^{-1}	Mortality due to predation for herbivorous fish
$m_{_O}$	0.1	yr^{-1}	Mortality due to predation for omnivorous fish
$m_{_P}$	0.1	yr^{-1}	Mortality due to predation for piscivorous fish
$\delta_{_O}$	0.38	Unitless	Percentage of omnivorous fish diet consisting of algae
$\delta_{_P}$	0.21	Unitless	Percentage of piscivorous fish diet consisting of herbivorous fish
$\delta_{_Z}^{H}$	0.1	Unitless	Percentage of top predator fish diet consisting of herbivorous fish
$\delta_{_Z}^{O}$	0.3	Unitless	Percentage of top predator fish diet consisting of omnivorous fish
$k_{_h}$	0 - 1	Unitless	Relative importance of local fish availability on harvesting rates
ν	0 - 1	Unitless	Dependence of harvesting on population growth

Table 4.1: Parameters related to fish vital processes used in Chapter 4. Mortality rates are assumed based on [28], $k_{_h}$ and ν are allowed to vary over broad potential ranges, and all other parameters are calculated based on FishBase data [88].

Param	Value	Units	Description	Reference
q_b	0.0013 - 0.2	mg cm^{-3}	Baseline sediment concentration in rivers due to erosion	[124]
q_c	0.043, 0.31	mg cm^{-3}	Additional river sediment concentration when land is 100% cleared	[187, 261]
λ	1	yr^{-1}	Rate at which sediment in rivers is exported to reefs	Assumed
e	0.1 - 0.5 - 0.9	yr^{-1}	Rate at which suspended sediment on reefs leaves the system	[258]
k_{Dep}	4400	100 $\times$ cm yr^{-1}	Constant governing sediment deposition from water column to seabed	[215, 11]
κ_r	365	100 $\times$ mg cm^{-2} yr^{-1}	Sedimentation rate at which coral lateral growth is halved	[89]
κ_b	29.2	100 $\times$ mg cm^{-2} yr^{-1}	Sedimentation rate at which brooding coral recruitment is halved	[89]
κ_s	29.2	100 $\times$ mg cm^{-2} yr^{-1}	Sedimentation rate at which spawning coral recruitment is halved	[89]
κ_d	47.5	100 $\times$ mg cm^{-2} yr^{-1}	Sedimentation rate at which coral death is doubled	[89]
$\tilde{\phi}$	60	mg^{-1} cm^3	Constant relating non-algal food availability for omnivorous fish and sediment concentration	[56]
r_X	0 - 0.23 - 0.25	yr^{-1}	Deforestation rate	[91, 229]
a_X	0.18 $\times$ 0.23	yr^{-1}	Forest regrowth rate	[250]

Table 4.2: Parameters related to sedimentation used in Chapter 4

initial conditions were taken to be their steady-state values when no deforestation takes place and all parameters are at their baseline values. This was done in order to isolate the transient dynamics produced by different local conditions for the same amount of deforestation pressure. In each simulation, we obtained the population of each fish functional group at $t = 20$.

To examine how fisheries might respond to changes in fish availability due to sedimentation, we simulated both the populations of each functional group and the amount of fish harvested, for static and dynamic harvesting rates. (For each functional group, the amount of harvested fish was obtained by integrating that functional group's population times its harvesting rate.) For a static baseline, we used the harvesting rates obtained from FishBase (see above). We then assumed a harvesting rate that would change for each functional group based on local availability of fish in that functional group, while the percentage of the total fish population being harvested would remain constant. We first estimated the rate for all functional groups combined by taking a weighted average of the rates h_H, h_O, h_P and h_Z, where the weights were set equal to the relative abundances of each functional group in the initial conditions we specified above. In other words, we defined the aggregate harvesting rate as follows:

$$h_{\text{Tot}} = \frac{h_H F_H(0) + h_O F_O(0) + h_P F_P(0) + h_Z F_Z(0)}{F_H(0) + F_O(0) + F_P(0) + F_Z(0)} \tag{4.16}$$

We then defined a harvesting rate for each functional group based solely on the relative availability of fish in that functional group as follows:

$$h_{\text{Var},I}(t) = \frac{F_I h_{\text{Tot}}}{F_H + F_O + F_P + F_Z}, \quad I \in \{H, O, P, Z\} \tag{4.17}$$

Since some fish species with high abundance (e.g. wrasses) are not expected to be of any commercial interest [161], we did not assume that the actual harvesting rates for each functional group would be solely based on relative fish abundances. Instead, we formulated harvesting rates $\bar{h}_H$, $\bar{h}_O$, $\bar{h}_P$, and $\bar{h}_Z$ for each functional group that would partly depend on the fishing rates parametrized from FishBase (i.e. the intrinsic demand for each functional group) and partially due to local fish availability. In other words, for a constant k_h representing the how important current local conditions are in determining demand for each functional group, we defined each $\bar{h}$ as follows:

$$\bar{h}_I(t) = \frac{h_I + k_h h_{\text{Var},I}}{1 + k_h}, \quad I \in \{H, O, P, Z\} \tag{4.18}$$

Following the construction of these time-dependent harvesting rates, we then generated time series of fish populations and fisheries yield (as above) for different values of k_h, namely $k_h = 0$ (the baseline with static fishing rates), $k_h = 0.1$, $k_h = 0.3$, and $k_h = 1$ (50 percent dependence on local fish availability). In these simulations, all parameters were assumed to be at their baseline values, e.g. $e = 0.5$ and $r_X = 0.23$, and we furthermore took $q_c = 0.043$ to represent lowland deforestation.

To test how robust reef fisheries' yield is to deforestation-driven sedimentation, as well as the persistence ability of reef fish, we simulated fish populations in a scenario where the amount of fish harvested was always constant, such as in a system with specified fishing quotas. (This contrasts with taking the number of harvested fish to be a percentage of the overall fish population.) Specifically, we assumed that over a unit of time, the total number of fish harvested during that time would always be equal to a value $\rho \times \xi$, where ξ is the number harvested at time $t = 0$ and ρ is a scaling constant. ξ is defined below:

$$\xi = h_H F_H(0) + h_O F_O(0) + h_P F_P(0) + h_Z F_Z(0) \tag{4.19}$$

We further assumed that the different fish functional groups were harvested according to their proportions of the population. This means that, for ω a factor to ensure that the total fish harvested remains constant, the number of fish harvested in each functional group I is as follows:

$$\left(\frac{F_I}{F_H + F_O + F_P + F_Z} \right) \omega F_I \tag{4.20}$$

In order to obtain ω, we first noted that the number of fish harvested at each time step always being equal to $\rho \times \xi$ implies the following:

$$\sum_I \left(\frac{F_I}{F_H + F_O + F_P + F_Z} \right) \omega F_I = \rho \xi \tag{4.21}$$

By factoring out and isolating ω, we get the following:

$$\omega = \rho \xi \left(\frac{F_H + F_O + F_P + F_Z}{F_H{}^2 + F_O{}^2 + F_P{}^2 + F_Z{}^2} \right) \tag{4.22}$$

The harvesting rate for each functional group I is the number of fish harvested in that functional group divided by its total population. If we denote the harvesting rate as

$h^{a}_{\mathrm{Var},I}$, with the a denoting that the amount harvested is what remains constant, we get the following:

$$h^{a}_{\mathrm{Var},I} = \frac{\omega F_I}{F_H + F_O + F_P + F_Z} = \frac{\rho \xi F_I}{{F_H}^2 + {F_O}^2 + {F_P}^2 + {F_Z}^2} \tag{4.23}$$

We then used a modified version of Equation 4.18, substituting $h^{a}_{\mathrm{Var},I}$ in place of $h_{\mathrm{Var},I}$ and taking $k_h = 1$, to obtain variable harvesting rates for each functional group that always summed to a constant value:

$$\bar{h}_I(t) = \frac{h_I + h^{a}_{\mathrm{Var},I}}{2}, \quad I \in \{H, O, P, Z\} \tag{4.24}$$

Anticipating that constant harvesting amounts could cause the fish to go extinct, we additionally imposed the constraint while running the model that if the population of a functional group was below 10^{-6}, it would be treated as 0. This constraint further implied that the amount of fish harvested in such cases would also be zero. Using these rates, we ran simulations for different values of ρ and r_X, for both lowland and highland deforestation scenarios. For each simulation, we obtained the amount of fish present at time $t = 50$. If this amount was zero, we additionally obtained the time at which the fish population first dropped below 10^{-6}. This calculation of fish extinction time was specifically done for herbivorous fish; since fish functional groups were harvested in this case according to their proportions of the total fish population, all functional groups that went extinct did so at the same time. (This put the threshold for local extinction of all fish functional groups combined at 4×10^{-6}.)

Furthermore, a relationship has been found between population and harvesting rate; intuitively, the demand for fish rises as population increases [219]. This can be expressed as the harvesting rate $h_I(t)$ for a given functional group I being multiplied by $1 + \nu N$, where the human population N is expressed as a proportion of the present-day value, and ν is a constant governing the population growth-harvesting relationship. In light of this, we evaluated the interaction effects between deforestation and increased fishing rates on both fish population size and fishing yield. This was done by running simulations for varying values of ν and r_X, and taking the population of all functional groups at time $t = 50$ years and the total number of fish harvested during the simulation. This was done for both lowland and highland deforestation scenarios.

4.5 Results

4.5.1 Fish resilience to deforestation-induced sedimentation depends on trophic level and local hydrological conditions

We found that deforestation had significant time-dependent effects on reef fish community composition, with different functional groups bearing the brunt of the burden caused by sedimentation in the medium-term and long-term (Figure 4.2). Generally, fish at lower trophic levels saw sharper declines first, while those at higher trophic levels were often harmed more in the long run. After 20 years of lowland deforestation, herbivorous fish populations usually showed the largest decreases (Figure 4.2a). The decline in herbivorous fish was more pronounced when off-shelf sediment export was higher; this was reversed for the other functional groups, with omnivorous fish becoming the hardest-hit functional group under conditions where most sediment was locally retained ($e = 0.1$). After 50 years of lowland deforestation, herbivorous fish populations decreased significantly (usually to 60-70 percent of their expected levels without deforestation), with these declines unaffected by off-shelf sediment export rates (Figure 4.2b). On the other hand, the declines of the other three functional groups were heavily dependent on local sediment dynamics in this scenario. Under moderate to high deforestation, omnivorous fish populations ranged anywhere from 20 to 90 percent of what they would be with full forest cover, depending on e. Piscivorous fish and top predators were able to maintain their numbers very well when sediment was mostly deposited away from reefs, but in the case where $e = 0.1$, both of these functional groups suffered comparable declines to herbivorous fish.

Deforestation on steep slopes caused the declines in fish populations to be much greater. After 20 years, populations of herbivorous and omnivorous fish had halved in the median scenario (Figure 4.2c), with the same dependence on e as that seen with lowland deforestation. Following 50 years, all fish functional groups had experienced large and sometimes catastrophic declines (Figure 4.2d). If the rate at which deforestation scales with population growth and the level of local sediment retention were sufficiently high, populations of omnivorous fish and top predators could reach critically low levels, with local extinction probable soon after. For high r_x and low e, herbivorous fish showed the most resilience, due to the total shift to algal turf dominance providing them with a steady food source. However, since this algal turf was unpalatable LSAT, herbivorous fish populations were far below what they would be without deforestation, and too low to support any species at higher trophic levels.

We also found that the effects of baseline local conditions on resilience of reef fish to deforestation-driven sedimentation was heterogeneous across functional groups. Taking the

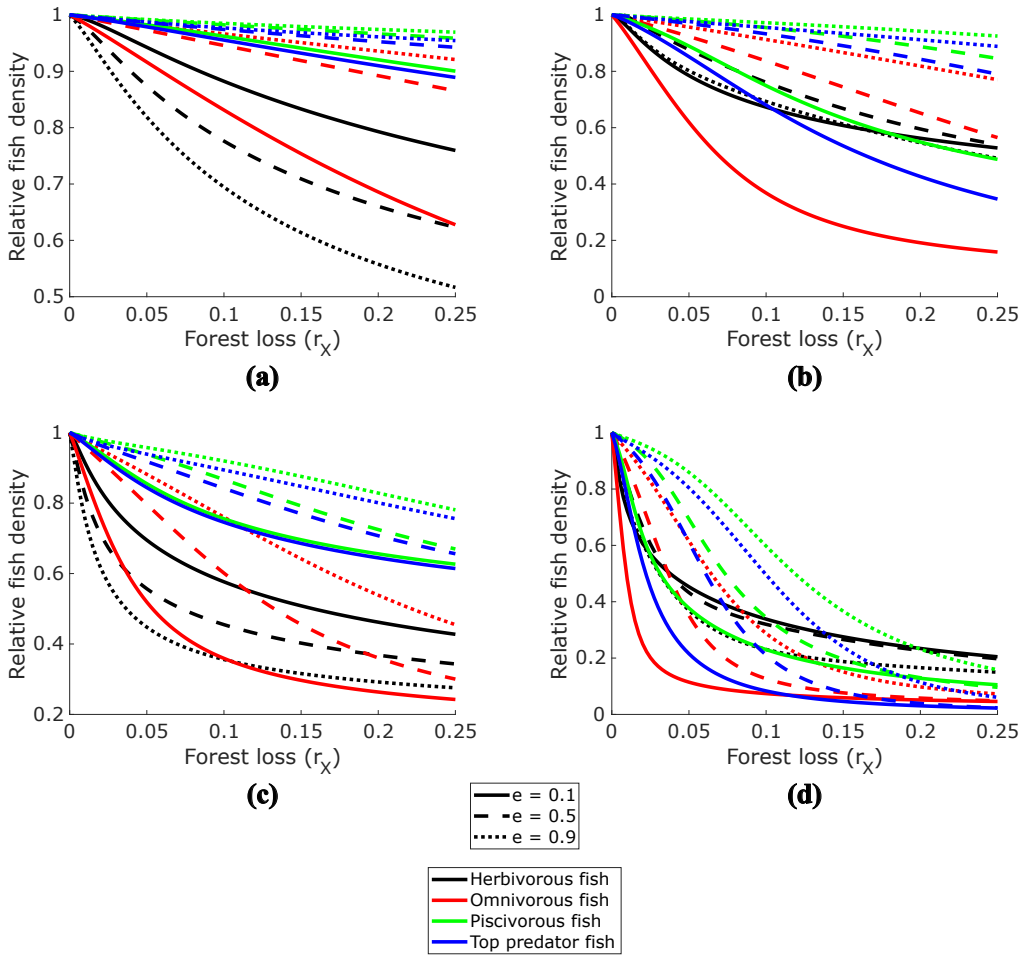

Figure 4.2: Abundances of fish functional groups after 20 years (Figure 4.2a) and 50 years (Figure 4.2b) of lowland deforestation, and 20 years (Figure 4.2c) and 50 years (Figure 4.2d) of deforestation on steep slopes, relative to the baseline case without deforestation. Note the difference in vertical axis scales.

population levels of each fish functional group following 20 years of heavy deforestation on steep slopes ($r_X = 0.23$, $q_c = 0.31$) revealed the expected patterns of fish resilience being greater for higher values of e and lower values of q_b. As was the case when we examined changes in fish populations as a function of deforestation rate (Figure 4.2), we found that more turbid starting conditions (low e, high q_b) affected fish at higher trophic levels less than it did those at lower ones, both in absolute terms and relative to their populations in more favourable conditions (Figure 4.3). Under the most turbid conditions,

the herbivorous fish population was about 30 percent of what it was under the least turbid ones (Figure 4.3a), and for omnivorous fish, this figure was about 25 percent (Figure 4.3b). This contrasts with piscivorous fish (40 percent; see Figure 4.3c) and top predators (45 percent; see Figure 4.3d). This suggests that under a wide range of potential local conditions, the initial effects of deforestation-driven sedimentation are to harm fish species at lower trophic levels. We additionally found that the dependence of fish populations following deforestation on baseline river sediment concentration q_b was sigmoidal, with large changes in fish population levels around 1×10^{-2} mg cm^{-3} for most functional groups, and at somewhat greater concentrations for herbivorous fish.

4.5.2 Flexible harvesting strategies can stabilize fish populations on reefs with heavy sedimentation

Within our simulations, varying which fish were harvested depending on their availability while keeping the same overall harvesting rate caused very large population increases in two of the model's four functional groups (Figure 4.4). Herbivorous fish and top predators, which had the highest baseline harvesting pressures, had about 60% and 50% higher populations after 50 years of lowland deforestation when $k_h = 1$ (indicating a harvesting strategy 50% based on fish availability) compared to the baseline scenario without harvesting flexibility ($k_h = 0$). The populations of omnivorous and piscivorous fish also increased with k_h, although these increases were of a lesser magnitude. Importantly, flexible harvesting also stabilized the populations of herbivorous fish and top predators: for $k_h = 1$, the populations of these two functional groups were nearly constant after $t = 20$, at levels significantly above their initial values (Figures 4.4a and 4.4d). It also attenuated the decline of piscivorous fish, which had a population at $t = 50$ approximately equal to its initial value in the case where $k_h = 1$, albeit with a decreasing trend (Figure 4.4c). In contrast, omnivorous fish saw relatively minor benefits from this strategy (Figure 4.4b), due to their high steady-state population without deforestation and low baseline harvesting rate.

Harvesting flexibility was also determined to provide substantial protection for most fish functional groups against the heavy sedimentation stress induced by highland deforestation (Figure 4.5). In the baseline highland deforestation scenario, where the harvesting rates for each functional group were kept at their observed values, all fish populations at least halved during our 50-year simulation window (Figure 4.5a). The halving time for herbivorous fish during highland deforestation could be as low as 10 years, depending on local conditions, and the populations of ordinarily robust functional groups of piscivorous fish and top predators typically halved in 30 to 40 years. However, assuming a flexible harvesting program (with $k_h = 1$) meant that halving did not occur for herbivorous fish or top

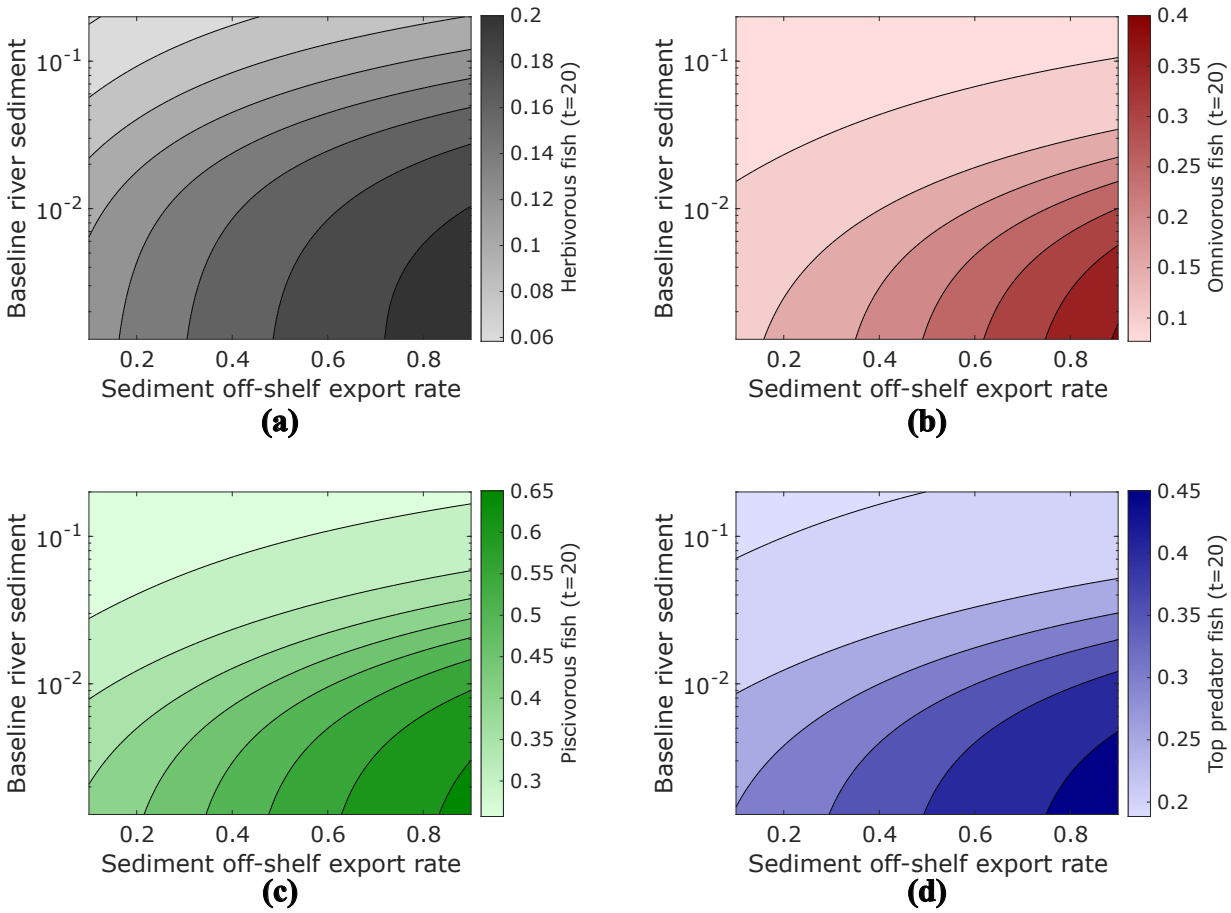

Figure 4.3: Population levels of herbivorous fish (Figure 4.3a), omnivorous fish (Figure 4.3b), piscivorous fish (Figure 4.3c), and top predator fish (Figure 4.3d) after 20 years of highland logging, showing dependence on baseline sediment levels from erosion q_b and off-shelf sediment export rate e. Initial conditions for fish functional groups were taken to be that functional group's theoretical maximum population (i.e. 1) in all cases.

predators within 50 years, regardless of local hydrodynamic conditions, and it only occurred for piscivorous fish when deforestation was especially severe, i.e. $r_X \gtrapprox 0.17$ (Figure 4.5b). For these three functional groups, flexible harvesting mitigated the worst of the damage caused by highland deforestation, reducing its effects to a magnitude similar to what may be expected under deforestation on flatter lowland terrain. Omnivorous fish only saw mild benefits, with flexible harvesting delaying their halving by a few years.

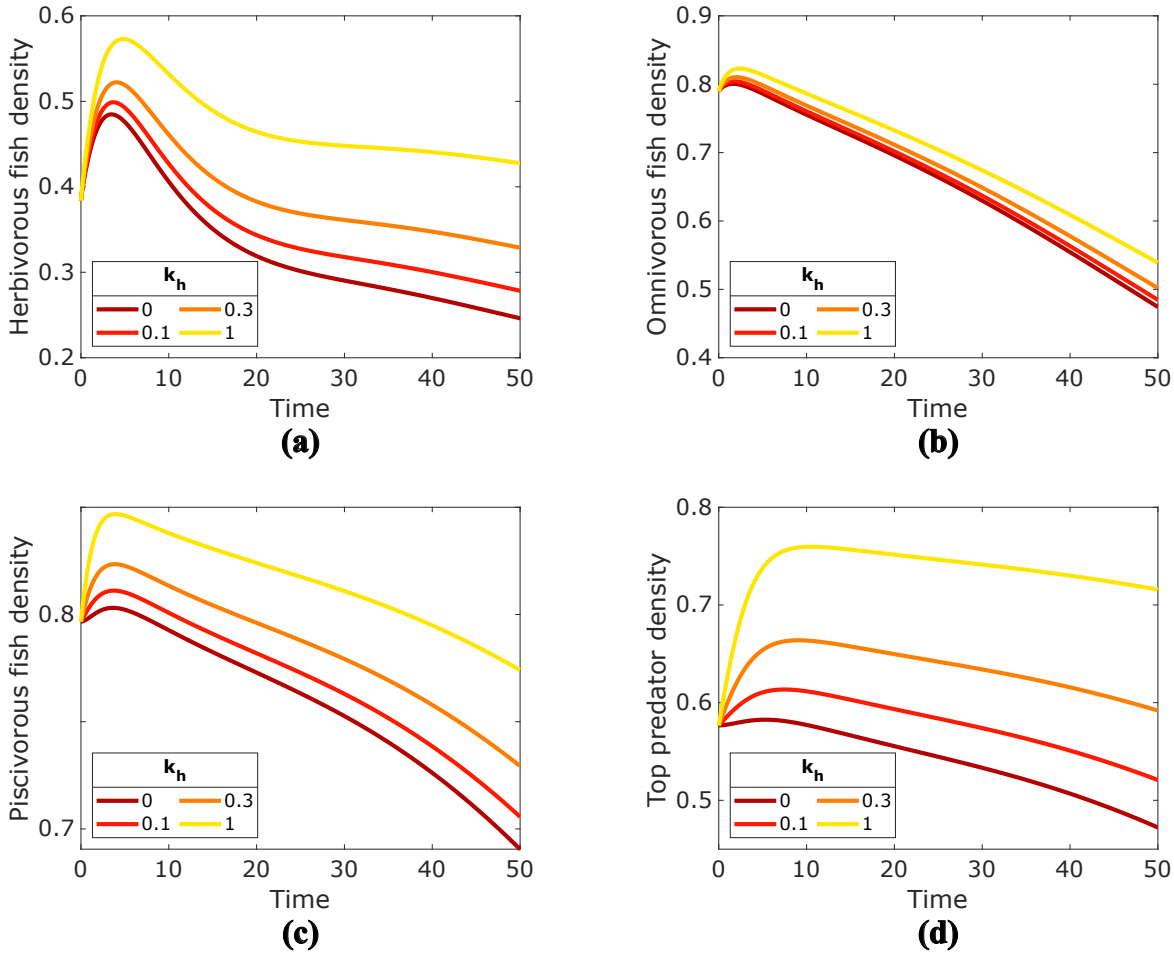

Figure 4.4: Populations of herbivorous fish (Figure 4.4a), omnivorous fish (Figure 4.4b), piscivorous fish (Figure 4.4c), and top predator fish (Figure 4.4d) for different values of the fishing flexibility constant k_h. Here, $e = 0.5$, $r_X = 0.23$, and $q_c = 0.043$.

4.5.3 Deforestation harms fisheries yield, and highland deforestation can cause it to collapse

We found that if harvesting rates start at their observed baseline values and increase with population growth, fish populations decline but total fish catch does not necessarily increase (Figure 4.6). Specifically, we found that increasing the rate ν at which demand for fish rises with population growth usually did not lead to greater numbers of fish harvested (Figures 4.6c and 4.6d), due to fish becoming more depleted under the lowland deforestation scenario

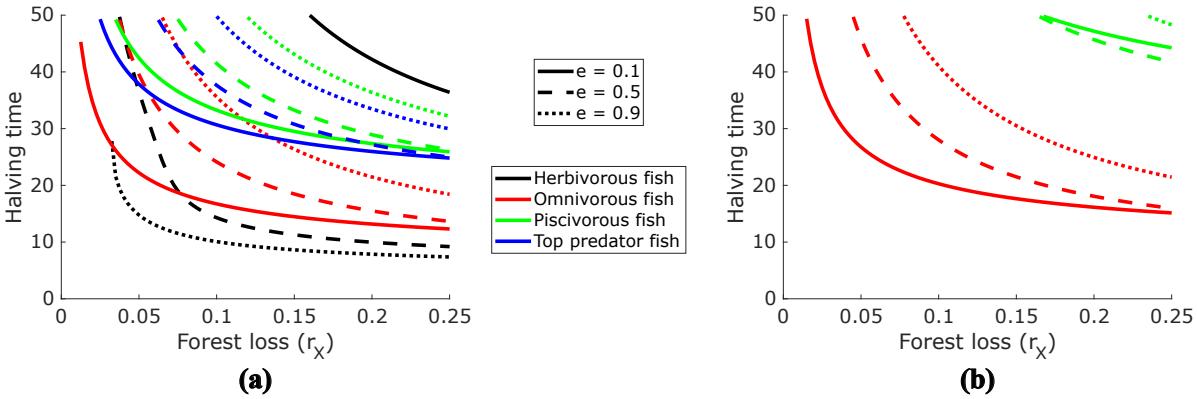

Figure 4.5: Time taken by fish functional groups to halve from their initial population sizes during highland deforestation, for different values of the forest loss constant r_x and the off-shelf sediment export rate e. Shown are the case where harvesting of all functional groups occurs at their baseline values (Figure 4.5a), and the case when harvesting partially depends on functional group availability with $k_h = 1$ (Figure 4.5b).

(Figure 4.6a) and being locally extirpated under the highland deforestation scenario (Figure 4.6b). We additionally found that if population growth leads to increased demand for fish, 50 years of highland deforestation would result in fish populations going to zero even if relatively little forest is removed (Figure 4.6b).

Our results similarly show that if fish harvesting is done according to fixed quotas, harvesting levels that would be sustainable without deforestation can instead lead to local fish extirpation when deforestation is severe enough (Figure 4.7). This effect was especially prominent in highland deforestation scenarios. We found that if the raw number of fish harvested in the Solomon Islands did not deviate from current levels (i.e. $\rho = 1$), which were evaluated as being sustainable under present conditions, the increases in sedimentation brought on by highland deforestation would reduce local fish populations to zero by $t = 50$ under all but the most optimistic scenarios (Figures 4.7b and 4.7d). This occurred in as few as 25 years when deforestation happened at the same rate as was observed in Borneo in previous decades (Figure 4.7d). Less extreme effects were observed under lowland deforestation. Fish population declines were still evident in that scenario, and local extirpation was still possible for the highest values of r_x. However, under lowland deforestation, maintaining harvesting quotas at 80% of estimated current levels resulted in reasonably healthy fish populations at $t = 50$ even under the highest values of r_x tested.

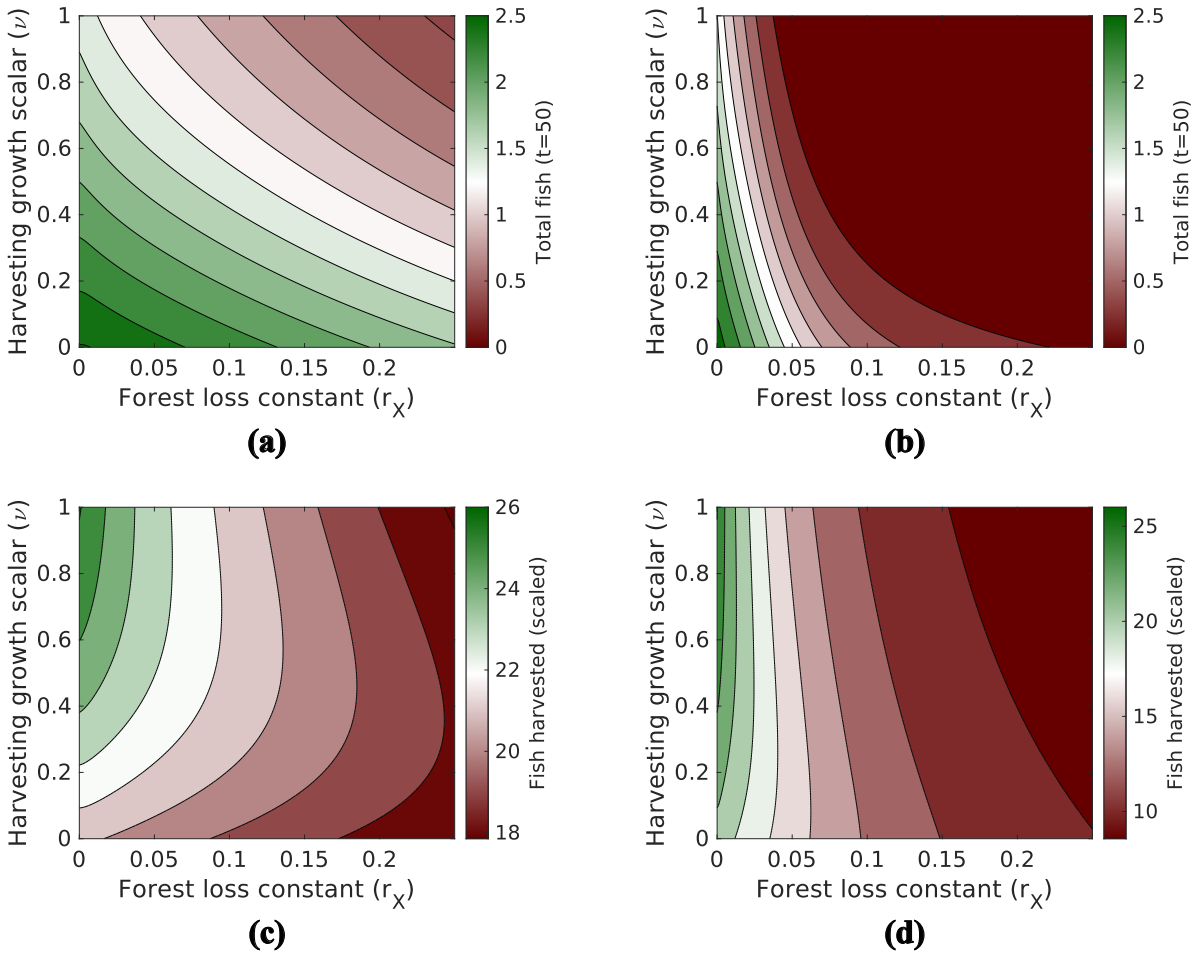

Figure 4.6: Fish populations from all functional groups after 50 years of deforestation (Figures 4.6a and 4.6b), as well as total fish harvested during that time (Figures 4.6c and 4.6d), when demand for fish increases with population growth. (Baseline harvesting rates are the constants shown in Table 1, i.e. $k_h = 0$.) Figures 4.6a and 4.6c show the case with lowland deforestation, while Figures 4.6b and 4.6d show the case with highland deforestation.

4.6 Discussion

In this paper, we use a dynamical system ridge-to-reef model of intermediate complexity to forecast the temporally-dependent effects of sedimentation due to deforestation on different reef fish functional groups in the Solomon Islands. We show that deforestation-driven

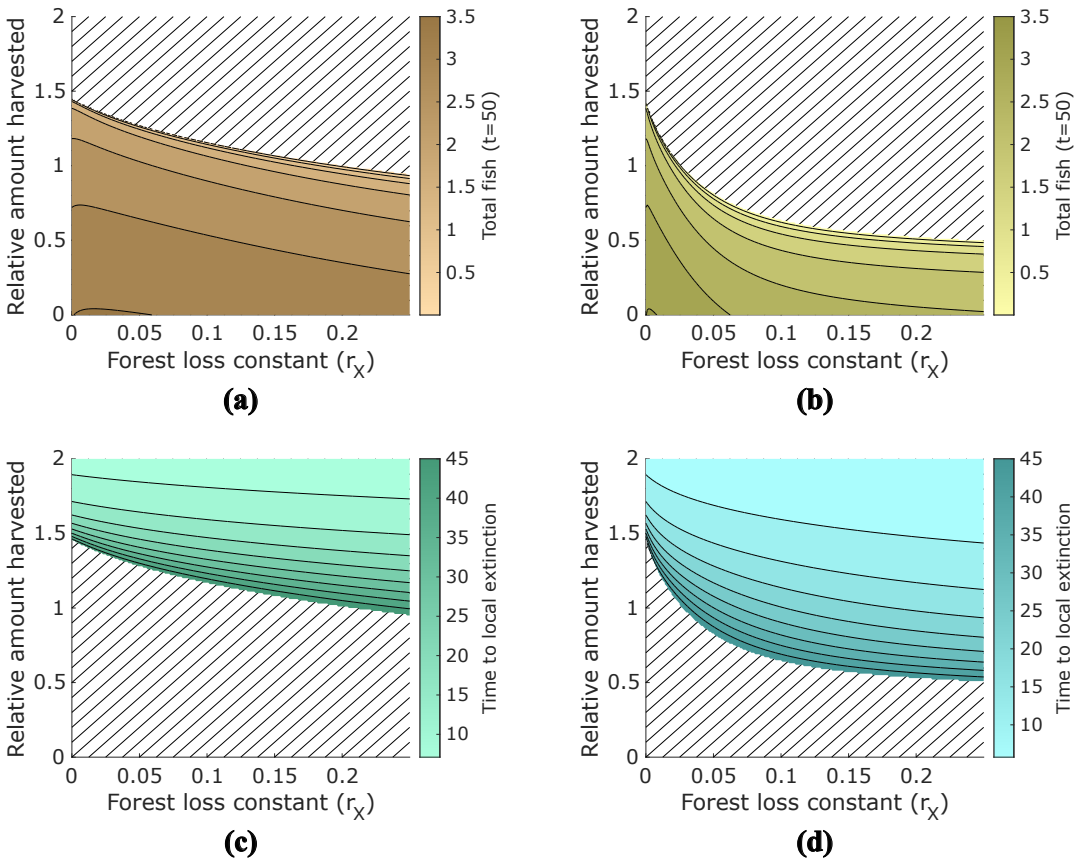

Figure 4.7: Robustness of reef fish and fisheries to changes caused by deforestation, assuming constant fishing quotas (specified by ρ, on the vertical axis). Figures 4.7a (lowland deforestation scenario) and 4.7b (highland deforestation scenario) show the amount of fish in all functional groups combined at $t = 50$, with diagonal hashing indicating that all fish populations were zero at this time. Figures 4.7c (lowland) and 4.7d (highland) show the time at which herbivorous fish became locally extinct in these cases, with diagonal hashing indicating that they did not go extinct.

sedimentation causes declines first in coral, then in herbivorous and omnivorous fish, and finally in fish at higher trophic levels, and we project herbivorous fish to be the hardest-hit fish functional group in the short-term but the most resilient one in the long-term. We evaluate the risk related to deforestation for four different functional groups (herbivorous, omnivorous, piscivorous, and top predator fish) based on local river turbidity and off-shelf sediment export rate, and find that the effects of deforestation can be magnified up to four

times in naturally turbid waters. We show that a fishing strategy featuring a constant total harvesting rate but flexible harvesting of different functional groups based on availability leads to substantially higher populations of herbivorous fish and top predators, with greater stability over time for these populations even with heavy sedimentation brought on by deforestation. We show that if population increases cause both greater deforestation and greater demand for fish, these increases in demand may not translate into greater fish catch due to local fish depletion. We show that harvesting at levels that would be sustainable under current conditions would instead lead to fish population collapses under highland deforestation, but that small to medium-scale lowland logging operations can be carried out without jeopardizing fish survival.

4.6.1 Temporal effects of deforestation on community composition, including trophic cascades

Our results show that after 20 years of deforestation and its associated sedimentation, herbivorous fish were more abundant in areas with less off-shelf sediment export (Figure 4.2). We also found that herbivorous fish populations showed a pronounced bump during the first 5-10 years of our deforestation simulations, peaking above their estimated pristine levels (Figure 4.4a). Both of these results point to coral being less resilient to high sediment levels than herbivorous fish, leading to coral being put under pressure first. This result has parallels in previous field work done in the Solomon Islands, in which coral appeared to decline in health over a 5-year period following the onset of heavy sedimentation (at or before the beginning of the study), but effects on fish abundance were less evident [102]. Similarly, field observations at a site in Hawaii in 1976 and 1996 that had been under intense sedimentation pressure due to offshore development showed a catastrophic decline in coral cover, but a mixture of decreasing and stable populations in reef fish [230]. These results support our findings that twenty years of heavy sedimentation is enough time for some fish taxa to collapse, depending on fishing pressure, but that coral would be more immediately susceptible to sedimentation's effects.

In our model, when large volumes of sediment are exported onto a reef and retained there, most coral dies and is replaced with algal turf, providing herbivorous fish with a short-term increase in food availability. However, this turf is typically LSAT, which is associated with low rates of herbivory. This means that under these conditions, herbivorous fish populations are significantly lower then their theoretical maxima, even in the most extreme cases when their predators are at or near extinction and the seabed is dominated by algal turf (Figure 4.2d). Another consequence of this is that after 50 years of deforestation and sediment buildup, the herbivorous fish population in the case with low off-shelf

sediment export ($e = 0.1$) is essentially the same as the other cases, as herbivorous fish cannot take advantage of the LSAT that predominates in that scenario (Figures 4.2b and 4.2d).

Piscivorous fish and top predators were in many cases quite resistant to the effects of deforestation, although this was complicated by the possibility of bottom-up trophic cascades. Whenever herbivorous fish populations crashed to very low levels, this was followed by similar declines in piscivorous fish and top predators about 20 years later, but this effect was not seen when herbivorous fish populations were only reduced by moderate amounts (Figures 4.2 and 4.5a). Additionally, in simulated areas where almost all sediment discharged from rivers is locally retained, we observed large declines in piscivorous fish and top predator populations approximately 15 years following declines in omnivorous fish, even though herbivorous fish were able to subsist on the massive amounts of low-quality algal turf (Figure 4.5a). This reduced the predation pressure on herbivorous fish, attenuating their decline even further due to this trophic feedback. It is known that herbivorous reef fish are sensitive to bottom-up control [214], whereas our results show that this sensitivity may be lessened for fish at higher trophic levels.

We can therefore identify three different regimes of fish population decline due to deforestation-driven sedimentation, with population reductions in the functional groups that we modelled happening at different speeds and in different orders in each regime. In areas with naturally high turbidity, we expect omnivorous fish to collapse first, followed by species at higher trophic levels, with herbivorous fish showing milder declines. When deforestation either happens on highland terrain or at a fast rate, we expect herbivorous fish to be the first to drop to critical levels, followed by omnivorous fish 10 to 20 years later, then fish at higher trophic levels. When deforestation happens relatively slowly and on flat lowland terrain, we expect herbivorous fish to exhibit moderate declines, followed by omnivorous fish soon after, but piscivorous fish and top predators should maintain relatively high abundance. Under these conditions, if deforestation is contained in relatively small areas (e.g. $r_x \approx 0.05$, about one fourth of the deforestation rate seen in Borneo in the past few decades) and local waters are not naturally turbid, losses in fish abundance should be minimal.

Our findings on the resistance to deforestation-driven sedimentation shown by fish at high trophic levels, as compared with herbivorous and omnivorous fish (Figures 4.2 and 4.3), are in concordance with a recent study on reefs in Western Australia by Moustaka *et al.* [178]. This study showed that abundances of herbivorous scrapers and planktivorous omnivores had significant negative correlations with water turbidity, but generalist carnivores were substantially less affected by it. Our model provides a mechanistic framework for explaining these results, and can be used for testing their robustness in other locations

due to the comprehensiveness of FishBase trophic, harvesting, and resilience data [88].

4.6.2 Interactions between deforestation and overfishing, and impact of flexible harvesting on sedimented reefs

Our simulations with fishing pressure on different reef fish functional groups defined both in terms of variable rates increasing with human population (Figure 4.6) and constant quota levels (Figure 4.7) show how interaction effects between overfishing and deforestation-driven sedimentation on reef fish abundance can change given local conditions. It has previously been experimentally shown that when nutrient levels are low, overfishing (simulated with herbivore exclusion cages) and sedimentation can have nonlinear masking effects on algal turf length, a proxy for turf quality due to its association with LSAT and SPAT, but for high nutrient levels this interaction becomes linear [85]. We similarly considered how varying levels of overfishing and deforestation (an upstream cause of sedimentation) can alter measures related to fish such as long-term population sizes, time to local extinction, and total catch over 50 years. For lowland deforestation, the interaction effects with fishing pressure were close to being linear (Figures 4.6a, 4.7a, and 4.7c), although nonlinearities were seen in the combined effects of lowland deforestation and growth in fish demand on fisheries yield (Figure 4.6c). However, exposure to both highland deforestation and high fishing rates led to compounding effects on fish local extinction risk (Figures 4.6b, 4.7b, and 4.7d). This shows the potential for "ecological surprises" under such scenarios, where small increases in rates of deforestation or fish harvesting could have outsize impacts on the ability of reef fish to persist.

We found flexible harvesting strategies to work very well in stabilizing fish populations, particularly those of herbivorous fish and top predators, both of which currently have high demand in the Solomon Islands. These strategies allowed both of these functional groups to persist at reasonable levels even in the face of severe sedimentation pressure caused by highland deforestation (Figure 4.5b). Flexible harvesting strategies such as the ones we recommend can be implemented in a variety of ways. For instance, reef fisheries target different species by using different gear, such as beach seines, spearguns, fish traps, nets, and hand lines [114], although some overlaps do exist. Fishing restrictions based on gear can therefore be used to redistribute, rather than reduce, a fishery's efforts [115], ideal for carrying out a strategy that keeps total fishing rate constant but varies which fish are targeted. Fishers have been more receptive to gear restrictions compared to the establishment of no-take areas [163], which is important as presenting management strategies acceptable to local fishers is far from trivial [199]. Such restrictions can also be dynamically updated based on field observations of which species need greater protection,

which would go a long way towards reducing risk from deforestation (see Figures 4.4 and 4.5).

The preferences of fishers have been previously noted to change as conditions on a reef do. The results of Rassweiler *et al.* suggest that the taxa preferred by fishers operating are different on healthy reefs and on degraded, macroalgae-dominated reefs, and imply that shifts towards macroalgae dominance could be accompanied by greater harvesting of rabbitfish [202]. Fishers in the Solomon Islands have also successfully responded in the past to the evolution of conditions in local fishing areas, by a combination of altering which gear and methods they used, which species they targeted, and which locations they visited [9]. Given this, it is likely that the implementation of flexible harvesting practices in response to greater sedimentation on reefs can be informed by existing local knowledge of which species to target under turbid conditions.

Chapter 5

Conclusion

5.1 Summary of findings

Our work in this thesis used three different mathematical models of coral reefs to investigate the impact of reef stressors over multiple spatial scales, and evaluate conservation prospects both now and in the future. This spatial focus was previously rare in both the mathematical and field literature on coral reefs, and hence explicitly considering spatial dynamics led to valuable insights for reef conservation. For instance, we found that coral populations are maximized when long, contiguous stretches of coastline are set aside as marine protected areas (MPAs), whereas herbivorous fish did better when MPAs were smaller and dispersed throughout unprotected areas (Figure 2.4). Ecologists have debated whether having large MPAs or smaller but interconnected MPAs results in optimal conservation outcomes [81]; we show here that the answer to that question can be different for two taxa that inhabit the same places and may be considered jointly in conservation efforts. We also found that managing crown-of-thorns starfish (CoTS) outbreaks with spatial dynamics in mind yields higher regional-level coral cover than if management of individual patches is done in a vacuum, consistent with past studies that have shown strictly local-scale CoTS management to have little effectiveness in preventing regional-scale outbreaks [198]. In reef areas with slow currents, or if only small areas of coastline can be managed, removing CoTS from areas where they have the highest likelihood of dispersing into other areas with high coral cover outperforms purely local strategies (Figure 3.6). Additionally, if resources exist for a wider area to be managed during a CoTS outbreak, removing CoTS from parts of a reef in which coral is most likely to recover becomes the better strategy. This is because under these conditions, CoTS in an area under management would be more likely to disperse into another area that is also being actively managed, so focusing

on preventing CoTS spread becomes less of an issue. Hence, the consideration of which strategy to use for CoTS removal still depends on spatial factors, even if the particular strategy that is eventually applied is a local one. Furthermore, our work on the effects of deforestation on reef fish shows that ecological processes that occur far away from reefs, in a completely different biome, can still nonetheless impact reef species greatly. An example of this is the difference in severity between lowland and highland deforestation on reef fish populations: when substantial deforestation pressure is present, persistence or extirpation of reef fish could depend on the topography of local river catchments (see [67] for another example of terrestrial topography being considered as a driver of coral reef health). These results highlight how interconnected different areas of a coral reef are, as well as how interconnected reefs as a whole are with the ecosystems that surround them.

One major theme present throughout this thesis is the fact that outcomes beneficial for both conservation and economic growth can be achieved. For instance, we found that transitions from a fishing-based economy to a tourism-based one in certain subsections of a reef can result in recovery first of herbivorous fish and subsequently of coral throughout the entire reef (Figure 2.7). Similarly, we found that temporary subsidies to reef-based tourism lasting a few years could, via feedback loops in our model, lead to substantial boosts or even long-term stability for herbivorous fish and coral populations (Figure 2.8). These results, coupled with our finding of a strong spillover effect for herbivorous fish (Figure 2.6), mean that reef fisheries in communities nearby an area undergoing an economic shift to tourism would substantially benefit from this shift as well. Hence, our results show that healthy reefs and profitable fishing and tourism industries can all coexist with each other, and that growing fish and coral populations can be accompanied by a growing economy. It has been shown that under certain conditions, fishing and tourism can coexist as economic strategies on reefs [82], as well as that a balance between those two economic strategies (roughly 50 percent preference for each) generates the most profit overall [268]. We provide evidence that such an arrangement would also ensure a reasonably healthy reef, with sustainable populations of both coral and reef fish. We additionally found that flexibility in harvesting different functional groups of reef fish, while maintaining the same overall fishing rates, can facilitate high and relatively stable populations of several fish functional groups in the Solomon Islands without sacrificing fisheries yield (Figure 4.4). Similarly, we found that if logging operations are restricted to lowland areas and the total amount of land cleared in these operations is not too high, reef fish can persist at levels close to those seen in pristine ecosystems (Figure 4.2). As with fishing and tourism, this means that the logging industry can coexist with a relatively healthy reef, although the margin for error in this case is comparatively smaller. Previous work has shown that striking a balance between logging and fishery output in another sensitive ecosystem (i.e. mangroves) is possible [98], and that forestry best practices can lessen the damage to reef fish stocks caused by

deforestation so long as local forests are still relatively intact [263]. Our work builds on this by demonstrating that if both forests and reef fisheries are managed effectively, development of both industries can be achieved while maintaining reasonably abundant fish populations. Since incompatibilities are common when considering the needs of many different economic and ecological stakeholders [42, 259], discovering paths to mutually beneficial outcomes (as was done in this thesis) is vital for balancing environmental protection with future economic development.

In a world that is constantly changing, the most effective conservation strategies will be ones that are flexible [71, 62]. We have shown this in our work, by highlighting the effectiveness of flexible methods of coral and reef fish conservation in the face of three very different problems faced by reefs. For instance, if overfishing has led to state shifts to macroalgae dominance on a large, contiguous reef area, but adjacent areas have been protected effectively and thus have healthy coral (see Figure 2.5), an ecosystem manager could come to the conclusion that establishing MPAs is the only way to preserve coral (see e.g. [49]). However, we present an alternative in the form of subsidies to tourism, which need not last for longer than a few years to set fish and coral recovery in motion (Figure 2.8); this strategy and MPA establishment can serve as complementary approaches within a manager's toolbox. In Barbados, policy planning areas for developing a sustainable tourism industry and increasing resilience to climate change overlap with each other [183], demonstrating a real-world example of how promoting tourism in reefside areas can assist with conservation. Additionally, our results show that reef fish, especially those that are herbivorous or occupy the upper reaches of the local food web, can become much more resilient to the sedimentation caused by deforestation if reef fisheries follow flexible harvesting guidelines (Figures 4.4 and 4.5). Although flexible harvesting is not a conservation strategy *per se*, our results dealing with it show how using an adaptable method can produce beneficial outcomes in domains other than the one that it is used for. Indeed, introducing flexibility in reef fishers' behaviour has been previously cited as a way to enhance reef resilience (within the context of ocean acidification), with funding to assist reef fishers in obtaining employment in ecotourism being explicitly mentioned [116]. Similarly, networks of both static and dynamic MPAs have recently been postulated as a way to enhance reef conservation under changing environmental conditions: some areas would be permanently set aside as MPAs, while the locations of other MPAs would be periodically adjusted based on local needs [62]. This strategy of temporal flexibility in MPA location could directly address the issues caused by habitat fragmentation that were brought up in this thesis. Additionally, we have demonstrated that each of four different strategies for removing CoTS from a reef being degraded by them can be optimal, depending on local and regional conservation priorities. As mentioned above, whether removing CoTS from areas based on their ability to spread or coral's ability to recover is the best strategy

depends on the amount of resources available for management (Figure 3.6). However, if authorities want to "play it safe" and ensure CoTS do not reach a critical mass on any one part of a reef, removing CoTS from the areas where they have the highest density is optimal (Figure 3.5), and using an average of these three strategies can also lead to appreciable gains in coral cover if a more holistic approach is desired (Figure 3.6). As neglecting CoTS management could lead to outbreaks, and hence coral devastation, over very large spatial scales (see e.g. [251, 107]), we have therefore demonstrated that flexible ecosystem management can make a huge difference in keeping coral reefs alive.

In a similar vein, we found that the interactions between several different coral reef stressors can change drastically over time, and we project that different stressors will increase and decrease in importance as areas adjacent to reefs develop and human influence on reefs becomes stronger. For instance, we predict that reefs under threat by CoTS outbreaks that are fairly pristine will be most affected by incremental gains in nutrient loading, whereas reefs adjacent to more heavily-populated areas will instead be more affected by incremental gains in fishing pressure (Figures 3.3 and 3.4). This meant that as fish harvesting rates increased in our simulations, the beneficiary of concurrent increases in nutrient loading rates changed from being herbivorous fish (that eat macroalgae) to the macroalgae themselves. We also found significant spatial differences in how reef stressors interact with each other. Specifically, on reefs with a relatively low burden of sedimentation, the damage to reef fish abundance caused by deforestation and that caused by overfishing were additive in nature, but on reefs adjacent to a watershed experiencing highland deforestation, the effects of deforestation-driven sedimentation and overfishing instead compounded on each other nonlinearly (Figures 4.6 and 4.7). Our results here are in agreement with the broad observations that complex, nonlinear interactions are common on reefs [85] and in ecological systems more generally [64], and reinforce our message on the importance of flexibility and adaptability in conservation measures. They also indicate that anticipating which stressors will impact reefs in the future, and at which magnitudes, is key for ensuring optimal conservation outcomes, stressing the importance of long-range mathematical modelling to find potential interactions that would be difficult to uncover by other means.

5.2 Future work

The work that makes up this thesis includes significant insights into how multiple stressors of coral reefs interact with each other, both now and in the future. Specifically, we covered how coral responds to pressure from overfishing, nutrient loading, CoTS outbreaks, and sedimentation in different combinations. These and other stressors such as ocean acidification [193, 131] and ocean warming [48, 193] will no doubt continue to exert influence on

coral reefs, and nonlinear (synergistic or antagonistic) interactions are common in marine systems [61, 64]. Therefore, studies on multi-stressor interaction are highly important for determining conservation priorities and establishing expectations for likely and worst-case scenarios. Despite this, studies that examine the interaction effects of four or more reef stressors are virtually nonexistent in the literature [74]. This can be attributed to the challenges in disentangling these effects when a large number of them are present, as well as the difficulty in setting up conditions to test these effects in the field for certain stressors (such as CoTS outbreaks or severe storms). However, these concerns apply less to mathematical coral reef models, and hence modelling can provide significant research contributions in determining how many different reef stressors interact with each other. Future work will fill this knowledge gap by using reef models to predict the interaction effects, both pairwise and in aggregate, that can be expected on coral reefs under threat from many sources.

In addition to the Solomon Islands, deforestation has been cited as a concern in other areas with offshore coral reefs, for example Vanuatu [50] and Madagascar [156]. In many such locations (especially volcanic high islands), future deforestation could be on elevated or steep terrain and thus result in large-scale sediment production. However, the fish community composition is often very different from island group to island group. This means that there also exists significant spatial variation in the growth and harvesting rates of fish at different trophic levels when viewed in the aggregate [88]. Similarly, we also found that different outcomes in the timing and order of the declines of fish functional groups were possible depending on local conditions (Figures 4.2 and 4.5). Because of these factors, our future work will include an island-by-island (and, for large islands, watershed-by-watershed) evaluation of which fish functional groups are the most vulnerable to the sedimentation caused by deforestation, as well as how to best protect them while maintaining adequate fisheries yield.

In our work on controlling CoTS outbreaks, we determined the best strategies for minimizing damage done to coral during potential outbreaks in Jeddah, Saudi Arabia and in Cebu City, Philippines, two cities with offshore coral that are within the existing range of CoTS. Since CoTS is a fast-spreading organism, and has established itself over a very wide range of locations in the Indo-Pacific region [107, 273], it would be able to devastate coral in a very large area if it were to further expand into areas where it is not native (e.g. the Caribbean). Therefore, in the future, we will use available local data to model the beginning of CoTS outbreaks on reefs outside the Indo-Pacific, and determine how much control would be needed to prevent CoTS from successfully invading these areas. We will similarly identify which local areas a hypothetical CoTS invasion would do the most damage in. Furthermore, the current range of CoTS includes reef areas that are very heterogeneous in terms of their environmental conditions; points of variation include ocean

current strength, nutrient runoff, future population growth, current coral cover, and fishing pressure. In order to provide comprehensive management recommendations for CoTS outbreaks throughout the Indo-Pacific, we will simulate such outbreaks and management strategies thereof in all possible areas for which a CoTS outbreak has been recorded in the literature. This will provide conservation managers valuable tools to protect coral in locations where CoTS management programs have not yet been established.

Along with increasing the total amount of nutrients exported into reef ecosystems, human population increases can also change the relative proportions in which common nutrients such as nitrogen and phosphorus are available [86]. Our studies on increases in nutrient loading looked specifically at nitrogen, since pristine reefs are commonly N-limited. We found that as nitrogen input onto reefs increased, further incremental gains in nitrogen input resulted in slower changes in system dynamics (Figures 2.2 and 3.4), corresponding to a shift to P-limitation. Changes in stoichiometry in aquatic ecosystems are capable of causing phenomena such as algal blooms [110] that happen over very short timescales, as well as affecting long-term evolutionary trajectories [277], and the ability of nutrient loading in general to cause regime shifts on coral reefs is well-known [17]. Hence, anthropogenic development, and the nutrient increases and stoichiometric changes that accompany it, could lead to abrupt tipping of coral reefs into algae-dominant alternative stable states. However, which areas are most at risk will depend on factors such as local currents and existing relative nutrient abundances. We can therefore use hydrodynamic modelling, population projections, and available local data to determine the sensitivity of different local reef areas to regime shifts based on altered stoichiometry.

As this thesis includes what is (to our knowledge) the first work that quantifies when and where coral can be expected to recover after economic transitions from a fishing-based economy to a tourism-based one, there exists a significant opening for future research on how economic factors can affect coral reef health. For instance, when evaluating the different responses to habitat fragmentation by coral and herbivorous fish (Figures 2.4, 2.5, and 2.6), we took local economic preferences for tourism and fishing to be equal across the system. However, it is possible that spatial variation in these preferences could itself cause habitat fragmentation. Therefore, in the future, we will determine whether reef degradation due to overfishing is more likely the result of high local fishing intensity (measured using harvesting rates) or local economic preferences starkly favouring fishing, by simulating fragmentation caused by each of those factors. This understanding of the root cause of overfishing-driven reef damage will allow policymakers to devise optimal strategies to preserve reef habitats without unnecessarily jeopardizing local reef fisheries. Additionally, while our results show the strength of the spillover effect for herbivorous reef fish, we did not consider fish in other functional groups in our study. Quantifying

the spillover effect for many different functional groups, and by extension determining the best possible MPA placement to optimize regional-scale fish populations across many different species of commercial and ecological interest, would be a boon to fisheries and conservationists alike.

5.3 Concluding comments

This thesis has used spatially explicit mathematical models of intermediate complexity to address three different problems that coral reefs face now and will continue to face, with greater intensity, going forward. This yielded results which linked robust theory with concrete conservation recommendations, which frameworks without a spatial component would miss. In recent years, the study of coral reefs has increasingly utilized mathematical analysis to produce novel insights and testable predictions, many of which have encouragingly been verified in the field. The work contained in this thesis greatly adds to this, by tackling problems that would be difficult to solve using field studies alone due to their spatial complexity. Future work will continue with this paradigm, using mathematical tools to promote healthy reefs and reefside communities in order to ensure a sustainable future for such an iconic part of Earth's oceans.

References

[1] Amin Abbasi, Somaiyeh MahmoudZadeh, and Amirmehdi Yazdani. A cooperative dynamic task assignment framework for COTSBot AUVs. *IEEE Transactions on Automation Science and Engineering*, pages 1–17, 2020.

[2] M. Abbiati, G. Buffoni, G. Caforio, G. Di Cola, and G. Santangelo. Harvesting, predation and competition effects on a red coral population. *Netherlands Journal of Sea Research*, 30:219–228, 1992.

[3] Rene A. Abesamis, Pablo Saenz-Agudelo, Michael L. Berumen, Michael Bode, Claro Renato L. Jadloc, Leilani A. Solera, Cesar L. Villanoy, Lawrence Patrick C. Bernardo, Angel C. Alcala, and Garry R. Russ. Reef-fish larval dispersal patterns validate no-take marine reserve network connectivity that links human communities. *Coral Reefs*, 36(3):791–801, 2017.

[4] Michael Lochinvar Sim Abundo, Jet Lawrence Belbes, Xinia Angela Cruz, Venice Erin Liong, Marc Caesar Talampas, Laura David, and Cesar Villanoy. Drifters as preliminary site assessment tool for ocean current-based renewable energy for straits and channels in the Philippines. In *2010 Conference Proceedings IPEC*. IEEE, 2010.

[5] Daron Acemoglu, Victor Chernozhukov, Iván Werning, and Michael Whinston. Optimal targeted lockdowns in a multi-group SIR model. Technical report, 2020.

[6] Maria Fernanda Adame, Melanie E. Roberts, David P. Hamilton, Christopher E. Ndehedehe, Vanessa Reis, Jing Lu, Matthew Griffiths, Graeme Curwen, and Mike Ronan. Tropical coastal wetlands ameliorate nitrogen export during floods. *Frontiers in Marine Science*, 6, 2019.

[7] Y Akita, T Kurihara, M Uehara, T Shiwa, and K Iwai. Impacts of overfishing and sedimentation on the feeding behavior and ecological function of herbivorous fishes in coral reefs. *Marine Ecology Progress Series*, 686:141–157, 2022.

[8] Radwan Al-Farawati, Mohamed Abdel Khalek El Sayed, and Najeeb M. A. Rasul. Nitrogen, phosphorus and organic carbon in the Saudi Arabian Red Sea coastal waters: Behaviour and human impact. In *Springer Oceanography*, pages 89–104. Springer International Publishing, 2018.

[9] Simon Albert, Shankar Aswani, Paul L. Fisher, and Joelle Albert. Keeping food on the table: Human responses and changing coastal fisheries in Solomon Islands. *PLOS ONE*, 10(7):e0130800, 2015.

[10] Simon Albert, Nathaniel Deering, Scravin Tongi, Avik Nandy, Allen Kisi, Myknee Sirikolo, Michael Maehaka, Nicholas Hutley, Shaun Kies-Ryan, and Alistair Grinham. Water quality challenges associated with industrial logging of a karst landscape: Guadalcanal, Solomon Islands. *Marine Pollution Bulletin*, 169:112506, 2021.

[11] Simon Albert, Paul L. Fisher, Badin Gibbes, and Alistair Grinham. Corals persisting in naturally turbid waters adjacent to a pristine catchment in Solomon Islands. *Marine Pollution Bulletin*, 94(1-2):299–306, 2015.

[12] Angel Alcala. *Directory of marine reserves in the Visayas, Philippines*. Foundation for the Philippine Environment and Sillliman University-Angelo King Center for Research and Environmental Management (SUAKCREM), Dumaguete City, Philippines, 2008.

[13] Mohammed Aljoufie and Alok Tiwari. Climate change adaptions for urban water infrastructure in Jeddah, Kingdom of Saudi Arabia. *Journal of Sustainable Development*, 8(3), 2015.

[14] G. R. Almany, S. R. Connolly, D. D. Heath, J. D. Hogan, G. P. Jones, L. J. McCook, M. Mills, R. L. Pressey, and D. H. Williamson. Connectivity, biodiversity conservation and the design of marine reserve networks for coral reefs. *Coral Reefs*, 28(2):339–351, 2009.

[15] Glenn R. Almany, Serge Planes, Simon R. Thorrold, Michael L. Berumen, Michael Bode, Pablo Saenz-Agudelo, Mary C. Bonin, Ashley J. Frisch, Hugo B. Harrison, Vanessa Messmer, Gerrit B. Nanninga, Mark A. Priest, Maya Srinivasan, Tane Sinclair-Taylor, David H. Williamson, and Geoffrey P. Jones. Larval fish dispersal in a coral-reef seascape. *Nature Ecology & Evolution*, 1(6), 2017.

[16] Li An, Frank Lupi, Jianguo Liu, Marc A. Linderman, and Jinyan Huang. Modeling the choice to switch from fuelwood to electricity. *Ecological Economics*, 42(3):445–457, 2002.

[17] Jesús Ernesto Arias-González, Tak Fung, Robert M. Seymour, Joaquín Rodrigo Garza-Pérez, Gilberto Acosta-González, Yves-Marie Bozec, and Craig R. Johnson. A coral-algal phase shift in Mesoamerica not driven by changes in herbivorous fish abundance. *PLOS ONE*, 12(4):e0174855, 2017.

[18] Russell C. Babcock, Jeffrey M. Dambacher, Elisabetta B. Morello, Éva E. Plagányi, Keith R. Hayes, Hugh P. A. Sweatman, and Morgan S. Pratchett. Assessing different causes of crown-of-thorns starfish outbreaks and appropriate responses for management on the Great Barrier Reef. *PLOS ONE*, 11(12):e0169048, 2016.

[19] Arieanna C. Balbar and Anna Metaxas. The current application of ecological connectivity in the design of marine protected areas. *Global Ecology and Conservation*, 17:e00569, 2019.

[20] Lee-Ann Barlow, Jacob Cecile, Chris T. Bauch, and Madhur Anand. Modelling interactions between forest pest invasions and human decisions regarding firewood transport restrictions. *PLoS ONE*, 9(4):e90511, 2014.

[21] Rebecca Bartley, Zoe T. Bainbridge, Stephen E. Lewis, Frederieke J. Kroon, Scott N. Wilkinson, Jon E. Brodie, and D. Mark Silburn. Relating sediment impacts on coral reefs to watershed sources, processes and management: A review. *Science of The Total Environment*, 468-469:1138–1153, 2014.

[22] David R. Bellwood and Christopher J. Fulton. Sediment-mediated suppression of herbivory on coral reefs: Decreasing resilience to rising sea-levels and climate change? *Limnology and Oceanography*, 53(6):2695–2701, 2008.

[23] David R. Bellwood and Terry P. Hughes. Regional-scale assembly rules and biodiversity of coral reefs. *Science*, 292(5521):1532–1535, 2001.

[24] Diana M. Beltrán, Nikolaos V. Schizas, Richard S. Appeldoorn, and Carlos Prada. Effective dispersal of Caribbean reef fish is smaller than current spacing among marine protected areas. *Scientific Reports*, 7(1), 2017.

[25] M. L. Berumen, A. S. Hoey, W. H. Bass, J. Bouwmeester, D. Catania, J. E. M. Cochran, M. T. Khalil, S. Miyake, M. R. Mughal, J. L. Y. Spaet, and P. Saenz-Agudelo. The status of coral reef ecology research in the Red Sea. *Coral Reefs*, 32(3):737–748, 2013.

[26] Charles Birkeland. Symbiosis, fisheries and economic development on coral reefs. *Trends in Ecology & Evolution*, 12(9):364–367, 1997.

[27] Julie C. Blackwood, Alan Hastings, and Peter J. Mumby. The effect of fishing on hysteresis in Caribbean coral reefs. *Theoretical Ecology*, 5(1):105–114, 2010.

[28] Julie C. Blackwood, Alan Hastings, and Peter J. Mumby. A model-based approach to determine the long-term effects of multiple interacting stressors on coral reefs. *Ecological Applications*, 21(7):2722–2733, 2011.

[29] Julie C. Blackwood, Colin Okasaki, Andre Archer, Eliza W. Matt, Elizabeth Sherman, and Kathryn Montovan. Modeling alternative stable states in Caribbean coral reefs. *Natural Resource Modeling*, 31(1):e12157, 2018.

[30] Mary C. Bonin, Glenn R. Almany, and Geoffrey P. Jones. Contrasting effects of habitat loss and fragmentation on coral-associated reef fishes. *Ecology*, 92(7):1503–1512, 2011.

[31] Arthur R. Bos, Girley S. Gumanao, Benjamin Mueller, and Marjho M.E. Saceda-Cardoza. Management of crown-of-thorns sea star (Acanthaster planci L.) outbreaks: Removal success depends on reef topography and timing within the reproduction cycle. *Ocean & Coastal Management*, 71:116–122, 2013.

[32] C Boström, SJ Pittman, C Simenstad, and RT Kneib. Seascape ecology of coastal biogenic habitats: advances, gaps, and challenges. *Marine Ecology Progress Series*, 427:191–217, 2011.

[33] Lisa Boström-Einarsson and Jairo Rivera-Posada. Controlling outbreaks of the coral-eating crown-of-thorns starfish using a single injection of common household vinegar. *Coral Reefs*, 35(1):223–228, 2015.

[34] L. W. Botsford, J. W. White, M.-A. Coffroth, C. B. Paris, S. Planes, T. L. Shearer, S. R. Thorrold, and G. P. Jones. Connectivity and resilience of coral reef metapopulations in marine protected areas: matching empirical efforts to predictive needs. *Coral Reefs*, 28(2):327–337, 2009.

[35] SJ Box and PJ Mumby. Effect of macroalgal competition on growth and survival of juvenile Caribbean corals. *Marine Ecology Progress Series*, 342:139–149, 2007.

[36] Yves-Marie Bozec, Lorenzo Alvarez-Filip, and Peter J. Mumby. The dynamics of architectural complexity on coral reefs under climate change. *Global Change Biology*, 21(1):223–235, 2014.

[37] Tom D. Brewer, Joshua E. Cinner, Rebecca Fisher, Alison Green, and Shaun K. Wilson. Market access, population density, and socioeconomic development explain diversity and functional group biomass of coral reef fish assemblages. *Global Environmental Change*, 22(2):399–406, 2012.

[38] Cheryl J. Briggs, Thomas C. Adam, Sally J. Holbrook, and Russell J. Schmitt. Macroalgae size refuge from herbivory promotes alternative stable states on coral reefs. *PLoS ONE*, 13(9):e0202273, 2018.

[39] Jon Brodie, Katharina Fabricius, Glenn De'ath, and Ken Okaji. Are increased nutrient inputs responsible for more outbreaks of crown-of-thorns starfish? an appraisal of the evidence. *Marine Pollution Bulletin*, 51(1-4):266–278, 2005.

[40] John F. Bruno and Elizabeth R. Selig. Regional decline of coral cover in the Indo-Pacific: Timing, extent, and subregional comparisons. *PLoS ONE*, 2(8):e711, 2007.

[41] Alexander Buck, Naomi Gardiner, and Lisa Boström-Einarsson. Citric acid injections: An accessible and efficient method for controlling outbreaks of the crown-of-thorns starfish Acanthaster cf. solaris. *Diversity*, 8(4):28, 2016.

[42] James R.A. Butler, Grace Y. Wong, Daniel J. Metcalfe, Miroslav Honzák, Petina L. Pert, Nalini Rao, Martijn E. van Grieken, Tina Lawson, Caroline Bruce, Frederieke J. Kroon, and Jon E. Brodie. An analysis of trade-offs between multiple ecosystem services and stakeholders linked to land use and water quality management in the Great Barrier Reef, Australia. *Agriculture, Ecosystems & Environment*, 180:176–191, 2013.

[43] Reniel B. Cabral, Darcy Bradley, Juan Mayorga, Whitney Goodell, Alan M. Friedlander, Enric Sala, Christopher Costello, and Steven D. Gaines. A global network of marine protected areas for food. *Proceedings of the National Academy of Sciences*, 117(45):28134–28139, 2020.

[44] Reniel B. Cabral, Steven D. Gaines, Brett A. Johnson, Tom W. Bell, and Crow White. Drivers of redistribution of fishing and non-fishing effort after the implementation of a marine protected area network. *Ecological Applications*, 27(2):416–428, 2017.

[45] M. Julian Caley, Kathryn A. Buckley, and Geoffrey P. Jones. Separating ecological effects of habitat fragmentation, degradation and loss on coral commensals. *Ecology*, 82(12):3435–3448, 2001.

[46] Carolina Camargo, Jorge H. Maldonado, Elvira Alvarado, Rocío Moreno-Sánchez, Sandra Mendoza, Nelson Manrique, Andrés Mogollón, Juan D. Osorio, Alejandro Grajales, and Juan Armando Sánchez. Community involvement in management for maintaining coral reef resilience and biodiversity in southern Caribbean marine protected areas. *Biodiversity and Conservation*, 18(4):935–956, 2008.

[47] James Cant, Roberto Salguero-Gómez, and Maria Beger. Transient demographic approaches can drastically expand the toolbox of coral reef science. *Coral Reefs*, 2022.

[48] Neal E. Cantin, Anne L. Cohen, Kristopher B. Karnauskas, Ann M. Tarrant, and Daniel C. McCorkle. Ocean warming slows coral growth in the Central Red Sea. *Science*, 329(5989):322–325, 2010.

[49] Laura Cardador, Lluís Brotons, François Mougeot, David Giralt, Gerard Bota, Manel Pomarol, and Beatriz Arroyo. Conservation traps and long-term species persistence in human-dominated systems. *Conservation Letters*, 8(6):456–462, 2015.

[50] Sophia Carodenuto, Benjamin Schwarz, Anjali Nelson, Godfrey Bome, and Glarinda Andre. Practice-based knowledge for REDD+ in Vanuatu. *Society & Natural Resources*, 35(2):220–241, 2022.

[51] Susana Carvalho, Benjamin Kürten, George Krokos, Ibrahim Hoteit, and Joanne Ellis. The Red Sea. In *World Seas: an Environmental Evaluation (Second Edition)*, pages 49–74. Elsevier, 2019.

[52] Yu-Chia Chang, Ruo-Shan Tseng, Peter C Chu, and Huan-Jie Shao. Global energy-saving map of strong ocean currents. *Journal of Navigation*, 69(1):75–92, 2015.

[53] Guangzhao Chen, Xia Li, Xiaoping Liu, Yimin Chen, Xun Liang, Jiye Leng, Xiaocong Xu, Weilin Liao, Yue'an Qiu, Qianlian Wu, and Kangning Huang. Global projections of future urban land expansion under shared socioeconomic pathways. *Nature Communications*, 11(1), 2020.

[54] Saad Chidami and Marc Amyot. Fish decomposition in boreal lakes and biogeochemical implications. *Limnology and Oceanography*, 53(5):1988–1996, 2008.

[55] J.H. Churchill, S.J. Lentz, J.T. Farrar, and Y. Abualnaja. Properties of Red Sea coastal currents. *Continental Shelf Research*, 78:51–61, 2014.

[56] James E. Cloern. Turbidity as a control on phytoplankton biomass and productivity in estuaries. *Continental Shelf Research*, 7(11-12):1367–1381, 1987.

[57] Sean R. Connolly and Andrew H. Baird. Estimating dispersal potential for marine larvae: dynamic models applied to scleractinian corals. *Ecology*, 91(12):3572–3583, 2010.

[58] Michael H. Cortez and Stephen P. Ellner. Understanding rapid evolution in predator-prey interactions using the theory of fast-slow dynamical systems. *The American Naturalist*, 176(5):E109–E127, 2010.

[59] Robert Costanza, Ralph d'Arge, Rudolf de Groot, Stephen Farber, Monica Grasso, Bruce Hannon, Karin Limburg, Shahid Naeem, Robert V. O'Neill, Jose Paruelo, Robert G. Raskin, Paul Sutton, and Marjan van den Belt. The value of the world's ecosystem services and natural capital. *Nature*, 387(6630):253–260, 1997.

[60] Mark J. Costello and David W. Connor. Connectivity is generally not important for marine reserve planning. *Trends in Ecology & Evolution*, 34(8):686–688, 2019.

[61] Caitlin Mullan Crain, Kristy Kroeker, and Benjamin S. Halpern. Interactive and cumulative effects of multiple human stressors in marine systems. *Ecology Letters*, 11(12):1304–1315, 2008.

[62] Cassidy C. D'Aloia, Ilona Naujokaitis-Lewis, Christopher Blackford, Cindy Chu, Janelle M. R. Curtis, Emily Darling, Frédéric Guichard, Shawn J. Leroux, Alexandre C. Martensen, Bronwyn Rayfield, Jennifer M. Sunday, Amanda Xuereb, and Marie-Josée Fortin. Coupled networks of permanent protected areas and dynamic conservation areas for biodiversity conservation under climate change. *Frontiers in Ecology and Evolution*, 7, 2019.

[63] Paul Dalzell. Catch rates, selectivity and yields of reef fishing. In *Reef Fisheries*, pages 161–192. Springer Netherlands, 1996.

[64] Emily S. Darling and Isabelle M. Côté. Quantifying the evidence for ecological synergies. *Ecology Letters*, 11(12):1278–1286, 2008.

[65] Homer Hermes de Dios and Filipina Sotto. Crown-of-thorns starfish (Acanthaster planci) population control technique and management strategies designed for developing country. *Journal of Science, Engineering and Technology*, 3:1–20, 2015.

[66] G. De'ath, K. E. Fabricius, H. Sweatman, and M. Puotinen. The 27-year decline of coral cover on the Great Barrier Reef and its causes. *Proceedings of the National Academy of Sciences*, 109(44):17995–17999, 2012.

[67] J. M. S. Delevaux, S. D. Jupiter, K. A. Stamoulis, L. L. Bremer, A. S. Wenger, R. Dacks, P. Garrod, K. A. Falinski, and T. Ticktin. Scenario planning with linked land-sea models inform where forest conservation actions will promote coral reef resilience. *Scientific Reports*, 8(1), 2018.

[68] A. Diedrich. The impacts of tourism on coral reef conservation awareness and support in coastal communities in Belize. *Coral Reefs*, 26(4):985–996, 2007.

[69] Manfredi DiLorenzo, Paolo Guidetti, Antonio DiFranco, Antonio Calò, and Joachim Claudet. Assessing spillover from marine protected areas and its drivers: A meta-analytical approach. *Fish and Fisheries*, 21(5):906–915, 2020.

[70] Amy L. Downing, Bryan L. Brown, Elizabeth M. Perrin, Timothy H. Keitt, and Mathew A. Leibold. Environmental fluctuations induce scale-dependent compensation and increase stability in plankton ecosystems. *Ecology*, 89(11):3204–3214, 2008.

[71] Martin Drechsler, Karin Johst, Frank Wätzold, and Michael I. Westphal. Integrating economic costs into the analysis of flexible conservation strategies. *Ecological Applications*, 16(5):1959–1966, 2006.

[72] SR Dudgeon, RB Aronson, JF Bruno, and WF Precht. Phase shifts and stable states on coral reefs. *Marine Ecology Progress Series*, 413:201–216, 2010.

[73] Nicholas K. Dulvy, Robert P. Freckleton, and Nicholas V. C. Polunin. Coral reef cascades and the indirect effects of predator removal by exploitation. *Ecology Letters*, 7(5):410–416, 2004.

[74] Joanne I. Ellis, Tahira Jamil, Holger Anlauf, Darren J. Coker, Joao Curdia, Judi Hewitt, Burton H. Jones, George Krokos, Benjamin Kürten, Dasari Hariprasad, Florian Roth, Susana Carvalho, and Ibrahim Hoteit. Multiple stressor effects on coral reef ecosystems. *Global Change Biology*, 25(12):4131–4146, 2019.

[75] Toby Elmhirst, Sean R. Connolly, and Terry P. Hughes. Connectivity, regime shifts and the resilience of coral reefs. *Coral Reefs*, 28(4):949–957, 2009.

[76] S. Enríquez, C. M. Duarte, and K. Sand-Jensen. Patterns in decomposition rates among photosynthetic organisms: the importance of detritus C:N:P content. *Oecologia*, 94(4):457–471, 1993.

[77] Michael Fabinyi. The intensification of fishing and the rise of tourism: Competing coastal livelihoods in the Calamianes Islands, Philippines. *Human Ecology*, 38(3):415–427, 2010.

[78] Michael Fabinyi. The role of land tenure in livelihood transitions from fishing to tourism. *Maritime Studies*, 19(1):29–39, 2020.

[79] K. E. Fabricius, K. Okaji, and G. De'ath. Three lines of evidence to link outbreaks of the crown-of-thorns seastar Acanthaster planci to the release of larval food limitation. *Coral Reefs*, 29(3):593–605, 2010.

[80] Katharina E. Fabricius. Factors determining the resilience of coral reefs to eutrophication: A review and conceptual model. In *Coral Reefs: An Ecosystem in Transition*, pages 493–505. Springer Netherlands, 2010.

[81] Lenore Fahrig. Ecological responses to habitat fragmentation per se. *Annual Review of Ecology, Evolution, and Systematics*, 48(1):1–23, 2017.

[82] Carles Falcó and Holly V. Moeller. Optimal spatial management in a multiuse marine habitat: Balancing fisheries and tourism. *Natural Resource Modeling*, 2021.

[83] Renata Ferrari, Manuel Gonzalez-Rivero, Juan Carlos Ortiz, and Peter J. Mumby. Interaction of herbivory and seasonality on the dynamics of Caribbean macroalgae. *Coral Reefs*, 31(3):683–692, 2012.

[84] B. Ferré, X. Durrieu de Madron, C. Estournel, C. Ulses, and G. Le Corre. Impact of natural (waves and currents) and anthropogenic (trawl) resuspension on the export of particulate matter to the open ocean. *Continental Shelf Research*, 28(15):2071–2091, 2008.

[85] Caitlin R. Fong, Sarah J. Bittick, and Peggy Fong. Simultaneous synergist, antagonistic and additive interactions between multiple local stressors all degrade algal turf communities on coral reefs. *Journal of Ecology*, 106(4):1390–1400, 2018.

[86] James W. Fourqurean and Joseph C. Zieman. Nutrient content of the seagrass Thalassia testudinum reveals regional patterns of relative availability of nitrogen and phosphorus in the Florida Keys USA. *Biogeochemistry*, 61(3):229–245, 2002.

[87] Alan D. Fox, David W. Corne, C. Gabriela Mayorga Adame, Jeff A. Polton, Lea-Anne Henry, and J. Murray Roberts. An efficient multi-objective optimization method for use in the design of marine protected area networks. *Frontiers in Marine Science*, 6, 2019.

[88] R. Froese and D. Pauly. Fishbase. *www.fishbase.org*, 2021.

[89] Tak Fung, Robert M. Seymour, and Craig R. Johnson. Alternative stable states and phase shifts in coral reefs under anthropogenic stress. *Ecology*, 92(4):967–982, 2011.

[90] Takuro Furusawa, Krishna Pahari, Masahiro Umezaki, and Ryutaro Ohtsuka. Impacts of selective logging on New Georgia Island, Solomon Islands evaluated using very-high-resolution satellite (IKONOS) data. *Environmental Conservation*, 31(4):349–355, 2004.

[91] David L. A. Gaveau, Douglas Sheil, Husnayaen, Mohammad A. Salim, Sanjiwana Arjasakusuma, Marc Ancrenaz, Pablo Pacheco, and Erik Meijaard. Rapid conversions and avoided deforestation: examining four decades of industrial plantation expansion in Borneo. *Scientific Reports*, 6(1), 2016.

[92] John Gibson. Forest loss and economic inequality in the Solomon Islands: Using small-area estimation to link environmental change to welfare outcomes. *Ecological Economics*, 148:66–76, 2018.

[93] Michael A. Gil, Silvan U. Goldenberg, Anne Ly Thai Bach, Suzanne C. Mills, and Joachim Claudet. Interactive effects of three pervasive marine stressors in a post-disturbance coral reef. *Coral Reefs*, 35(4):1281–1293, 2016.

[94] Christopher H. R. Goatley and David R. Bellwood. Sediment suppresses herbivory across a coral reef depth gradient. *Biology Letters*, 8(6):1016–1018, 2012.

[95] Christopher H. R. Goatley, Roberta M. Bonaldo, Rebecca J. Fox, and David R. Bellwood. Sediments and herbivory as sensitive indicators of coral reef degradation. *Ecology and Society*, 21(1), 2016.

[96] ME Goecker, KL Heck, and JF Valentine. Effects of nitrogen concentrations in turtlegrass Thalassia testudinum on consumption by the bucktooth parrotfish Sparisoma radians. *Marine Ecology Progress Series*, 286:239–248, 2005.

[97] Shanna Grafeld, Kirsten L. L. Oleson, Lida Teneva, and John N. Kittinger. Follow that fish: Uncovering the hidden blue economy in coral reef fisheries. *PLOS ONE*, 12(8):e0182104, 2017.

[98] Monica Grasso. Ecological–economic model for optimal mangrove trade off between forestry and fishery production: comparing a dynamic optimization and a simulation model. *Ecological Modelling*, 112(2-3):131–150, 1998.

[99] Dominique Gravel, Frédéric Guichard, Michel Loreau, and Nicolas Mouquet. Source and sink dynamics in meta-ecosystems. *Ecology*, 91(7):2172–2184, 2010.

[100] Yi Guan, Sönke Hohn, Christian Wild, and Agostino Merico. Vulnerability of global coral reef habitat suitability to ocean warming, acidification and eutrophication. *Global Change Biology*, 26(10):5646–5660, 2020.

[101] Georgina G. Gurney, Jessica Melbourne-Thomas, Rollan C. Geronimo, Perry M. Aliño, and Craig R. Johnson. Modelling coral reef futures to inform management: Can reducing local-scale stressors conserve reefs under climate change? *PLoS ONE*, 8(11):e80137, 2013.

[102] B. S. Halpern, K. A. Selkoe, C. White, S. Albert, S. Aswani, and M. Lauer. Marine protected areas and resilience to sedimentation in the Solomon Islands. *Coral Reefs*, 32(1):61–69, 2012.

[103] Richard J. Hamilton, Glenn R. Almany, Christopher J. Brown, John Pita, Nathan A. Peterson, and J. Howard Choat. Logging degrades nursery habitat for an iconic coral reef fish. *Biological Conservation*, 210:273–280, 2017.

[104] Nicholas M. Hammerman, Alberto Rodriguez-Ramirez, Timothy L. Staples, Thomas M. DeCarlo, Vincent Saderne, George Roff, Nicole Leonard, Jian xin Zhao, Susann Rossbach, Michelle N. Havlik, Carlos M. Duarte, and John M. Pandolfi. Variable response of Red Sea coral communities to recent disturbance events along a latitudinal gradient. *Marine Biology*, 168(12), 2021.

[105] M. H. Hamza, A. S. Al-Thubaiti, M. Dhieb, A. Bel Haj Ali, M. S. Garbouj, and M. Ajmi. Dasymetric mapping as a tool to assess the spatial distribution of population in Jeddah City (Kingdom of Saudi Arabia). *Current Urban Studies*, 04(03):329–342, 2016.

[106] Charles Hannah, Alain Vezina, and Mike St. John. The case for marine ecosystem models of intermediate complexity. *Progress in Oceanography*, 84(1-2):121–128, 2010.

[107] Hugo Harrison, Morgan Pratchett, Vanessa Messmer, Pablo Saenz-Agudelo, and Michael Berumen. Microsatellites reveal genetic homogeneity among outbreak populations of crown-of-thorns starfish (Acanthaster cf. solaris) on Australia's Great Barrier Reef. *Diversity*, 9(1):16, 2017.

[108] Herlina Hartanto, Ravi Prabhu, Anggoro S.E Widayat, and Chay Asdak. Factors affecting runoff and soil erosion: plot-level soil loss monitoring for assessing sustainability of forest management. *Forest Ecology and Management*, 180(1-3):361–374, 2003.

[109] K. E. Havens, J. R. Beaver, D. A. Casamatta, T. L. East, R. T. James, P. Mccormick, E. J. Phlips, and A. J. Rodusky. Hurricane effects on the planktonic food web of a large subtropical lake. *Journal of Plankton Research*, 33(7):1081–1094, 2011.

[110] Christopher M. Heggerud, Hao Wang, and Mark A. Lewis. Transient dynamics of a stoichiometric cyanobacteria model via multiple-scale analysis. *SIAM Journal on Applied Mathematics*, 80(3):1223–1246, 2020.

[111] Kirsten A. Henderson, Chris T. Bauch, and Madhur Anand. Alternative stable states and the sustainability of forests, grasslands, and agriculture. *Proceedings of the National Academy of Sciences*, 113(51):14552–14559, 2016.

[112] Mohamed E. Hereher. Vulnerability assessment of the Saudi Arabian Red Sea coast to climate change. *Environmental Earth Sciences*, 75(1), 2015.

[113] AJ Heyward and JD Collins. Growth and sexual reproduction in the scleractinian coral Montipora digitata (Dana). *Marine and Freshwater Research*, 36(3):441, 1985.

[114] Christina C. Hicks and Timothy R. McClanahan. Assessing gear modifications needed to optimize yields in a heavily exploited, multi-species, seagrass and coral reef fishery. *PLoS ONE*, 7(5):e36022, 2012.

[115] Ray Hilborn, André E. Punt, and José Orensanz. Beyond band-aids in fisheries management: fixing world fisheries. *Bulletin of Marine Science*, 74(3):493–507, 2004.

[116] Nathalie Hilmi, David Osborn, Sevil Acar, Tamatoa Bambridge, Frederique Chlous, Mine Cinar, Salpie Djoundourian, Gunnar Haraldsson, Vicky W.Y. Lam, Samir Maliki, Annick de Marffy Mantuano, Nadine Marshall, Paul Marshall, Nicolas Pascal, Laura Recuero-Virto, Katrin Rehdanz, and Alain Safa. Socio-economic tools to mitigate the impacts of ocean acidification on economies and communities reliant on coral reefs — a framework for prioritization. *Regional Studies in Marine Science*, 28:100559, 2019.

[117] A. S. Hoey and D. R. Bellwood. Cross-shelf variation in the role of parrotfishes on the Great Barrier Reef. *Coral Reefs*, 27(1):37–47, 2007.

[118] Josef Hofbauer and Karl Sigmund. *Evolutionary games and population dynamics*. Cambridge University Press, 1998.

[119] Peter Houk, David Benavente, John Iguel, Steven Johnson, and Ryan Okano. Coral reef disturbance and recovery dynamics differ across gradients of localized stressors in the Mariana Islands. *PLoS ONE*, 9(8):e105731, 2014.

[120] R. N. Hughes. *Oceanography and marine biology. an annual review.* CRC Press, Taylor & Francis Group, Boca Raton, Florida, 2014.

[121] T. P. Hughes and J. H. Connell. Multiple stressors on coral reefs: A long -term perspective. *Limnology and Oceanography*, 44(3part2):932–940, 1999.

[122] Keng-Lou James Hung, John S. Ascher, and David A. Holway. Urbanization-induced habitat fragmentation erodes multiple components of temporal diversity in a Southern California native bee assemblage. *PLOS ONE*, 12(8):e0184136, 2017.

[123] Sijia Huo, Mengmeng Wang, Guolong Chen, Huiqin Shu, and Ruixia Yang. Monitoring and assessment of endangered UNESCO World Heritage Sites using space technology: a case study of East Rennell, Solomon Islands. *Heritage Science*, 9(1), 2021.

[124] Nicholas Hutley, Mandus Boselalu, Amelia Wenger, Alistair Grinham, Badin Gibbes, and Simon Albert. Evaluating the effect of data-richness and model complexity in the prediction of coastal sediment loading in Solomon Islands. *Environmental Research Letters*, 15(12):124044, 2020.

[125] Clinton Innes, Madhur Anand, and Chris T. Bauch. The impact of human-environment interactions on the stability of forest-grassland mosaic ecosystems. *Scientific Reports*, 3(1), 2013.

[126] David M. P. Jacoby, Francesco Ferretti, Robin Freeman, Aaron B. Carlisle, Taylor K. Chapple, David J. Curnick, Jonathan J. Dale, Robert J. Schallert, David Tickler, and Barbara A. Block. Shark movement strategies influence poaching risk and can guide enforcement decisions in a large, remote marine protected area. *Journal of Applied Ecology*, 57(9):1782–1792, 2020.

[127] R. L. Jefferies, R. F. Rockwell, and K. F. Abraham. Agricultural food subsidies, migratory connectivity and large-scale disturbance in Arctic coastal systems: A case study. *Integrative and Comparative Biology*, 44(2):130–139, 2004.

[128] E. B. Dale Jones, Gene S. Helfman, Joshua O. Harper, and Paul V. Bolstad. Effects of riparian forest removal on fish assemblages in southern Appalachian streams. *Conservation Biology*, 13(6):1454–1465, 1999.

[129] S. D. Jupiter, R. Weeks, A. P. Jenkins, D. P. Egli, and A. Cakacaka. Effects of a single intensive harvest event on fish populations inside a customary marine closure. *Coral Reefs*, 31(2):321–334, 2012.

[130] André Kamdem Toham and Guy G. Teugels. First data on an Index of Biotic Integrity (IBI) based on fish assemblages for the assessment of the impact of deforestation in a tropical West African river system. *Hydrobiologia*, 397:29–38, 1998.

[131] Pamela Z. Kamya, Maria Byrne, Alexia Graba-Landry, and Symon A. Dworjanyn. Near-future ocean acidification enhances the feeding rate and development of the herbivorous juveniles of the crown-of-thorns starfish, Acanthaster planci. *Coral Reefs*, 35(4):1241–1251, 2016.

[132] Lisa Kanary, Jeffrey Musgrave, Rebecca C. Tyson, Andrea Locke, and Frithjof Lutscher. Modelling the dynamics of invasion and control of competing green crab genotypes. *Theoretical Ecology*, 7(4):391–406, 2014.

[133] Eric Katovai, Alana L. Burley, and Margaret M. Mayfield. Understory plant species and functional diversity in the degraded wet tropical forests of Kolombangara Island, Solomon Islands. *Biological Conservation*, 145(1):214–224, 2012.

[134] Alexander Kattan, Darren J. Coker, and Michael L. Berumen. Reef fish communities in the central Red Sea show evidence of asymmetrical fishing pressure. *Marine Biodiversity*, 47(4):1227–1238, 2017.

[135] JK Keesing, AR Halford, and KC Hall. Mortality rates of small juvenile crown-of-thorns starfish Acanthaster planci on the Great Barrier Reef: implications for population size and larval settlement thresholds for outbreaks. *Marine Ecology Progress Series*, 597:179–190, 2018.

[136] Julie B. Kellner, James N. Sanchirico, Alan Hastings, and Peter J. Mumby. Optimizing for multiple species and multiple values: tradeoffs inherent in ecosystem-based fisheries management. *Conservation Letters*, 4(1):21–30, 2011.

[137] Richard Kenchington and Graeme Kelleher. Crown-of-thorns starfish management conundrums. *Coral Reefs*, 11(2):53–56, 1992.

[138] Quy Van Khuc, Bao Quang Tran, Patrick Meyfroidt, and Mark W. Paschke. Drivers of deforestation and forest degradation in Vietnam: An exploratory analysis at the national level. *Forest Policy and Economics*, 90:128–141, 2018.

[139] J. R. King and G. A. McFarlane. Marine fish life history strategies: applications to fishery management. *Fisheries Management and Ecology*, 10(4):249–264, 2003.

[140] Brian P. Kinlan, Steven D. Gaines, and Sarah E. Lester. Propagule dispersal and the scales of marine community process. *Diversity and Distributions*, 11(2):139–148, 2005.

[141] IB Kuffner, LJ Walters, MA Becerro, VJ Paul, R Ritson-Williams, and KS Beach. Inhibition of coral recruitment by macroalgae and cyanobacteria. *Marine Ecology Progress Series*, 323:107–117, 2006.

[142] C. Kuster, V.C. Vuki, and L.P. Zann. Long-term trends in subsistence fishing patterns and coral reef fisheries yield from a remote Fijian island. *Fisheries Research*, 76(2):221–228, 2005.

[143] Brian E. Lapointe, Rachel A. Brewton, Laura W. Herren, James W. Porter, and Chuanmin Hu. Nitrogen enrichment, altered stoichiometry, and coral reef decline at Looe Key, Florida Keys, USA: a 3-decade study. *Marine Biology*, 166(8), 2019.

[144] Brian E. Lapointe, Mark M. Littler, and Diane S. Littler. A comparison of nutrient-limited productivity in macroalgae from a Caribbean barrier reef and from a mangrove ecosystem. *Aquatic Botany*, 28(3-4):243–255, 1987.

[145] François X. Latrille, Sterling B. Tebbett, and David R. Bellwood. Quantifying sediment dynamics on an inshore coral reef: Putting algal turfs in perspective. *Marine Pollution Bulletin*, 141:404–415, 2019.

[146] Benjamin J Laurel and Ian R Bradbury. "big" concerns with high latitude marine protected areas (MPAs): trends in connectivity and MPA size. *Canadian Journal of Fisheries and Aquatic Sciences*, 63(12):2603–2607, 2006.

[147] RJ Lennox, A Filous, SJ Cooke, and AJ Danylchuk. Substantial impacts of subsistence fishing on the population status of an endangered reef predator at a remote coral atoll. *Endangered Species Research*, 38:135–145, 2019.

[148] Xia Li, Guangzhao Chen, Xiaoping Liu, Xun Liang, Shaojian Wang, Yimin Chen, Fengsong Pei, and Xiaocong Xu. A new global land-use and land-cover change product at a 1-km resolution for 2010 to 2100 based on human–environment interactions. *Annals of the American Association of Geographers*, 107(5):1040–1059, 2017.

[149] Ardea M. Licuanan, Michelle Z. Reyes, Katrina S. Luzon, Marie Angelica A. Chan, and Wilfredo Y. Licuanan. Initial findings of the nationwide assessment of Philippine coral reefs. *Philippine Journal of Science*, 146(2):177–185, 2017.

[150] T. Lindeberg. Scale-space for discrete signals. *IEEE Transactions on Pattern Analysis and Machine Intelligence*, 12(3):234–254, 1990.

[151] Zhifeng Liu, Chunyang He, and Jianguo Wu. The relationship between habitat loss and fragmentation during urbanization: An empirical evaluation from 16 world cities. *PLOS ONE*, 11(4):e0154613, 2016.

[152] Alfred James Lotka. *Elements of physical biology*. Williams & Wilkins, 1925.

[153] Ryan J. Lowe and James L. Falter. Oceanic forcing of coral reefs. *Annual Review of Marine Science*, 7(1):43–66, 2015.

[154] J.S. Lucas. Growth, maturation and effects of diet in Acanthaster planci (L.) (Asteroidea) and hybrids reared in the laboratory. *Journal of Experimental Marine Biology and Ecology*, 79(2):129–147, 1984.

[155] María Maestro, Ma Luisa Pérez-Cayeiro, Juan Adolfo Chica-Ruiz, and Harry Reyes. Marine protected areas in the 21st century: Current situation and trends. *Ocean & Coastal Management*, 171:28–36, 2019.

[156] Joseph Maina, Hans de Moel, Jens Zinke, Joshua Madin, Tim McClanahan, and Jan E. Vermaat. Human deforestation outweighs future climate change impacts of sedimentation on coral reefs. *Nature Communications*, 4(1), 2013.

[157] CS Mantyka and DR Bellwood. Macroalgal grazing selectivity among herbivorous coral reef fishes. *Marine Ecology Progress Series*, 352:177–185, 2007.

[158] R.J. Marriott, B.D. Mapstone, and G.A. Begg. Age-specific demographic parameters, and their implications for management of the red bass, Lutjanus bohar (Forsskal 1775): A large, long-lived reef fish. *Fisheries Research*, 83(2-3):204–215, 2007.

[159] Brezo Martínez, Lorena Sordo Pato, and Jose Manuel Rico. Nutrient uptake and growth responses of three intertidal macroalgae with perennial, opportunistic and summer-annual strategies. *Aquatic Botany*, 96(1):14–22, 2012.

[160] S.A. Matthews, K. Shoemaker, Morgan S. Pratchett, and C. Mellin. COTSMod: A spatially explicit metacommunity model of outbreaks of crown-of-thorns starfish and coral recovery. In *Advances in Marine Biology*, pages 259–290. Elsevier, 2020.

[161] T. R. McClanahan and R. Arthur. The effect of marine reserves and habitat on populations of East African coral reef fishes. *Ecological Applications*, 11(2):559–569, 2001.

[162] Tim R. McClanahan, Christina C. Hicks, and Emily S. Darling. Malthusian overfishing and efforts to overcome it on Kenyan coral reefs. *Ecological Applications*, 18(6):1516–1529, 2008.

[163] T.R. McClanahan. Human and coral reef use interactions: From impacts to solutions? *Journal of Experimental Marine Biology and Ecology*, 408(1-2):3–10, 2011.

[164] Eliot J. B. McIntire and Alex Fajardo. Beyond description: the active and effective way to infer processes from spatial patterns. *Ecology*, 90(1):46–56, 2009.

[165] Lucy A. McKergow, Ian P. Prosser, Andrew O. Hughes, and Jon Brodie. Regional scale nutrient modelling: exports to the Great Barrier Reef World Heritage Area. *Marine Pollution Bulletin*, 51(1-4):186–199, 2005.

[166] M McLean, D Mouillot, and A Auber. Ecological and life history traits explain a climate-induced shift in a temperate marine fish community. *Marine Ecology Progress Series*, 606:175–186, 2018.

[167] John W. McManus, Lambert A.B. Menez, Kathleen N. Kesner-Reyes, Sheila G. Vergara, and M.C. Ablan. Coral reef fishing and coral-algal phase shifts: implications for global reef status. *ICES Journal of Marine Science*, 57(3):572–578, 2000.

[168] John W. McManus and Johanna F. Polsenberg. Coral–algal phase shifts on coral reefs: Ecological and environmental aspects. *Progress in Oceanography*, 60(2-4):263–279, 2004.

[169] Carl G. Meyer, Yannis P. Papastamatiou, and Timothy B. Clark. Differential movement patterns and site fidelity among trophic groups of reef fishes in a Hawaiian marine protected area. *Marine Biology*, 157(7):1499–1511, 2010.

[170] K. Miller and C. Mundy. Rapid settlement in broadcast spawning corals: implications for larval dispersal. *Coral Reefs*, 22(2):99–106, 2003.

[171] Russell Milne, Chris T. Bauch, and Madhur Anand. Local overfishing patterns have regional effects on health of coral, and economic transitions can promote its recovery. *Bulletin of Mathematical Biology*, 84(4), 2022.

[172] Russell Milne and Frederic Guichard. Coupled phase-amplitude dynamics in heterogeneous metacommunities. *Journal of Theoretical Biology*, 523:110676, 2021.

[173] I. Montero-Serra, C. Linares, D. F. Doak, J. B. Ledoux, and J. Garrabou. Strong linkages between depth, longevity and demographic stability across marine sessile species. *Proceedings of the Royal Society B: Biological Sciences*, 285(1873):20172688, 2018.

[174] PJ Moran, G De'ath, VJ Baker, DK Bass, CA Christie, IR Miller, BA Miller-Smith, and AA Thompson. Pattern of outbreaks of crown-of-thorns starfish (Acanthaster planci L.) along the Great Barrier Reef since 1966. *Marine and Freshwater Research*, 43(3):555, 1992.

[175] EB Morello, ÉE Plagányi, RC Babcock, H Sweatman, R Hillary, and AE Punt. Model to manage and reduce crown-of-thorns starfish outbreaks. *Marine Ecology Progress Series*, 512:167–183, 2014.

[176] Andrew Morozov, Karen Abbott, Kim Cuddington, Tessa Francis, Gabriel Gellner, Alan Hastings, Ying-Cheng Lai, Sergei Petrovskii, Katherine Scranton, and Mary Lou Zeeman. Long transients in ecology: Theory and applications. *Physics of Life Reviews*, 32:1–40, 2020.

[177] Safa Motesharrei, Jorge Rivas, and Eugenia Kalnay. Human and nature dynamics (HANDY): Modeling inequality and use of resources in the collapse or sustainability of societies. *Ecological Economics*, 101:90–102, 2014.

[178] Molly Moustaka, Tim J. Langlois, Dianne McLean, Todd Bond, Rebecca Fisher, Peter Fearns, Passang Dorji, and Richard D. Evans. The effects of suspended sediment on coral reef fish assemblages and feeding guilds of north-west Australia. *Coral Reefs*, 37(3):659–673, 2018.

[179] Richard N. Muallil, Melchor R. Deocadez, Renmar Jun S. Martinez, Wilfredo L. Campos, Samuel S. Mamauag, Cleto L. Nañola, and Porfirio M. Aliño. Effectiveness of small locally-managed marine protected areas for coral reef fisheries management in the Philippines. *Ocean & Coastal Management*, 179:104831, 2019.

[180] Peter J Mumby and Alan Hastings. The impact of ecosystem connectivity on coral reef resilience. *Journal of Applied Ecology*, 45(3):854–862, 2007.

[181] Peter J. Mumby, Alan Hastings, and Helen J. Edwards. Thresholds and the resilience of Caribbean coral reefs. *Nature*, 450(7166):98–101, 2007.

[182] Peter J. Mumby, Robert S. Steneck, and Alan Hastings. Evidence for and against the existence of alternate attractors on coral reefs. *Oikos*, 122(4):481–491, 2012.

[183] Michelle Mycoo. Sustainable tourism, climate change and sea level rise adaptation policies in Barbados. *Natural Resources Forum*, 38(1):47–57, 2013.

[184] Marc O. Nadon. Stock assessment of the coral reef fishes of Hawaii, 2016. 2017.

[185] Masako Nakamura, Yoshimi Higa, Naoki Kumagai, and Ken Okaji. Using long-term removal data to manage a crown-of-thorns starfish population. *Diversity*, 8(4):24, 2016.

[186] Arzoo Narang and Partha Sharathi Dutta. Climate warming and dispersal strategies determine species persistence in a metacommunity. *Theoretical Ecology*, 15(1):81–92, 2022.

[187] David T. Neil, Alan R. Orpin, Peter V. Ridd, and Bofu Yu. Sediment yield and impacts from river catchments to the Great Barrier Reef lagoon: a review. *Marine and Freshwater Research*, 53(4):733, 2002.

[188] Craig E Nelson, Alice L Alldredge, Elizabeth A McCliment, Linda A Amaral-Zettler, and Craig A Carlson. Depleted dissolved organic carbon and distinct bacterial communities in the water column of a rapid-flushing coral reef ecosystem. *The ISME Journal*, 5(8):1374–1387, 2011.

[189] Quach Thi Khanh Ngoc. Assessing the value of coral reefs in the face of climate change: The evidence from Nha Trang Bay, Vietnam. *Ecosystem Services*, 35:99–108, 2019.

[190] T.A. Norton. Dispersal by macroalgae. *British Phycological Journal*, 27(3):293–301, 1992.

[191] M. M. Nugues and C. M. Roberts. Coral mortality and interaction with algae in relation to sedimentation. *Coral Reefs*, 22(4):507–516, 2003.

[192] Richard Randolph Olson. In situ culturing as a test of the larval starvation hypothesis for the crown-of-thoms starfish, Acanthaster planci 1. *Limnology and Oceanography*, 32(4):895–904, 1987.

[193] J. M. Pandolfi, S. R. Connolly, D. J. Marshall, and A. L. Cohen. Projecting coral reef futures under global warming and ocean acidification. *Science*, 333(6041):418–422, 2011.

[194] MF Pedersen and J Borum. Nutrient control of estuarine macroalgae: growth strategy and the balance between nitrogen requirements and uptake. *Marine Ecology Progress Series*, 161:155–163, 1997.

[195] Philippine Statistics Authority. 2020 Census of Population and Housing, 2021.

[196] Morgan Pratchett, Ciemon Caballes, Jennifer Wilmes, Samuel Matthews, Camille Mellin, Hugh Sweatman, Lauren Nadler, Jon Brodie, Cassandra Thompson, Jessica Hoey, Arthur Bos, Maria Byrne, Vanessa Messmer, Sofia Fortunato, Carla Chen, Alexander Buck, Russell Babcock, and Sven Uthicke. Thirty years of research on crown-of-thorns starfish (1986–2016): Scientific advances and emerging opportunities. *Diversity*, 9(4):41, 2017.

[197] Morgan Pratchett, Symon Dworjanyn, Benjamin Mos, Ciemon Caballes, Cassandra Thompson, and Shane Blowes. Larval survivorship and settlement of crown-of-thorns starfish (Acanthaster cf. solaris) at varying algal cell densities. *Diversity*, 9(1):2, 2017.

[198] Morgan S. Pratchett and Graeme S. Cumming. Managing cross-scale dynamics in marine conservation: Pest irruptions and lessons from culling of crown-of-thorns starfish (Acanthaster spp.). *Biological Conservation*, 238:108211, 2019.

[199] Chi Nguyen Thi Quynh, Steven Schilizzi, Atakelty Hailu, and Sayed Iftekhar. Fishers' preference heterogeneity and trade-offs between design options for more effective monitoring of fisheries. *Ecological Economics*, 151:22–33, 2018.

[200] M Rasheed, MI Badran, C Richter, and M Huettel. Effect of reef framework and bottom sediment on nutrient enrichment in a coral reef of the Gulf of Aqaba, Red Sea. *Marine Ecology Progress Series*, 239:277–285, 2002.

[201] Andrew Rassweiler, Christopher Costello, and David A. Siegel. Marine protected areas and the value of spatially optimized fishery management. *Proceedings of the National Academy of Sciences*, 109(29):11884–11889, 2012.

[202] Andrew Rassweiler, Scott D. Miller, Sally J. Holbrook, Matthew Lauer, Mark A. Strother, Sarah E. Lester, Thomas C. Adam, Jean Wencélius, and Russell J. Schmitt. How do fisher responses to macroalgal overgrowth influence the resilience of coral reefs? *Limnology and Oceanography*, 67(S1), 2021.

[203] R. E. Reichelt, R. H. Bradbury, and P. J. Moran. Distribution of Acanthaster planci outbreaks on the Great Barrier Reef between 1966 and 1989. *Coral Reefs*, 9(3):97–103, 1990.

[204] A.J Reichelt-Brushett and P.L Harrison. The effect of copper on the settlement success of larvae from the scleractinian coral Acropora tenuis. *Marine Pollution Bulletin*, 41(7-12):385–391, 2000.

[205] Andries Richter and Vasilis Dakos. Profit fluctuations signal eroding resilience of natural resources. *Ecological Economics*, 117:12–21, 2015.

[206] Michael J Risk. Assessing the effects of sediments and nutrients on coral reefs. *Current Opinion in Environmental Sustainability*, 7:108–117, 2014.

[207] Callum M. Roberts. Effects of fishing on the ecosystem structure of coral reefs. *Conservation Biology*, 9(5):988–995, 1995.

[208] Alice Rogers, Alastair R. Harborne, Christopher J. Brown, Yves-Marie Bozec, Carolina Castro, Iliana Chollett, Karlo Hock, Cheryl A. Knowland, Alyssa Marshell, Juan C. Ortiz, Tries Razak, George Roff, Jimena Samper-Villarreal, Megan I. Saunders, Nicholas H. Wolff, and Peter J. Mumby. Anticipative management for coral reef ecosystem services in the 21st century. *Global Change Biology*, 21(2):504–514, 2014.

[209] M. L. Rosenzweig and R. H. MacArthur. Graphical representation and stability conditions of predator-prey interactions. *The American Naturalist*, 97(895):209–223, 1963.

[210] S. M. Ross and A. Dykes. Soil conditions, erosion and nutrient loss on steep slopes under mixed dipterocarp forest in Brunei Darussalam. In *Monographiae Biologicae*, pages 259–270. Springer Netherlands, 1996.

[211] Jennifer L. Ruesink and Ligia Collado-Vides. Modeling the increase and control of Caulerpa taxifolia, an invasive marine macroalga. *Biological Invasions*, 8(2):309–325, 2006.

[212] A. Ruiz-Frau, H. Hinz, G. Edwards-Jones, and M.J. Kaiser. Spatially explicit economic assessment of cultural ecosystem services: Non-extractive recreational uses of the coastal environment related to marine biodiversity. *Marine Policy*, 38:90–98, 2013.

[213] Garry R. Russ, Angel C. Alcala, Aileen P. Maypa, Hilconida P. Calumpong, and Alan T. White. Marine reserve benefits local fisheries. *Ecological Applications*, 14(2):597–606, 2004.

[214] Garry R. Russ, Sarah-Lee A. Questel, Justin R. Rizzari, and Angel C. Alcala. The parrotfish–coral relationship: refuting the ubiquity of a prevailing paradigm. *Marine Biology*, 162(10):2029–2045, 2015.

[215] Hermann Rügner, Marc Schwientek, Barbara Beckingham, Bertram Kuch, and Peter Grathwohl. Turbidity as a proxy for total suspended solids (TSS) and particle facilitated pollutant transport in catchments. *Environmental Earth Sciences*, 69(2):373–380, 2013.

[216] Giovanni Santangelo, Lorenzo Bramanti, and Mimmo Iannelli. Population dynamics and conservation biology of the over-exploited Mediterranean red coral. *Journal of Theoretical Biology*, 244(3):416–423, 2007.

[217] Megan Irene Saunders, Scott Atkinson, Carissa Joy Klein, Tony Weber, and Hugh P. Possingham. Increased sediment loads cause non-linear decreases in seagrass suitable habitat extent. *PLOS ONE*, 12(11):e0187284, 2017.

[218] Russell J. Schmitt, Sally J. Holbrook, Samantha L. Davis, Andrew J. Brooks, and Thomas C. Adam. Experimental support for alternative attractors on coral reefs. *Proceedings of the National Academy of Sciences*, 116(10):4372–4381, 2019.

[219] Jennifer C Selgrath, Sarah E Gergel, and Amanda C J Vincent. Incorporating spatial dynamics greatly increases estimates of long-term fishing effort: a participatory mapping approach. *ICES Journal of Marine Science*, 75(1):210–220, 2017.

[220] Maria Isabel S. Senal, Gil S. Jacinto, Maria Lourdes San Diego-McGlone, Fernando Siringan, Peter Zamora, Lea Soria, M. Bayani Cardenas, Cesar Villanoy, and Olivia Cabrera. Nutrient inputs from submarine groundwater discharge on the Santiago reef flat, Bolinao, Northwestern Philippines. *Marine Pollution Bulletin*, 63(5-12):195–200, 2011.

[221] Andrew A. Shantz, Mark C. Ladd, and Deron E. Burkepile. Algal nitrogen and phosphorus content drive inter- and intraspecific differences in herbivore grazing on a Caribbean reef. *Journal of Experimental Marine Biology and Ecology*, 497:164–171, 2017.

[222] Tatsuya Shinnaka, Mitsuhiko Sano, Kou Ikejima, Prasert Tongnunui, Masahiro Horinouchi, and Hisashi Kurokura. Effects of mangrove deforestation on fish assemblage at Pak Phanang Bay, southern Thailand. *Fisheries Science*, 73(4):862–870, 2007.

[223] Roy C. Sidle, Alan D. Ziegler, Junjiro N. Negishi, Abdul Rahim Nik, Ruyan Siew, and Francis Turkelboom. Erosion processes in steep terrain—truths, myths, and uncertainties related to forest management in Southeast Asia. *Forest Ecology and Management*, 224(1-2):199–225, 2006.

[224] Martin D. Smith, Cathy A. Roheim, Larry B. Crowder, Benjamin S. Halpern, Mary Turnipseed, James L. Anderson, Frank Asche, Luis Bourillón, Atle G. Guttormsen, Ahmed Khan, Lisa A. Liguori, Aaron McNevin, Mary I. O'Connor, Dale Squires, Peter Tyedmers, Carrie Brownstein, Kristin Carden, Dane H. Klinger, Raphael Sagarin, and Kimberly A. Selkoe. Sustainability and global seafood. *Science*, 327(5967):784–786, 2010.

[225] Stephen V. Smith, Dennis P. Swaney, Liana Talaue-McManus, Jeremy D. Bartley, Peder T. Sandhei, Casey J. McLaughlin, Vilma C. Dupra, Chris J. Crossland, Robert W. Buddemeier, Bruce A. Maxwell, and Fredrik Wulff. Humans, hydrology, and the distribution of inorganic nutrient loading to the ocean. *BioScience*, 53(3):235, 2003.

[226] Lara Patricia A. Sotto, Arthur H. W. Beusen, Cesar L. Villanoy, Lex F. Bouwman, and Gil S. Jacinto. Nutrient load estimates for Manila Bay, Philippines using population data. *Ocean Science Journal*, 50(2):467–474, 2015.

[227] David Souter, Serge Planes, Jérémy Wicquart, Murray Logan, David Obura, and Francis Staub, editors. *Status of Coral Reefs of the World: 2020*. Global Coral Reef Monitoring Network, 2020.

[228] Barbara Spiecker, Tarik C. Gouhier, and Frédéric Guichard. Reciprocal feedbacks between spatial subsidies and reserve networks in coral reef meta-ecosystems. *Ecological Applications*, 26(1):264–278, 2016.

[229] Statistics Indonesia. Penduduk Indonesia menurut Provinsi 1971, 1980, 1990, 1995, 2000 dan 2010, 2021. in Indonesian.

[230] Yuko Stender, Paul L. Jokiel, and Ku'ulei S. Rodgers. Thirty years of coral reef change in relation to coastal construction and increased sedimentation at Pelekane Bay, Hawai'i. *PeerJ*, 2:e300, 2014.

[231] Robert S. Steneck, Suzanne N. Arnold, Robert Boenish, Ramón de León, Peter J. Mumby, Douglas B. Rasher, and Margaret W. Wilson. Managing recovery resilience in coral reefs against climate-induced bleaching and hurricanes: A 15 year case study from Bonaire, Dutch Caribbean. *Frontiers in Marine Science*, 6, 2019.

[232] Kelly R. Stewart, Rebecca L. Lewison, Daniel C. Dunn, Rhema H. Bjorkland, Shaleyla Kelez, Patrick N. Halpin, and Larry B. Crowder. Characterizing fishing effort and spatial extent of coastal fisheries. *PLoS ONE*, 5(12):e14451, 2010.

[233] Curt D. Storlazzi, Maarten van Ormondt, Yi-Leng Chen, and Edwin P. L. Elias. Modeling fine-scale coral larval dispersal and interisland connectivity to help designate mutually-supporting coral reef marine protected areas: Insights from Maui Nui, Hawaii. *Frontiers in Marine Science*, 4, 2017.

[234] Hugh Sweatman. No-take reserves protect coral reefs from predatory starfish. *Current Biology*, 18(14):R598–R599, 2008.

[235] Alina M. Szmant. Reproductive ecology of Caribbean reef corals. *Coral Reefs*, 5(1):43–53, 1986.

[236] Shojiro Tanaka and Ryuei Nishii. A model of deforestation by human population interactions. *Environmental and Ecological Statistics*, 4(1):83–92, 1997.

[237] Yiwen Tao, Sue Ann Campbell, and Francis J. Poulin. Dynamics of a diffusive nutrient-phytoplankton-zooplankton model with spatio-temporal delay. *SIAM Journal on Applied Mathematics*, 81(6):2405–2432, 2021.

[238] Yiwen Tao and Jingli Ren. The stability and bifurcation of homogeneous diffusive predator–prey systems with spatio–temporal delays. *Discrete & Continuous Dynamical Systems - B*, 27(1):229, 2022.

[239] Chris Taylor and David B. Lindenmayer. Temporal fragmentation of a critically endangered forest ecosystem. *Austral Ecology*, 45(3):340–354, 2020.

[240] Sterling B. Tebbett and David R. Bellwood. Algal turf sediments on coral reefs: what's known and what's next. *Marine Pollution Bulletin*, 149:110542, 2019.

[241] Sterling B. Tebbett, Christopher H.R. Goatley, Robert P. Streit, and David R. Bellwood. Algal turf sediments limit the spatial extent of function delivery on coral reefs. *Science of The Total Environment*, 734:139422, 2020.

[242] Vivek A. Thampi, Madhur Anand, and Chris T. Bauch. Socio-ecological dynamics of Caribbean coral reef ecosystems and conservation opinion propagation. *Scientific Reports*, 8(1), 2018.

[243] Damian P. Thomson, Russell C. Babcock, Richard D. Evans, Ming Feng, Molly Moustaka, Melanie Orr, Dirk Slawinski, Shaun K. Wilson, and Andrew S. Hoey. Coral larval recruitment in north-western Australia predicted by regional and local conditions. *Marine Environmental Research*, 168:105318, 2021.

[244] Molly A. Timmers, Kimberly R. Andrews, Chris E. Bird, Marta J. deMaintenton, Russell E. Brainard, and Robert J. Toonen. Widespread dispersal of the crown-of-thorns sea star, Acanthaster planci, across the Hawaiian Archipelago and Johnston Atoll. *Journal of Marine Biology*, 2011:1–10, 2011.

[245] Molly A. Timmers, Christopher E. Bird, Derek J. Skillings, Peter E. Smouse, and Robert J. Toonen. There's no place like home: Crown-of-thorns outbreaks in the Central Pacific are regionally derived and independent events. *PLoS ONE*, 7(2):e31159, 2012.

[246] Monica G. Turner, William H. Romme, Robert H. Gardner, and William W. Hargrove. Effects of fire size and pattern on early succession in Yellowstone National Park. *Ecological Monographs*, 67(4):411–433, 1997.

[247] United Nations, Department of Economic and Social Affairs, Population Division. World urbanization prospects: The 2018 revision, online edition, 2018.

[248] United Nations, Department of Economic and Social Affairs, Population Division. World population prospects 2019: Online edition, 2019.

[249] Sven Uthicke, Britta Schaffelke, and Maria Byrne. A boom–bust phylum? ecological and evolutionary consequences of density variations in echinoderms. *Ecological Monographs*, 79(1):3–24, 2009.

[250] C. Vancutsem, F. Achard, J.-F. Pekel, G. Vieilledent, S. Carboni, D. Simonetti, J. Gallego, L. E. O. C. Aragão, and R. Nasi. Long-term (1990–2019) monitoring of forest cover changes in the humid tropics. *Science Advances*, 7(10), 2021.

[251] Jarno Vanhatalo, Geoffrey R. Hosack, and Hugh Sweatman. Spatiotemporal modelling of crown-of-thorns starfish outbreaks on the Great Barrier Reef to inform control strategies. *Journal of Applied Ecology*, 54(1):188–197, 2016.

[252] J.E.N. Veron, Lyndon M. Devantier, Emre Turak, Alison L. Green, Stuart Kininmonth, Mary Stafford-Smith, and Nate Peterson. Delineating the Coral Triangle. *Galaxea, Journal of Coral Reef Studies*, 11(2):91–100, 2009.

[253] Ghislain Vieilledent, Clovis Grinand, and Romuald Vaudry. Forecasting deforestation and carbon emissions in tropical developing countries facing demographic expansion: a case study in Madagascar. *Ecology and Evolution*, 3(6):1702–1716, 2013.

[254] Peter M. Vitousek, John D. Aber, Robert W. Howarth, Gene E. Likens, Pamela A. Matson, David W. Schindler, William H. Schlesinger, and David G. Tilman. Human alteration of the global nitrogen cycle: Sources and consequences. *Ecological Applications*, 7(3):737–750, 1997.

[255] V. Volterra. Variations and fluctuations of the number of individuals in animal species living together. *ICES Journal of Marine Science*, 3(1):3–51, 1928.

[256] Maren Voss, Hermann W. Bange, Joachim W. Dippner, Jack J. Middelburg, Joseph P. Montoya, and Bess Ward. The marine nitrogen cycle: recent discoveries, uncertainties and the potential relevance of climate change. *Philosophical Transactions of the Royal Society B: Biological Sciences*, 368(1621):20130121, 2013.

[257] Ama Wakwella, Peter J. Mumby, and George Roff. Sedimentation and overfishing drive changes in early succession and coral recruitment. *Proceedings of the Royal Society B: Biological Sciences*, 287(1941):20202575, 2020.

[258] J.P Walsh and C.A Nittrouer. Contrasting styles of off-shelf sediment accumulation in New Guinea. *Marine Geology*, 196(3-4):105–125, 2003.

[259] Shuhong Wang, Suisui Chen, Hongyan Zhang, and Malin Song. The model of early warning for China's marine ecology-economy symbiosis security. *Marine Policy*, 128:104476, 2021.

[260] Fiona J. Webster, Russell C. Babcock, Mike Van Keulen, and Neil R. Loneragan. Macroalgae inhibits larval settlement and increases recruit mortality at Ningaloo Reef, Western Australia. *PLOS ONE*, 10(4):e0124162, 2015.

[261] Amelia S Wenger, Scott Atkinson, Talitha Santini, Kim Falinski, Nicholas Hutley, Simon Albert, Ned Horning, James E M Watson, Peter J Mumby, and Stacy D Jupiter. Predicting the impact of logging activities on soil erosion and water quality in steep, forested tropical islands. *Environmental Research Letters*, 13(4):044035, 2018.

[262] Amelia S. Wenger, Katharina E. Fabricius, Geoffrey P. Jones, and Jon E. Brodie. Effects of sedimentation, eutrophication, and chemical pollution on coral reef fishes. In Camilo Mora, editor, *Ecology of Fishes on Coral Reefs*, pages 145–153. Cambridge University Press, 2015.

[263] Amelia S. Wenger, Daniel Harris, Samuel Weber, Ferguson Vaghi, Yashika Nand, Waisea Naisilisili, Alec Hughes, Jade Delevaux, Carissa J. Klein, James Watson,

Peter J. Mumby, and Stacy D. Jupiter. Best-practice forestry management delivers diminishing returns for coral reefs with increased land-clearing. *Journal of Applied Ecology*, 57(12):2381–2392, 2020.

[264] Dale Weston, Katharina Hauck, and Richard Amlôt. Infection prevention behaviour and infectious disease modelling: a review of the literature and recommendations for the future. *BMC Public Health*, 18(1), 2018.

[265] Clive R. Wilkinson. Global and local threats to coral reef functioning and existence: review and predictions. *Marine and Freshwater Research*, 1999.

[266] Jennifer Wilmes, Samuel Matthews, Daniel Schultz, Vanessa Messmer, Andrew Hoey, and Morgan Pratchett. Modelling growth of juvenile crown-of-thorns starfish on the northern Great Barrier Reef. *Diversity*, 9(1):1, 2016.

[267] Kennedy Wolfe, Alexia Graba-Landry, Symon A. Dworjanyn, and Maria Byrne. Superstars: Assessing nutrient thresholds for enhanced larval success of Acanthaster planci, a review of the evidence. *Marine Pollution Bulletin*, 116(1-2):307–314, 2017.

[268] Bui Bich Xuan and Claire W. Armstrong. Trading off tourism for fisheries. *Environmental and Resource Economics*, 73(2):697–716, 2018.

[269] Toshimasa Yamamoto and Takanao Otsuka. Experimental validation of dilute acetic acid solution injection (Acanthaster planci). *Naturalistae*, 17:63–65, 2013.

[270] Max Yaremchuk and Tangdong Qu. Seasonal variability of the large-scale currents near the coast of the Philippines. *Journal of Physical Oceanography*, 34(4):844–855, 2004.

[271] Nina Yasuda, Satoshi Nagai, Masami Hamaguchi, Ken Okaji, Karin Gérard, and Kazuo Nadaoka. Gene flow of Acanthaster planci (L.) in relation to ocean currents revealed by microsatellite analysis. *Molecular Ecology*, 18(8):1574–1590, 2009.

[272] Lauren A. Yeager, Jenelle Estrada, Kylie Holt, Spencer R. Keyser, and Tobi A. Oke. Are habitat fragmentation effects stronger in marine systems? a review and meta-analysis. *Current Landscape Ecology Reports*, 5(3):58–67, 2020.

[273] Hideaki Yuasa, Rei Kajitani, Yuta Nakamura, Kazuki Takahashi, Miki Okuno, Fumiya Kobayashi, Takahiro Shinoda, Atsushi Toyoda, Yutaka Suzuki, Nalinee Thongtham, Zac Forsman, Omri Bronstein, Davide Seveso, Enrico Montalbetti,

Coralie Taquet, Gal Eyal, Nina Yasuda, and Takehiko Itoh. Elucidation of the speciation history of three sister species of crown-of-thorns starfish (Acanthaster spp.) based on genomic analysis. *DNA Research*, 28(4), 2021.

[274] Jesse R. Zaneveld, Deron E. Burkepile, Andrew A. Shantz, Catharine E. Pritchard, Ryan McMinds, Jérôme P. Payet, Rory Welsh, Adrienne M. S. Correa, Nathan P. Lemoine, Stephanie Rosales, Corinne Fuchs, Jeffrey A. Maynard, and Rebecca Vega Thurber. Overfishing and nutrient pollution interact with temperature to disrupt coral reefs down to microbial scales. *Nature Communications*, 7(1), 2016.

[275] Jaquelini O. Zeni, María Angélica Pérez-Mayorga, Camilo A. Roa-Fuentes, Gabriel L. Brejão, and Lilian Casatti. How deforestation drives stream habitat changes and the functional structure of fish assemblages in different tropical regions. *Aquatic Conservation: Marine and Freshwater Ecosystems*, 29(8):1238–1252, 2019.

[276] Hongwei Zhao, Meile Yuan, Maryna Strokal, Henry C. Wu, Xianhua Liu, AlberTinka Murk, Carolien Kroeze, and Ronald Osinga. Impacts of nitrogen pollution on corals in the context of global climate change and potential strategies to conserve coral reefs. *Science of The Total Environment*, 774:145017, 2021.

[277] Shengnan Zhao, Sanling Yuan, and Hao Wang. Adaptive dynamics of a stoichiometric phosphorus–algae–zooplankton model with environmental fluctuations. *Journal of Nonlinear Science*, 32(3), 2022.

[278] Alan D Ziegler, Thomas W Giambelluca, Liem T Tran, Thomas T Vana, Michael A Nullet, Jefferson Fox, Tran Duc Vien, Jitti Pinthong, J.F Maxwell, and Steve Evett. Hydrological consequences of landscape fragmentation in mountainous northern Vietnam: evidence of accelerated overland flow generation. *Journal of Hydrology*, 287(1-4):124–146, 2004.

[279] Kamila Żychaluk, John F. Bruno, Damian Clancy, Tim R. McClanahan, and Matthew Spencer. Data-driven models for regional coral-reef dynamics. *Ecology Letters*, 15(2):151–158, 2011.

APPENDICES

Appendix A

Crown-of-thorns starfish model parametrization and explanation of management strategies

A.1 Parametrization of local processes in the model

The lifespan of a crown-of-thorns starfish has been observed as being between 5 and 8 years [154, 196], while reef-forming corals typically live for approximately ten times that length [173], so we took ε to be 0.1. (Macroalgae lifespan is on the same order as that of corals [173], so we did not use a separate timescale for macroalgae despite their high growth rates.) Coral mortality has been estimated at a rate of 44 percent per year [28], with 30 percent of that coming from predation [35], so we took l_S to be 0.3 and m_C to be 0.14. We took m_S to be the low rate of 0.1, as field studies on juvenile CoTS have shown that their mortality decreases sharply after the first few months of life [135], suggesting that adult CoTS mortality is also low (approximately in line with coral mortality). We took a baseline value of 30 for k_S under the assumptions that k_S would be on the same order of magnitude as q and that the resulting curve would resemble that found in [160] for nutrient concentrations characteristic of our study areas (the Red Sea [200] and the Philippines [220]; see Appendix B). We also tested the cases where $k_S = 10$ and $k_S = 3$, representing cases where CoTS larval survival is less dependent on nutrient density.

Parameters not related to CoTS were similarly obtained using field data. The growth rate of herbivorous fish r_H was taken to be 0.7, and the half-saturation constant for herbivorous fish growth k_H was taken to be 0.5. k_H was chosen to be the midpoint of the theoretical range of algal cover, i.e. $[0, 1]$; r_H was chosen so that at maximum algal cover, the intrinsic growth rate of herbivorous fish would match that of Blackwood *et al.* [28], which ultimately comes from data on fish doubling times curated by FishBase [88]. This step was necessary because Blackwood *et al.* took the carrying capacity of herbivorous fish (rather than their growth rate) to depend on the amount of algae present, and our model is therefore mechanistically different. Macroalgae are known to have high growth rates: rates of increase of 10x and upwards have been observed in the field [211], and a growth rate as high as 15x has been deemed biologically plausible [228]. Therefore, we used a value of 12 for r_M. We took k_M to be the median value observed from two studies that modelled macroalgae nitrogen uptake kinetics using experimental data [194, 159], which was 80 kmol N after converting units. Natural mortality rates for macroalgae and herbivorous fish were taken to be $m_H = m_M = 0.1$, corresponding to the values in [228]. We took $\gamma = 1$ under the assumption that all detritus would decay in a year (see e.g. [76, 54]), and $f = 20$ kmol N under the assumption that the amount of nutrients entering the water above a reef from detritus decomposition would be an order of magnitude less than the amount gained from terrestrial runoff [256], which was estimated at ≈ 200 kmol N over a 1 km^2 offshore area with moderately high population density. We took the nitrogen flushing rate e to be the relatively high value of 0.6 (see e.g. [188, 153] for examples of high rates of nutrient exchange between waters above reefs and those further offshore); lateral movement of nu-

trients along the coastline by currents is covered by probability distributions θ_{N_i} for each patch i (see below). All local parameters are further described in Tables A.1 and A.2.

Param	Value	Units	Description	Reference
r_H	0.7	yr^{-1}	Herbivorous fish maximum intrinsic growth rate	[88, 28]
k_H	0.5	unitless	Half-saturation constant for herbivorous fish growth	[88, 28]
m_H	0.1	yr^{-1}	Mortality rate for herbivorous fish from causes other than harvesting	[228]
h_H	0 - 0.4	yr^{-1}	Fish harvesting rate	[63, 184, 147]
r_C	5	yr^{-1}	Coral intrinsic growth rate	[216]
m_C	0.14	yr^{-1}	Coral natural mortality rate	[35, 28]
r_M	12	yr^{-1}	Macroalgae maximum intrinsic growth rate	[211]
k_M	80	kmol N	Half-saturation constant for growth of macroalgae	[194, 159]
m_M	0.1	yr^{-1}	Macroalgae natural mortality rate	[228]
γ	1	yr^{-1}	Detritus decomposition rate	[76, 54]
q	0 - 245	kmol N yr^{-1}	Nitrogen loading rate	[254, 225]
e	0.6	yr^{-1}	Nitrogen flushing rate	[188, 153]
f	20	kmol N	Scaling constant for conversion of detritus into nutrients	[256]

Table A.1: Parameters associated with local interactions not involving crown-of-thorns starfish in the model in Chapter 3

A.2 Parametrization of dispersal distributions

Most macroalgae propagules are retained locally, with pelagic duration on the order of 0.1 day [140] and average dispersal distances being in the tens or hundreds of meters [190, 140]. Therefore, we took $k_{\text{PLD},M} = 0.1$, and $\sigma_M = 0.75$ to represent a narrow distribution. Coral pelagic larval duration is typically less than two weeks, with much variation in observations [204, 170, 57], so we took $k_{\text{PLD},C} = 7$ and $\sigma_C = 1.5$. θ_{H_i}, θ_{D_i} and θ_{N_i} for each patch i represented passive dispersal kernels for herbivorous fish, detritus and nutrients. The means of θ_{D_i} and θ_{N_i} were taken to be $i + k_{\text{curr}}k_{\text{sc}}$ as detritus and nutrients were assumed

Param	Value	Units	Description	Reference
l_S	0.3	yr^{-1}	Rate at which CoTS consumes coral	[35]
r_S	4	unitless	Scalar for converting eaten coral into CoTS larvae	Fitted
k_S	3 - 30 - 30	kmol N	Half-saturation constant for CoTS larval survival	[160]
m_S	0.1	yr^{-1}	CoTS natural mortality rate	[135]
ε	0.1	unitless	Timescale separation constant	[154, 196, 173]
$k_{\text{PLD},C}$	7	unitless	Offset of θ_C means, based on coral pelagic larval duration	[204, 170, 57]
$k_{\text{PLD},M}$	0.1	unitless	Offset of θ_M means, based on macroalgae pelagic larval duration	[190, 140]
$k_{\text{PLD},S}$	14	unitless	Offset of θ_S means, based on CoTS pelagic larval duration	[192, 266, 197]
k_{curr}	0 - 2	unitless	Offset of most dispersal kernel means, based on current strength	[203, 270, 55, 52]
k_{sc}	0.5	unitless	Scaling constant used in replicating conditions on the Great Barrier Reef	Fitted

Table A.2: Parameters associated with crown-of-thorns starfish, as well as organismal dispersal, in the model in Chapter 3

to be carried by the currents, while the mean of θ_{H_i} was taken to be i as herbivorous fish were assumed to swim freely. The standard deviation of the three passive dispersal kernels was assumed to be 1 in all cases. (For herbivorous fish, this is in line with telemetry observations suggesting adult dispersal capabilities of up to 1.6 km of coastline, with rare occurrences of dispersal beyond that [169].) We varied k_{curr} depending on the area being simulated, taking $k_{\text{curr}} = 2$ for fast currents (e.g. the east coast of the Philippines [270, 52]), $k_{\text{curr}} = 1$ for moderate currents (e.g. the Great Barrier Reef [203] and most areas of the Philippines [52]), and $k_{\text{curr}} = 0.5$ for slow currents (e.g. the Red Sea [55]). We fit k_{sc} following the incorporation of CoTS into the model (see below).

CoTS pelagic larval duration has been observed in the range of 10 to 40 days [266], with mean settlement time reported as two weeks [192] or 17 to 22 days [197]. We took $k_{\text{PLD},S} = 14$, and $\sigma_S = 1.5$ for a wide distribution. Finally, taking values of $r_S = 4$ and $k_{\text{sc}} = 0.5$ yielded results that accurately described many of the phenomena observed for Great Barrier Reef CoTS outbreaks. This included an invasion front that appeared to progress at a rate of 80-90 km per year [203, 174], a time lag of 2 years between initial larval settlement and CoTS population sizes reaching outbreak levels [192, 251], and a second outbreak approximately 15 years after the first one [196], as well as an annual reproduction cycle for CoTS [31]; see Figure B.1a. The value chosen for r_S also reduces the stiffness of the system. When evaluated on the timescale as the rest of the model, the maximal growth rate for CoTS is $r_S \cdot l_S \cdot \frac{1}{\varepsilon} = 12$. This is equal to our maximal growth rate for macroalgae, and less than the maximal growth rate for macroalgae considered in [228], in which a model similar to ours was successfully integrated using a nonstiff solver. Information on the distributions used in the model is additionally contained in Table A.3.

A.3 Choice of study cities

In order to simulate the effects of future increases of fishing pressure and nutrient loading rate on crown-of-thorns starfish (CoTS) outbreaks, we chose two cities for case studies. These were Cebu City in the Philippines, and Jeddah in Saudi Arabia. Both Cebu City [149, 219] and Jeddah [112, 227] are adjacent to large coral reefs, and CoTS outbreaks have been recently observed in both the Philippines [31, 65] and the Red Sea [273, 104] where the cities are located. The two cities are both large and expected to experience substantial further growth [247], providing an appropriate opportunity to test how urban growth will affect CoTS outbreaks. Additionally, the marine areas adjacent to Cebu City and Jeddah have very different characteristics, allowing us to evaluate the robustness of our predictions. The Red Sea is oligotrophic [51], due to low population density in the deserts surrounding it, as well as slow currents [55] that limit exchange of water with the

Distribution	Mean	Std. Dev.	Description
θ_{H_i}	i	1	Passive dispersal kernel for herbivorous fish in patch i
θ_{C_i}	$i + k_{\text{PLD},C} k_{\text{curr}} k_{\text{sc}}$	1.5	Dispersal kernel for coral larvae produced in patch i (including population growth function)
θ_{M_i}	$i + k_{\text{PLD},M} k_{\text{curr}} k_{\text{sc}}$	0.75	Dispersal kernel for macroalgae propagules produced in patch i (including population growth function)
θ_{D_i}	$i + k_{\text{curr}} k_{\text{sc}}$	1	Passive dispersal kernel for detritus in patch i
θ_{N_i}	$i + k_{\text{curr}} k_{\text{sc}}$	1	Passive dispersal kernel for nutrients in patch i
θ_{B_i}	i	1	Distribution governing how much time fishing boats based in patch i spend in each patch in the system
θ_{S_i}	$i + k_{\text{PLD},S} k_{\text{curr}} k_{\text{sc}}$	1.5	Dispersal kernel for CoTS larvae produced in patch i (including population growth function)

Table A.3: Gaussian distributions used for dispersal of model components in Chapter 3

neighbouring Indian Ocean. In contrast, the interior waters of the Philippines (such as those off the coast of Cebu) have relatively faster currents, of about the same strength as those on the Great Barrier Reef [52] (which our model was initially fit for). Rural areas of the Philippines also have higher population density than the areas surrounding the Red Sea [195, 247]; aside from the city of Mecca, much of the land in the vicinity of Jeddah is sparsely populated desert. This indicates greater amounts of nutrient input in the areas surrounding Cebu, as compared to Jeddah [225].

A.4 Spatial representation of the two study cities

For each of our two study cities, we used a 100-patch model to represent 100 km of coastline centred on the city in question. Each of the 100 patches was designated as either urban or non-urban: the number of urban patches was chosen to be equal to the length of the coastline (in km) that was urbanized according to the baseline scenarios in prior studies [148, 53]. In Jeddah, the simulated urbanized area was contiguous, while in Cebu City, the simulations for 2021 broke up the urbanized area into two components separated by outlying areas in Mactan and Cordova that were not considered urban.

Because of the fact that the coastline in Cebu City was broken up into two urbanized areas that were asymmetrically divided by a non-urbanized area, it was necessary to specify the current direction for use in the dispersal kernels θ. This was done in order to simulate CoTS larvae (and other model components) dispersing in the direction of the current rather than against it. Since currents offshore of Cebu City flow from southwest to northeast [4], we assumed that CoTS larvae entering the Cebu City area would arrive from the southwest. (In Jeddah, this specification was irrelevant, as the urban area formed a contiguous stretch of coastline and was therefore symmetric.)

We simulated dynamics on reefs adjacent to our two cities over two different 30-year time frames: from 2020 to 2050 and from 2050 to 2080. When simulating CoTS outbreaks starting in 2050, we altered the number of urban patches to match the expansion of the two cities' urban footprints, using projections [148, 53] based on the Intergovernmental Panel on Climate Change's Shared Socioeconomic Pathways and Special Report on Emissions Scenarios. Likewise, when simulating continuous growth of our two study cities until 2050, we assumed that q would increase (see below) in all patches that were considered urban in 2050, to represent the urbanization process. Cebu City was predicted to be a contiguous urban area in 2050, with the non-urban area in Mactan and Cordova being fully urbanized.

A.5 Initial conditions for case study simulations

For both cities, the fishing rate h_H was assumed to be 0.2 in 2020. This value is significantly above rates associated with small-scale subsistence fishing [63], but not high enough to cause the fish population to completely collapse [28, 242]. We chose such a value for our simulations of Jeddah because the abundance of herbivorous fish (the functional group represented in our model) in the central Red Sea near Jeddah is about a third of the value recorded on the less-populated Sudanese side of the Red Sea [134], and fishing pressure there has been recorded as high but mostly sustainable [51]. A recent review of conditions on Philippine coral reefs found that the marine protected areas closest to Cebu City were not overfished, while non-protected areas near them were overfished but retained some fish biomass [179]. Considering these conditions holistically, we decided on an initial fishing rate of 0.2 for the waters directly adjacent to Cebu City, although we note that this may be an underestimate.

With regards to nutrient availability, each type of patch (urban and non-urban) that we simulated in our two cities had values of q based on its population density using a formula from [225]. This formula considered nutrient loading from basins with unspecified areas, measured in square kilometers, and was implied to hold for local runoff. Since we used a spatial resolution of 1 km, we therefore considered nutrient input into an offshore area of 1 km^2 from an adjacent terrestrial area of the same size. At the start of our simulations, we took q to be 90 in the urban agglomeration of Cebu City and 40 in the surrounding non-urban areas, based on population numbers from the 2020 Philippine Census for municipalities in Metro Cebu and elsewhere in Cebu province [195]. For Jeddah, we used a value of $q = 90$ for urban areas based on previously reported population density numbers for the city [105], and $q = 15$ in non-urban areas. We kept q constant within the built-up areas of each city, and assumed that increases in q in these areas would be spatially uniform (see below), to eliminate potential confounding due to uneven increases in urban density.

In both simulated cities, patches outside the urbanized area started with 50 percent coral cover and 10 percent macroalgae cover ($C(t = 0) = 0.5$, $M(t = 0) = 0.1$), in line with recent field observations in the Philippines and the northern Red Sea [227]. In patches offshore from urbanized areas, we took initial values for C and M to instead be 0.3 and 0.7, respectively, to represent a shift away from coral dominance due to better conditions for macroalgae (e.g. higher nutrient input). To simulate the beginning of an outbreak, initial values for CoTS were taken to be 0.5 in the patch furthest upstream and 0 everywhere else. Initial herbivorous fish densities were assumed to be 0.5 across the system, representing relatively healthy levels, and initial levels of nutrients and detritus were assumed to be their long-term average values when the model reaches its steady state.

A.6 Simulated fishing rate increases

Increases in h_H were assumed to scale with projected increases in population, as this relationship is well-documented for commercial fishing [232]. Fishing effort in a reef ecosystem adjacent to Cebu City increased by at minimum 150 percent from 1960 to 2010 [219], while the municipalities making up Metro Cebu grew by about 350 percent over the same timeframe. We assumed a similar relationship in Jeddah, and took the rate of increase of h_H to be $\frac{3}{7}$ times the rate of population increase in both cities. To fit future values of h_H, we used population projections for Jeddah from [13] (with a linear extrapolation from 2040 to 2050 based on the 2030-2040 growth rate), and estimates for urban population growth in the Philippines from the United Nations [247]. Harvesting rate was increased at the same rate systemwide, in order to account for the fact that areas where fishing effort is high are often some distance away from population centres and often change over time [219]. The value of h_H reached at the end of the simulation was additionally used as the value for h_H in our simulations with constant fishing pressure starting in 2050.

A.7 Simulated nutrient loading rate increases

We simulated increases in nutrient loading in two different ways, representing density increases in urban areas and urbanization of previously rural or non-urbanized areas. For the former, our simulations representing 2050 featured greater values of q in urban patches based on projected increases in nutrient loading by that year. In Cebu City, this was based on the median projected increase in the Manila Bay region [226] elsewhere in the Philippines (scaled to account for a start date of 2020 rather than 2010), under the assumption that growth in Cebu City would be similar. In Jeddah, this was based on projections of wastewater output until 2040 [13], which were then linearly extrapolated to 2050. This is because wastewater is a large contributor to the elevated nitrogen and phosphorus levels found off the coast of Jeddah, in comparison to open waters in the Red Sea [8]. Additionally, we increased q at the same rate in patches that were not considered urban at the start of our simulations but were projected to be urbanized by 2050 [148, 53]. (This caused q to be lower in those patches throughout the simulation than ones that were already urbanized, making this a relatively optimistic scenario.) As with h_H, the final value reached by q was used as its (non-varying) value in our simulations starting in 2050.

A.8 Criteria for prioritizing patches for CoTS removal

As part of our simulations of local CoTS removal, we devised three mathematical criteria for CoTS management based on available data, plus a fourth defined as the average of the first three. These were based on management priorities set out for CoTS on the Great Barrier Reef. The first management criterion we used was the density of CoTS in each patch i, relative to the systemwide average:

$$\Phi_{\mathrm{CoTS}}(i) = \begin{cases} S_i \left(\frac{1}{100} \sum_{j=1}^{100} S_j \right)^{-1}, & S_i \geq 0.01 \\ 0, & S_i < 0.01 \end{cases} \tag{A.1}$$

The second criterion that we used was the ability of local coral to recover. We represented this by the proportion of the seabed covered either by coral or bare rock (i.e. not macroalgae) compared to the systemwide average, as macroalgae overgrows coral and inhibits coral larval settlement, but bare rock can be freely colonized by coral. We used the following formulation for this criterion:

$$\Phi_{\mathrm{Rec}}(i) = \begin{cases} (1 - M_i) \left(\frac{1}{100} \sum_{j=1}^{100} (1 - M_j) \right)^{-1}, & S_i \geq 0.01 \\ 0, & S_i < 0.01 \end{cases} \tag{A.2}$$

The third criterion that we used was the extent to which local CoTS could cause an outbreak to spread. For this criterion, we evaluated how dangerous CoTS in each patch i could be to other patches in the system, which we did by taking the sum over all patches j of the coral cover in that patch (C_j) multiplied by the probability that CoTS larvae originating in patch i would settle in patch j ($\theta_{S_i}(j)$). We then normalized this quantity relative to its systemwide average. This resulted in the following formulation:

$$\Phi_{\mathrm{Spr}}(i) = \begin{cases} \left(\sum_{j=1}^{100} \theta_{S_i}(j) C_j \right) \left(\frac{1}{100} \sum_{k=1}^{100} \sum_{j=1}^{100} \theta_{S_k}(j) C_j \right)^{-1}, & S_i \geq 0.01 \\ 0, & S_i < 0.01 \end{cases} \tag{A.3}$$

The averaged criterion was assumed to be an unweighted average of the three specific criteria, i.e. $\Phi_{\mathrm{Avg}}(i) = \frac{1}{3} \left(\Phi_{\mathrm{CoTS}}(i) + \Phi_{\mathrm{Rec}}(i) + \Phi_{\mathrm{Spr}}(i) \right)$.

Appendix B

Crown-of-thorns starfish model simulations with static fishing and nutrient loading rates

In order to fit model parameters (as detailed in the Methods section of the main manuscript), we ran the model with parameter values characteristic of parts of the Great Barrier Reef adjacent to rural areas (Figure B.1a). In these simulations, we took $q = 15$ based on applying the formula in [225] to population density numbers in central and northern Queensland, and $k_{\text{curr}} = 1$ by default. We assumed static values of q and h_H, in order to eliminate any confoundation caused by future changes in conditions and hence best approximate CoTS population dynamics during the most recent Great Barrier Reef outbreak. We also performed such simulations for the Red Sea off the coast of Jeddah (Figure B.1b) and the interior waters of the Philippines, such as those near Cebu City (Figure B.1c). This was done in order to generate baseline expectations for CoTS population dynamics in those regions, which could be compared to our future projections there. Additional simulations with static q and h_H were performed for the east coast of the Philippines (Figure B.1d), as an example of an area with strong currents [270] where CoTS larvae would likely be dispersed into other ocean areas instead of being retained locally.

As part of the baseline expectations we generated for our study cities of Cebu City and Jeddah, we simulated average coral cover in each patch offshore from those cities over 30-year intervals (2020 to 2050, and 2050 to 2080) with q and h_H constant. This allowed us to compare the resilience of coral to hypothetical outbreaks starting in 2020 and 2050; maintaining constant values for q and h_H was necessary in this case as data projecting land use, nutrient input, and population growth was unavailable post-2050 on the spatial scales that we performed our analysis on. The results of these simulations for Cebu City are shown in Figure B.2a, including one case starting in 2050 where a marine protected area was set up in parts of Mactan and Cordova Islands and development was restricted there, and one case in which these conservation strategies were not implemented. The simulation results for Jeddah can be seen in Figure B.2c. Additionally, to test how robust our predictions are to potential uncertainty in how dependent CoTS larvae are on available phytoplankton (and hence nutrients), we repeated the above simulations with k_S taking a value of 3 (an order of magnitude lower than our baseline value of 30), representing the hypothesis that CoTS larvae can survive in relatively large quantities regardless of nutrient levels. The results of these simulations are shown in Figures B.2b and B.2d.

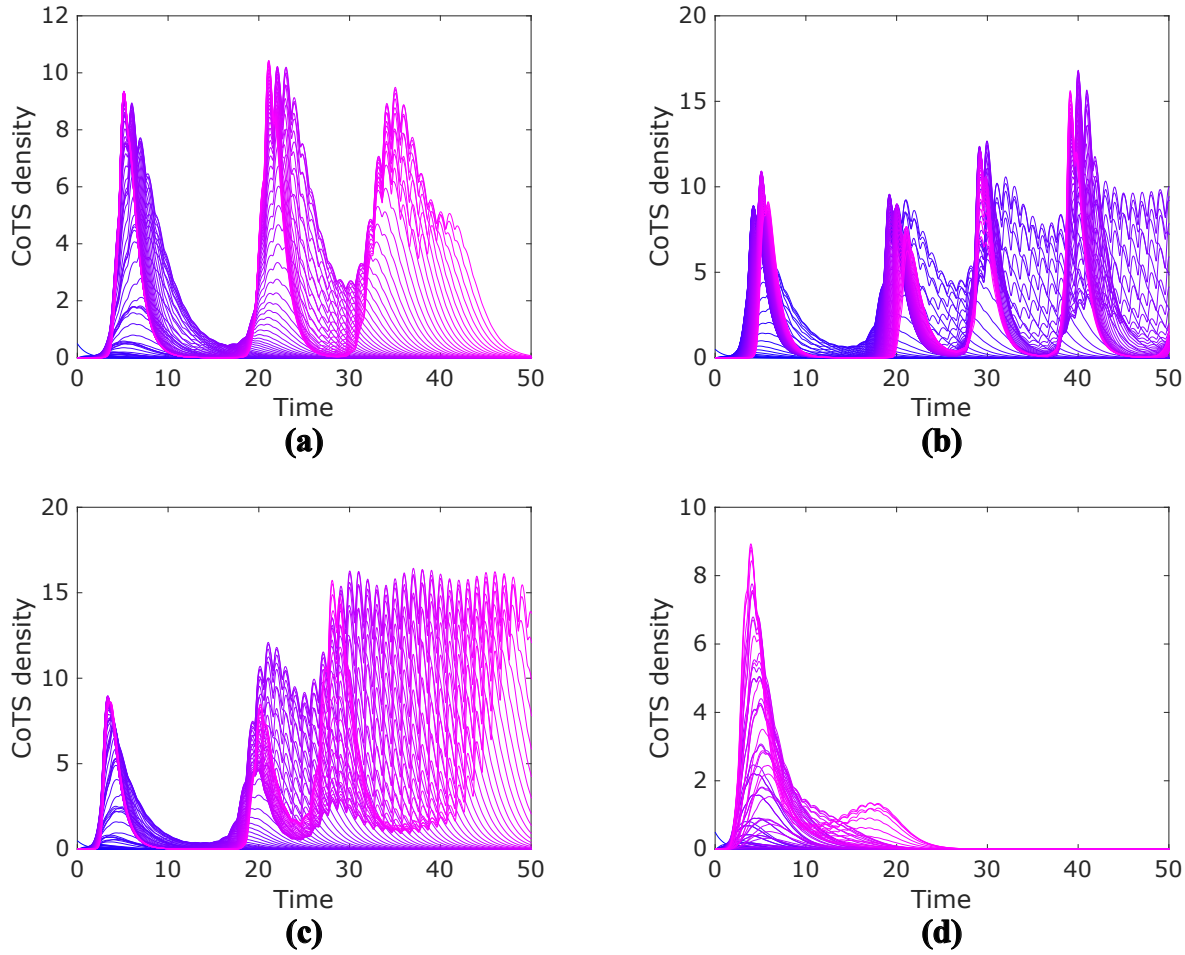

Figure B.1: Time series showing simulated CoTS population in conditions similar to those on the Great Barrier Reef, Red Sea, Philippines interior waters, and Philippines east coast. Simulations were initialized with $S_i\,(t=0)=0.5$ for $i=1$ and 0 otherwise, representing the start of an invasion of CoTS into previously uncolonized areas. Time series for individual patches are coloured on a scale from blue (close to outbreak starting point) to magenta (far away from outbreak starting point).

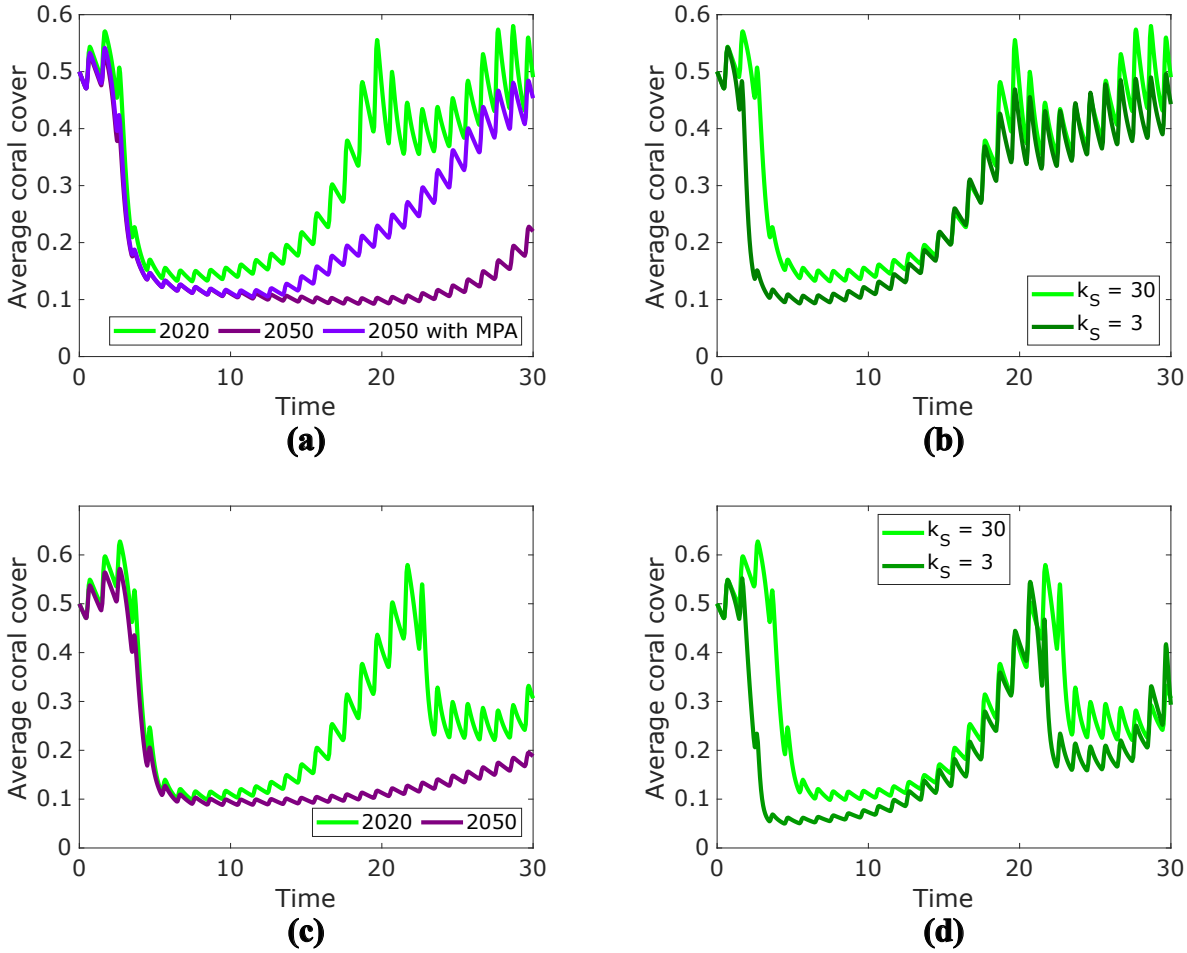

Figure B.2: Case studies for Cebu City, Philippines and Jeddah, Saudi Arabia, in which nutrient loading rate q and harvesting rate h_H remained constant over time. Figures B.2a and B.2b show coral dynamics in Cebu, while figures B.2c and B.2d show dynamics in Jeddah. Figures B.2a and B.2c show average coral cover during and after a simulated crown-of-thorns starfish outbreak in 2020 and 2050; figure B.2a (these simulations in Cebu) includes another case in 2050 where an MPA is established and development is restricted in some areas of Mactan and Cordova Islands. Figures B.2b and B.2d show potential variation in CoTS outbreak severity from dependence of CoTS larval survival on nutrient availability (k_S).